

IN-73
14952

NASA Contractor Report 187527

p. 77

(NASA-CR-187527) SCIENCE REQUIREMENTS FOR
HEAVY NUCLEI COLLECTION (HNC) EXPERIMENT ON
NASA LONG DURATION EXPOSURE FACILITY (LDEF)
MISSION 2 Final Report (California Univ.)
77 p CSCL 20H G3/73

N91-23887

Unclas
0014952

**SCIENCE REQUIREMENTS FOR HEAVY NUCLEI
COLLECTION (HNC) EXPERIMENT ON NASA LONG
DURATION EXPOSURE FACILITY (LDEF) MISSION II**

P. Buford Price

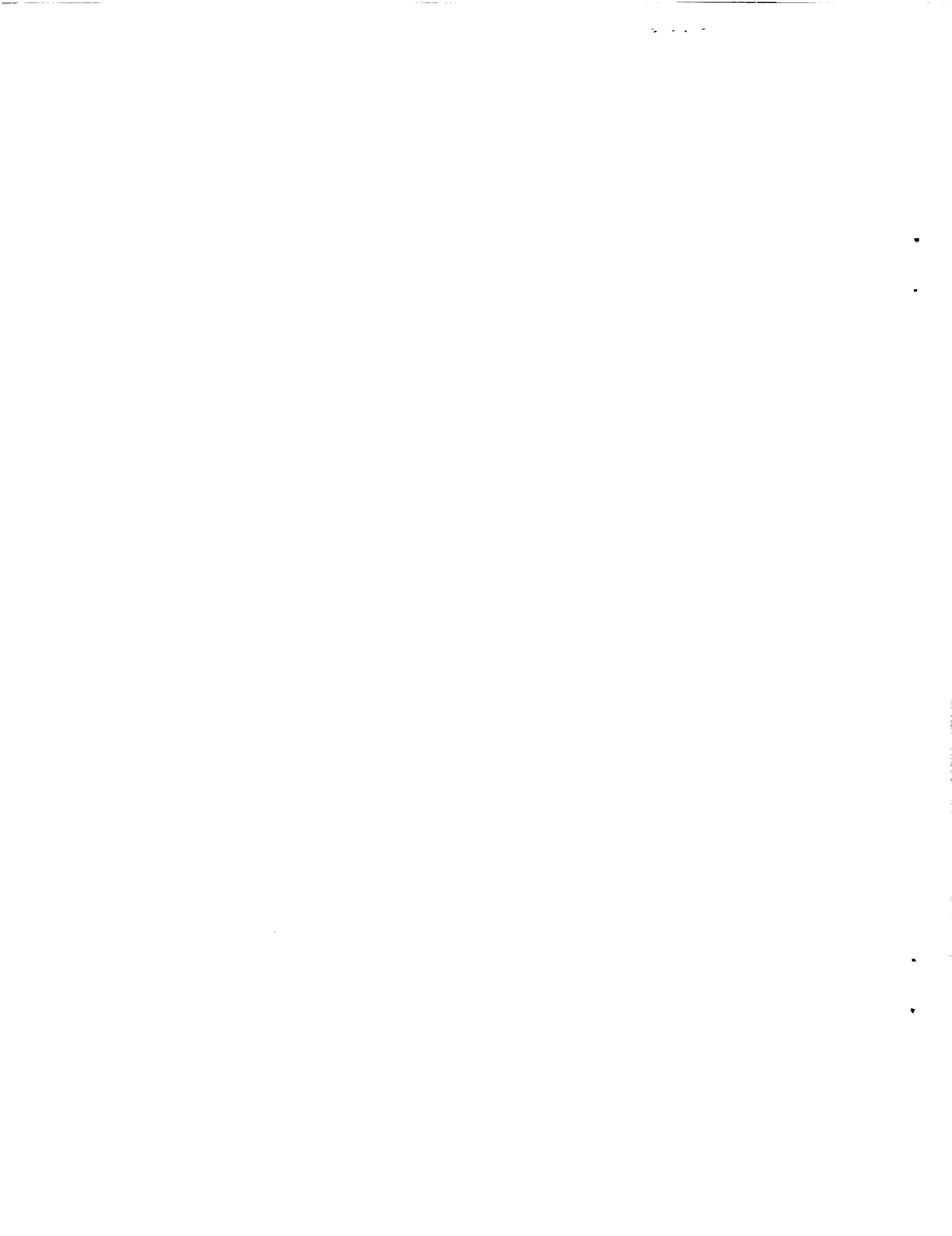
**UNIVERSITY OF CALIFORNIA
Berkeley, California**

**Contract NAS1-17806
June 1991**



National Aeronautics and
Space Administration

Langley Research Center
Hampton, Virginia 23665-5225



Final Report: Science Requirements for Heavy Nuclei Collection Experiment on LDEF Mission II

1. Introduction

This report contains several documents. The first summarizes the procedures which, if followed, will ensure attainment of the goal of resolution of individual charges of the ultraheavy nuclei. For a fuller discussion, one should consult the University of California (Berkeley) Ph. D. thesis of Dr. Jaime Drach, dated February, 1987. The second summarizes the procedures that should be followed in processing the HNC detectors after recovery, and the data analysis.

During the study, the Challenger accident occurred and ultimately the second LDEF mission was cancelled. We discovered a new type of detector made of phosphate glass, with properties superior to those of the plastic detectors intended for the HNC mission. The opportunity arose to propose an attached payload for the Space Station Freedom, and the third document in this final report is a copy of that proposal, which describes how the glass detectors would be used to achieve better performance with less post-flight labor. The fourth and final document is a short summary of two modes of the HNC -- one for the Freedom and one for deployment on the Soviet Mir Space Station. If all goes well, one or both of these versions of HNC should provide the astrophysical community with data of unprecedented quality and quantity on the ultraheavy cosmic rays.

.....

.....

.....

Attainment of High Charge Resolution

P.B. Price

1. Introduction

The following is a brief layman's summary of the procedures by which the HNC mission is able to attain its goal of a charge standard deviation no worse than 0.25 e for the actinide elements. Its purpose is to expand upon the information given in the flow chart labeled "Attainment of High Charge Resolution." At the end of this summary is a list of papers in which each of the technical points is discussed in detail. All of the papers have appeared in refereed journals.

2. High-quality detectors

a) Z/β intervals covered by the various HNC detectors

Figure 1 shows the reduced track etch rate as a function of Z/β for the three types of plastic track detectors to be used on HNC and for a very promising new phosphate glass detector, VG-13, which should be considered seriously for an add-on experiment on the LDEF reflight.

b) CR-39 (DOP) with antioxidant

This material is made by American Acrylic to our specifications, using the cure cycle and mold gasket developed by J. Adams; using French Allymer monomer; using G. Tarlé's DOP additive for a smooth post-etch surface; and using Tarlé's antioxidant for long-term stability in air.

Our group, as well as Henshaw (Bristol), Somogy (Hungary), and Almasy (LBL), have found that CR-39 undergoes slow changes in response and in general etch rate, V_G , as a function of time after manufacture as well as after irradiation. We have found, however, that addition of the antioxidant developed by Tarlé results in a detector that shows no systematic change in V_T or in V_G (track etch rate) over times of at least seven months at room temperature (see Fig. 8 and discussion in sections 5 and 6). As a further precaution, the detectors that were recently made for HNC are now stored at -16°C and will be returned to a room at -16°C after the mission. The sheets that were calibrated with uranium ions at the Bevalac in April, 1986 are also being maintained at -16°C at the University of Michigan.

Uniformity tests by Ahlen on samples of the batch of CR-39 made for HNC and irradiated with Fe ions show that it meets our specifications.

c) Rodyne

This detector was made for HNC to our specifications in thicknesses of 127 and 254 μm by Coburn Industries. Uniformity tests by Ahlen on samples with and without antioxidant, irradiated with uranium ions, showed that samples without antioxidant were best. An experiment in which samples both with and without antioxidant were irradiated with fission fragments, then were heated at 120°C for a week in air, showed that no surface degradation of either type of Rodyne took place. A similar test on CR-39 showed that an antioxidant was essential in protecting that polymer from thermal oxidation.

d) Cronar

This detector is made by DuPont in several thicknesses. It, like all polyester films, is biaxially stretched during manufacture, which gives it desirable chemical and physical properties but results in a preferred polymer orientation that gives rise to a refractive index that varies in three directions, rather like mica, and can result in slightly anisotropic V_G in the film plane if the amount of stretch in the two orthogonal directions is not the same. We chose 100 μm Cronar over 178 μm Cronar because V_G is approximately independent of azimuth angle in the film plane for the 100 μm material, whereas it is anisotropic in the 178 μm material.

One side of Cronar is coated with a ~ 100 Angstrom layer of proprietary material that comes off without any problem during etching and has no perceptible effect on track registration.

3. Demonstration of charge resolution with Bevalac calibrations

a) Many independent dE/dx detectors

We have published several papers [1-6] demonstrating that, for relativistic nuclei throughout the interval $10 \leq Z \leq 92$, the standard deviation in measured charge decreases as $1/\sqrt{n}$, where n is the number of etch pits on independent surfaces of sheets in a stack and the charge is calculated from the average value of the diameter or length of the n etch pits. The three types of plastic detectors are optimized for different but overlapping intervals of Z/β : as shown in Fig. 2, CR-39 (DOP) is suitable for $10 \leq Z/\beta \leq 60$ when etch pit mouths are measured but can also provide data for $Z/\beta \geq 60$ when etch pit lengths are measured. As Fig. 3 shows, Rodyne is suitable for $55 \leq Z/\beta \leq 92$ when mouths are measured and for $Z/\beta \geq 92$ when lengths are measured. As Fig. 4 shows, Cronar is suitable for $76 \leq Z/\beta \leq 115$ when mouths are measured. The sensitivity depends somewhat on etching temperature in NaOH.

b) Copper foils to strip electrons from heavy elements

We have shown [3] both experimentally and theoretically that for uranium nuclei at energies above about 800 MeV/nucleon the insertion of thin copper foils periodically in the stack narrows the charge state distribution, removes the correlation of

charge state from one plastic sheet to the next, and improves the charge resolution by allowing the $1/\sqrt{n}$ dependence of the charge standard deviation on n to hold for values of n as large as ~ 20 . Copper is better than a heavier element like lead because its nonradiative capture cross section does not grow as fast as that for lead as energy decreases. As an example, for uranium at 960 MeV/nucleon calculations supported by experimental measurements show that the charge state populations are 0.9 in 92+, 0.09 in 91+, and 0.01 in 90+ with a copper foil, compared with 0.67 in 92+, 0.3 in 91+, and 0.03 in 90+ with a pure plastic stack.

For nuclei lighter than uranium a larger fraction of ions are fully stripped at a given energy/nucleon, and the copper is even more effective.

At energies below ~ 400 MeV/nucleon copper becomes increasingly ineffective at stripping the K electrons. At very low energies, below about 100 MeV/nucleon, the interaction lengths for both stripping and capture of electrons become much shorter than a typical cone length, and the concept of effective charge becomes applicable, with many changes of ionic charge occurring along each etched cone. Our studies of cone length distributions for uranium ions slowing to rest in a thick stack [5] indicate that the charge resolution is as good at low energies as at high energies. Our data on uranium at energies of a few hundred MeV/nucleon are not extensive enough for us to make a definitive statement about resolution at intermediate energies. Since, with the thick stacks on HNC, heavy ions of intermediate energies will be brought to rest and their etch pits measured at low as well as at intermediate energies, we expect to be able to attain high charge resolution over the complete energy spectrum.

c) Charge resolution for particles of known velocity

Table 1 lists some of the charge standard deviations already achieved in measurements of a single etchpit for various values of Z based on results reported in refs. [1-6] using Bevalac beams for which β is known and is always > 0.87 . It also lists charge standard deviations achieved by averaging measurements of n etchpits. In every case $\sigma_Z(n) \approx \sigma_Z(1)/\sqrt{n}$.

4. Determination of charge and velocity from track etch rate and its gradient in a thick stack.

In the actual HNC mission the velocities will not be known. Table 2 gives the charge standard deviations expected on the basis of extensive Monte Carlo simulations done by J. Drach [18] for various values of Z and β . We assumed no fading, no dependence of response on track registration temperature, and no track aging effect. The calculations were done for a stack of standard thickness and for one of half the standard thickness. The results for half thickness indicate how resolution deteriorates for those particles that catastrophically interact about halfway through the stack, leaving no fragment large enough to be detected. Fortunately, most of the time the major fragment would be detectable at least in the CR-39 sheets, so that the charges before and after fragmentation, together with the velocity, can be fitted at the price of one additional degree of freedom.

Thus, the Monte Carlo results for the full-thickness stack are almost always the relevant ones.

A critical parameter in the calculations is the standard deviation in the measurement of either minor axis or cone length. In section I of Table 2 we show the results based on experimental measurements of standard deviation of minor axis (refs. 4,6) and of track length (refs. 5,7). Note, in particular, that the length standard deviations we used are based mainly on values attained ten years ago in the Skylab ultraheavy cosmic ray experiment (see Fig. 5) using Lexan detectors.

We believe the standard deviations used in section I of the table are overly pessimistic. By using Rodyne and Cronar, which have smoother post-etch surfaces than Lexan, we expect to attain length standard deviations smaller than those observed on Skylab, and by using semi-automated measurement techniques to be described below, it should be possible to reduce the fractional error in track etch rate by about a factor two. This is a consequence of using all of the information in the microscope image instead of only a diameter or length, and by avoiding drift in response due to scanner fatigue or other bias. The Monte Carlo results in section II of Table 2 were obtained assuming a factor two reduction in standard deviation of minor axis or length. We see from these entries that for all charges and over all of the spectrum of energies except those around 4 GeV/nucleon it should be possible to attain a charge resolution better than 0.25e, provided all the sheets are included in the analysis. In addition, we call attention to the result that, at energies below about 1.5 GeV/nucleon, it should be possible to attain $\sigma_Z < 0.25e$ using only the skeleton etch (see Flowchart for list of sheets to be used in the skeleton etch) of nine layers of Rodyne and five layers of Cronar.

5. Elimination of track fading by maintaining $T < 0^\circ\text{C}$ during the mission

From the laboratory annealing results and the track-fading model reported in ref. [8] and summarized in Fig. 6, we conclude that in Rodyne no decrease in reduced track etch rate should occur during a ~3 year mission if the stacks are maintained at a temperature less than 0°C . We also conclude from these results and the model, and from the comparative track-aging data in Fig. 8, that at most a barely perceptible decrease would occur during a year or longer at room temperature. Referring to Fig. 8, we note that during seven months of aging of samples irradiated at the Bevalac the reduced track etch rates in those aged at 22°C do not diverge from the etch rates in those aged at -16°C . This result is true both for samples aged in air and samples aged in argon. The same insensitivity to aging temperature is true of Cronar samples as seen in Fig. 8.

For CR-39 (DOP) the interpretation of data from laboratory annealing experiments is less clear-cut, probably because during annealing other processes simultaneously occur - - oxidation and further polymerization being two examples. Note that Fig. 8 shows that the reduced track etch rates for samples aged at 22°C and at -16°C show no tendency to diverge with time. Measurements of V_G show that the general etch rate of the CR-39 samples shows no systematic change during the seven months of aging.

After the mission we propose to store Cronar and CR-39 at -16°C except when working with specific sheets, and to store Rodyne at a temperature of ~ 0 to 5°C , low enough to completely eliminate track-fading but high enough to counteract the track-aging phenomenon to be discussed in the next section.

6. Effect of track-aging on charge resolution

Ref. [9] discusses our laboratory track-aging studies of all three detectors. Data for uranium tracks with $Z/\beta = 124$ in Cronar and Rodyne samples kept at room temperature in air show (Fig. 7) that the reduced track etch rate in Cronar does not appear to change with time during the first ten months after the irradiation. Unless there happens to be a nearly exact compensation between two competing processes of aging and fading, this result indicates that neither aging or fading is significant in Cronar at room temperature during ten months and suggests that during a time of several years, no aging or fading should occur during storage at -16°C . However, for uranium tracks with $Z/\beta = 124$ in Rodyne the reduced track etch rate increases roughly logarithmically with time after irradiation and shows no sign of leveling off after ten months.

To study this poorly understood effect further, on June 30, 1985, we began a series of experiments on samples of Cronar and Rodyne exposed to gold ions with $Z/\beta = 93.6$ and on CR-39 (DOP) (with 10^{-4} antioxidant) exposed to iron ions with $Z/\beta = 27.7$. The irradiations were done at room temperature in air or in an argon atmosphere, and subsequent aging was done under four conditions: air at 22°C , air at -16°C , argon at 22°C , and argon at -16°C . Results to date, shown in Fig. 8, extend over about seven months. First of all, note that fluctuations in data points are larger than normal, for two reasons: the beams had to penetrate the lid of a 1.3-cm aluminum box before reaching the detectors, so they contained fragments which increased the errors; during the seven month period the age and concentration of sodium hydroxide solution and of etch products in the etch tanks varied. To correct for these variations we measured the general etch rate for each set of samples, both by including a sample irradiated with fission fragments for diameter measurements and by measuring the geometry of the etched tracks so as to be able to extract the value of V_G from the data. The corrections are subject to rather large errors, and we will discuss the importance of independent measurements of V_G at the end of this document.

For all of the plastic detectors we found that s was somewhat greater for samples aged in air than for samples aged in argon. In none of the four environments did CR-39 or Cronar show evidence of a growth of s due to aging. Rodyne irradiated and kept in argon shows no growth in track etch rate due to aging at either 22°C or at -16°C but has a reduced track etch rate $\sim 30\%$ lower than Rodyne irradiated and kept in air. Rodyne in air at 22°C shows a positive, roughly logarithmic aging effect over times of a few months, with slope much smaller than the slope of the aging effect for uranium ions (Fig. 7). For Rodyne in air at -16°C the effect is smaller and may even be zero. Systematic fluctuations in the values of s for a specific aging time are due to uncertainty in the correct value of V_G for that etch. These systematic fluctuations can be eliminated in the future by following a new procedure, to be discussed below, to measure V_G more accurately.

The data in Fig. 8 strongly suggest that storage of all detectors in argon would eliminate the aging effect. However, to avoid losing sensitivity, we propose not to use an argon atmosphere. Instead, we propose to keep all stacks in air at a temperature below 0°C during the mission and then to keep the Rodyne -- the only detector that shows an aging effect -- at a temperature ~0 to 10°C for at least two years after the mission before etching any layers other than the skeleton-etch layers. Due to the logarithmic dependence of track etch rate on time, aging at an optimal temperature of a few deg. C for two years after the mission should reduce the fractional difference in ages between the youngest and oldest tracks and decrease the difference in etch rates of these tracks, without at the same time causing track-fading. The optimal temperature will have to be established by further experiment. Quantitative examples are given in ref. [9] and in the Flowchart document. The CR-39 and Cronar will be kept at -16°C. For them, track-aging will not occur.

7. Correction for registration temperature effect using an event thermometer

Refs. [10-13] from the Dublin group report that in the temperature interval 18 to -78°C, which includes the interval expected for the HNC mission, the shift in apparent charge of ultraheavy nuclei with $Z/\beta \sim 100$ recorded in dry air at 1 atm measured in Rodyne is $\sim -0.16e/\text{degree}$. They find that the fractional shift in apparent charge is an increasing function of Z/β . For CR-39 irradiated in dry air at 1 atm the shift in apparent charge is higher by a factor ~ 2 to 3 at the same Z/β . In Fig. 9, from ref. [14], we show that in the interval +18 to -76°C the shift in apparent charge in Cronar is about an order of magnitude smaller than in Rodyne. Our results for Rodyne agree well with results of the Dublin group for Lexan. For $Z/\beta = 93.8$, the shift in apparent charge in Cronar is $-0.014e/\text{degree}$. In the entire temperature interval, 0°C to -50°C relevant to the HNC mission, the apparent charge of Au ions shifts by only $\sim 1e$.

In Fig. 10, from ref. [14], we show that in CR-39 exposed to 1.8 GeV/nucleon Fe and fragments the apparent charge decreases by $\sim 1e$ at Fe for a decrease in air pressure from 1 atm to 0.3 atm and by $\sim 4e$ at Fe for a decrease from 1 atm to vacuum. This shift, which occurred within an hour after changing the pressure, is a lower limit on the final shift that occurs in CR-39 samples irradiated many hours after having been exposed to high vacuum.

Fig. 10 also shows that the shift in reduced track etch rate goes through a maximum at a temperature around -40°C for CR-39 exposed to nuclei with $22 \leq Z \leq 26$. The results summarized above, together with results by Adams and Beahm [15], show that the event thermometer on HNC needs to record the temperature of CR-39 and Rodyne to within 1°C in order to attain the goal of a charge standard deviation of 0.25e for both the mid-Z nuclei and the actinides. The HNC event thermometer was designed with these requirements in mind. For Cronar a knowledge of temperature to within $\pm 15^\circ\text{C}$ should be sufficient, and in the unlikely event of a total failure of the event thermometer, it should still be possible to use Cronar to obtain the desired charge resolution for nuclei with $Z \geq 78$ recorded on those trays with temperature excursions less than $\sim \pm 20^\circ\text{C}$.

8. Automation of measurements to increase accuracy and remove subjective bias

Figures 11 to 14 give examples of the two types of automated measurement techniques we developed in 1986. The first technique, in which the dimensions of the mouths of conical etchpits are measured, is applicable to normally incident or inclined tracks with $s < 5$. Figure 11 shows (a) the image, digitized by means of a CCD camera, of a field of view containing two circular etchpits due to 800 MeV/nucleon gold ions in a Cronar detector; (b) the gradient image after thresholding; and (c) the superimposed circles that fit the two etchpit mouths best. Figure 12 shows the gradient image of an elliptical etch pit of a 1.8 GeV/nucleon iron ion in CR-39 (DOP) and the superimposed best-fit ellipse. It now takes ~ 1 second per ellipse to automatically find and fit several etchpit mouths in a field of view. If the zenith angle has already been measured, the ellipse data provide an adequate measure of Z/β for cones with $s < 5$. If the zenith angle is not known, the ellipse parameters determine it to within ~ 1 to 20° . To do better one can determine zenith angle from a measurement of sheet thickness together with a measurement of the shift in position of the bottom ellipse with respect to the top ellipse.

The second technique, applicable for cones with $s > 5$, is described in ref. 16 and illustrated in figures 13 and 14. In its fully automated form, a laser autofocus will maintain focus on the top surface until an event is found; then the fine-focus knob will be driven with a motor successively in increments of a few microns to various depths at which the image will be digitized and a pixelwise minimum will be generated between this image and the preceding one. The final image will be a composite of the darkest pixels in each column down through the field of view of the plastic sheet. It will produce a well-focussed two-dimensional image of the three-dimensional etch pit. The next steps will be to produce a gradient image, clean it, find its dimensions, and relate these dimensions to the original three-dimensional cone.

9. Conclusions Regarding Overall Charge Resolution

The Monte Carlo simulations show that inherent detector resolution is adequate to identify cosmic rays over the entire charge region of interest up to the actinide elements and over essentially all energies, provided systematic effects are understood and corrected for. The following systematic effects need to be taken into account:

- a. Thermally activated track-fading, which can be eliminated by maintaining detectors at a temperature below $\sim 0^\circ\text{C}$.
- b. Track-aging, an approximately logarithmic growth of detector sensitivity with time, which occurs only in Rodyne at temperatures somewhat above -16°C . Further study will show whether the aging effect occurs at 0°C , the highest temperature expected on the HNC experiment. If it does, the fractional spread of values of apparent charge for each species could be reduced by aging of Rodyne for at least two years after completion of the mission. During this aging the other detectors could be analyzed.

c. Dependence of detector sensitivity on detector temperature, which can be corrected for by an event thermometer.

d. Sheet-to-sheet variations in detector sensitivity. These variations are likely to cause a problem only for CR-39 sheets, which are cast in a batch process, but not for Rodyne or Cronar sheets, which are made by extrusion in a continuous film. With automated techniques, variations in sensitivity from sheet to sheet can be corrected by measuring a population of minimum-ionizing cosmic ray Fe tracks in each CR-39 sheet. Small variations from sheet to sheet of Rodyne or Cronar can be corrected for by requiring consistency in the response to the numerous platinum-group tracks passing through each stack.

e. Variations in general etch rate from tankload to tankload. This important source of systematic error, which explains fluctuations of groups of data from sheets etched at the same time in the track-aging study, can be eliminated as follows: Using the procedure developed by Fujii et al. (17), we mask one control sheet of each type of plastic with epoxy resin so that a step in sheet thickness develops during etching. The surface of the control sheet is then coated with an evaporated aluminum film. Using a Tolansky multiple-beam interferometry attachment, we measure the step height by observing the displacement of the interference fringes. This permits V_G to be measured to much better than 1% for each batch of etched samples.

f. Systematic measurement errors. We have found that automation removes sources of systematic error due to observer fatigue or long-term drift in criteria. Using a CCD camera instead of a Vidicon, we have seen no variation of response with location in the field of view. The gradual accumulation of dirt in etched cones in the sample that is left on a microscope stage for a long time, and the presence of incompletely removed etch products in etched cones of some detectors, can be eliminated by adhering to rigorous standards of cleanliness such as are routine in the semiconductor industry. The room designated for measurements, and its occupants, must follow the same protocol used in the semiconductor industry.

10. Summary

a. If systematic errors, track fading and track aging are negligible, if the event thermometer works, and if errors with automation are as small as expected, then --

- 1) $\sigma_Z \leq 0.25$ for nuclei with $Z \geq 70$ in the actinide stacks except in one energy interval around 4 GeV/nucleon.
- 2) $\sigma_Z \leq 0.25$ for mid-Z nuclei in the mid-Z stacks except in the same energy interval.
- 3) Satisfactory measurements can be made of actinide nuclei in the mid-Z stacks.

- 4) Mid-Z nuclei can be studied in the actinide stacks with high resolution only at energies below ~ 1 GeV/nucleon.
- b. Track fading is negligible at $T \leq 0^\circ\text{C}$.
 - c. Track aging may not occur at $T \leq 0^\circ\text{C}$.
 - d. The event thermometer is essential for the successful use of Rodyne and CR-39. Useful data could be obtained with Cronar if the event thermometer were to fail.
 - e. Expected sheet-to-sheet variations in sensitivity can be corrected for with automation (minimum-ionizing Fe tracks in CR-39; minimum ionizing Pt tracks in Rodyne and Cronar).
 - f. The value of V_G for each tankload can be measured to $<1\%$ by Tolansky interferometry.
 - g. Automation, image processing techniques, and cleanroom conditions can ensure maintenance of a single-cone standard deviation about half that achieved to date.

References

1. G. Tarlé, S.P. Ahlen and P.B. Price, *Nature* 293, 556 (1981).
2. P.B. Price, M.L. Tincknell, G. Tarlé, S.P. Ahlen, K.A. Frankel and S. Perlmutter, *Phys. Rev. Lett.* 50, 566 (1983).
3. M.H. Salamon, J. Drach, Shi-lun Guo, P.B. Price and G. Tarlé, *Nucl. Instr. Meth.* 224, 217 (1984).
4. M.H. Salamon, P.B. Price, M. Tincknell, Shi-lun Guo and G. Tarlé, *Nucl. Instr. Meth.* B6, 504 (1984).
5. Shi-lun Guo, J. Drach, P.B. Price, M.H. Salamon, M.L. Tincknell, S.P. Ahlen and G. Tarlé, *Nucl. Tracks* 9, 183 (1984).
6. J. Drach, P.B. Price and M.H. Salamon (Cronar resolution), to be published.
7. E.K. Shirk and P.B. Price, *Ap. J.* 220, 719 (1978).
8. M.H. Salamon, P.B. Price and J. Drach (annealing), submitted to *Nucl. Instr. Meth.* (1986).
9. P.B. Price, M.H. Salamon and J. Drach (track-aging), to be published.
10. D. O'Sullivan and A. Thompson, *Nucl. Tracks* 4, 271 (1980).
11. D. O'Sullivan, A. Thompson, J.A. Adams and L.P. Beahm, *Nucl. Tracks* 8, 143 (1984).
12. A. Thompson and D. O'Sullivan, *Nucl. Tracks* 8, 567 (1984).
13. A. Thompson, D. O'Sullivan and C. Domingo, preprint.
14. J. Drach, P.B. Price and M.H. Salamon (effect of temperature and oxygen pressure on sensitivity of CR-39, Rodyne and Cronar track detectors), to be published.
15. J.H. Adams and L.P. Beahm, preprint.
16. P.B. Price and W. Krischer, *Nucl. Instr. Meth.* A234, 158 (1985).
17. M. Fujii, J. Nishimura and T. Kobayashi, *Nucl. Instr. Meth.* 226, 496 (1984)
18. J. Drach, Ph.D. thesis, University of California, Berkeley, February, 1987.

Table 1. Attainment of High Charge Resolution

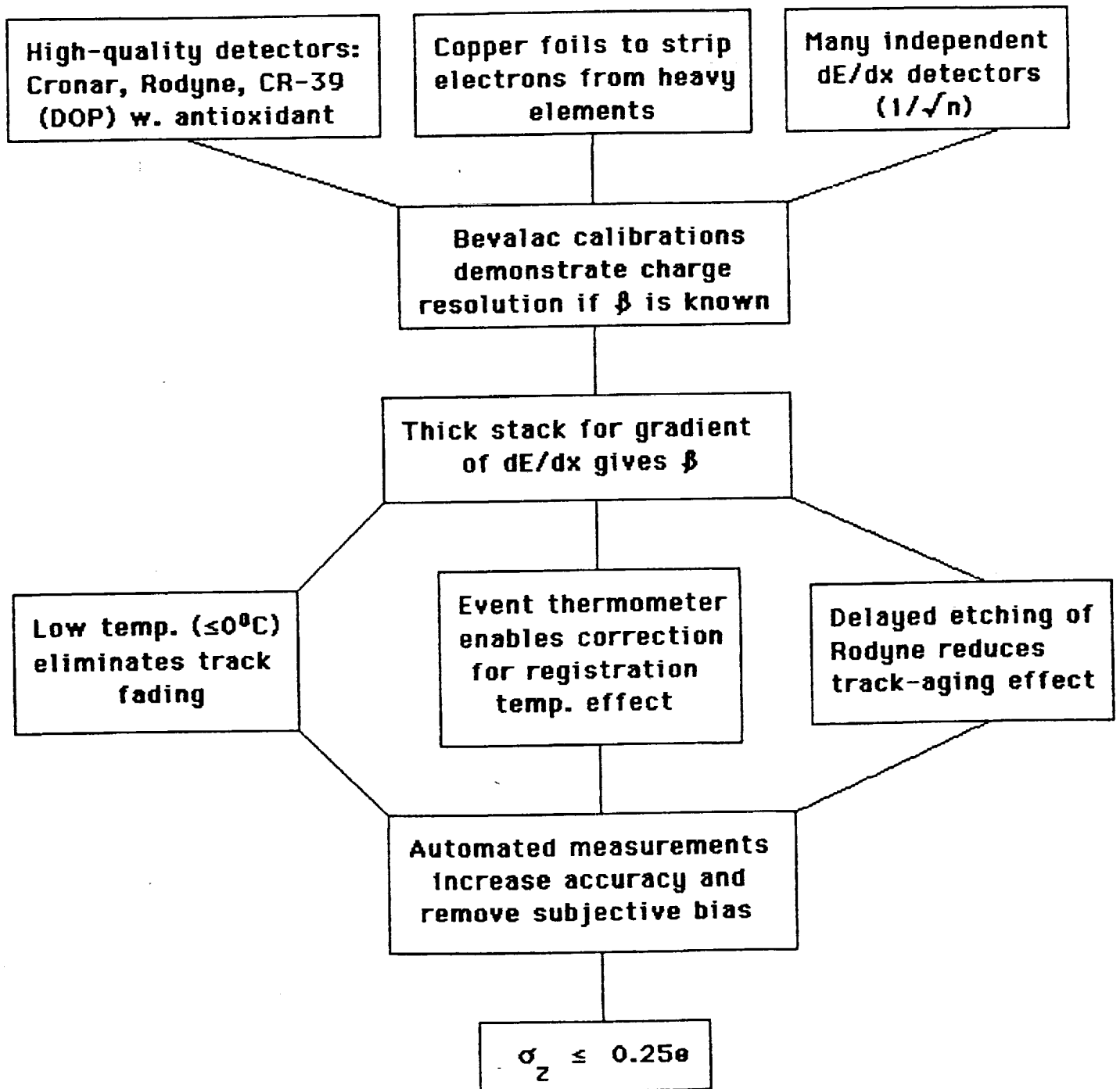


Table 2. Monte Carlo Calculations of Charge Standard Deviations for Particles with Unknown Velocities Detected in HNC

I. Actinide stack; aging effect neglected; conservative measurement errors taken from refs. 4 to 7.

		Energy (GeV/nucleon)					
		0.5	0.7	1	2	4	8
		<u>Z = 92</u>					
full thickness	skeleton	0.10	0.10	0.40	0.82	1.03	0.50
	Cronar	0.13	0.14	0.19	0.45	0.72	0.35
	Rodyne	0.13	0.12	0.23	0.54	0.77	0.34
	all	0.12	0.14	0.17	0.38	0.54	0.26

half thickness	Cronar	0.43		0.60	0.92	1.28	0.69
	Rodyne	0.54		0.59	1.00	1.17	0.64
	all	0.34		0.47	0.81	1.03	0.62

		<u>Z = 79</u>					
full thickness	skeleton	0.17	0.16	0.30	0.69	0.91	0.40
	Cronar	0.13	0.11	0.18	0.38	0.67	0.25
	Rodyne	0.13	0.13	0.20	0.46	0.69	0.30
	all	0.13	0.11	0.15	0.31	0.54	0.20

half thickness	Cronar	0.27		0.58	0.90	0.92	0.56
	Rodyne	0.33		0.54	0.93	1.02	0.58
	all	0.22		0.41	0.69	0.80	0.53

		<u>Z = 70</u>					
full thickness	skeleton	0.11	0.11	0.29	0.60	0.81	0.33
	Cronar	0.13	0.15	0.17	N/A	N/A	N/A
	Rodyne	0.13	0.17	0.22	0.43	0.63	0.25
	all	0.13	0.14	0.14	N/A	N/A	N/A

half thickness	Cronar	0.26		0.53	N/A	N/A	N/A
	Rodyne	0.23		0.49	0.89	0.81	0.50
	all	0.17		0.40	N/A	N/A	N/A

Table 2. (cont.)

II. Actinide stack; aging effect neglected; measurement errors assumed to be reduced by 50% by processing the entire image.

		Energy (GeV/nucleon)					
		0.5	0.7	1	2	4	8
		Z = 92					
full thickness	skeleton	0.10	0.10	0.21	0.41	0.67	0.37
	Cronar	0.12	0.14	0.11	0.22	0.44	0.24
	Rodyne	0.10	0.14	0.13	0.28	0.50	0.26
	all	0.11	0.14	0.07	0.22	0.35	0.22

half thickness	Cronar	0.25		0.38	0.57	0.78	0.55
	Rodyne	0.31		0.35	0.68	0.89	0.49
	all	0.21		0.25	0.41	0.60	0.49
		Z = 79					
full thickness	skeleton	0.15	0.16	0.19	0.27	0.60	0.33
	Cronar	0.18	0.14	0.09	0.22	0.30	0.21
	Rodyne	0.16	0.13	0.12	0.27	0.40	0.23
	all	0.13	0.13	0.08	0.19	0.25	0.21

half thickness	Cronar	0.16		0.34	0.52	0.57	0.47
	Rodyne	0.20		0.31	0.60	0.63	0.44
	all	0.10		0.23	0.40	0.47	0.43
		Z = 70					
full thickness	skeleton	0.13		0.17	0.24	0.45	0.27
	Cronar	0.14		0.10	N/A	N/A	N/A
	Rodyne	0.12		0.12	0.23	0.28	0.20
	all	0.11		0.07	N/A	N/A	N/A

half thickness	Cronar	0.16		0.32	N/A	N/A	N/A
	Rodyne	0.12		0.26	0.51	0.54	0.38
	all	0.10		0.20	N/A	N/A	N/A

14 sh 0.2cm
VG-13

14 sh 2mm
VG-13

Table 2. (cont.)

III. Mid-Z stack; conservative measurement errors taken from refs. 4 to 7.

		Energy (GeV/nucleon)					
		0.5	0.7	1	2	4	8
		<u>Z = 51</u>					
full	skeleton CR-39	0.13		0.42	1.05	0.74	0.49
thickness	all CR-39	0.13	0.17	0.22	0.40	0.44	0.21
		<u>Z = 92</u>					
full	skeleton	0.12	0.12	0.39	0.82	1.13	0.56
	Cronar	0.13	0.14	0.27	0.55	0.96	0.44
thickness	Rodyne	0.11	0.13	0.32	0.64	0.98	0.50
	all	0.11	0.15	0.20	0.40	0.66	0.34

IV. Actinide stack; conservative measurement errors (ref. 4).

		Energy (GeV/nucleon)					
		0.5	0.7	1	2	4	8
		<u>Z = 51</u>					
full	all CR-39	0.13	0.24	0.33	0.77	0.59	0.39
thickness							

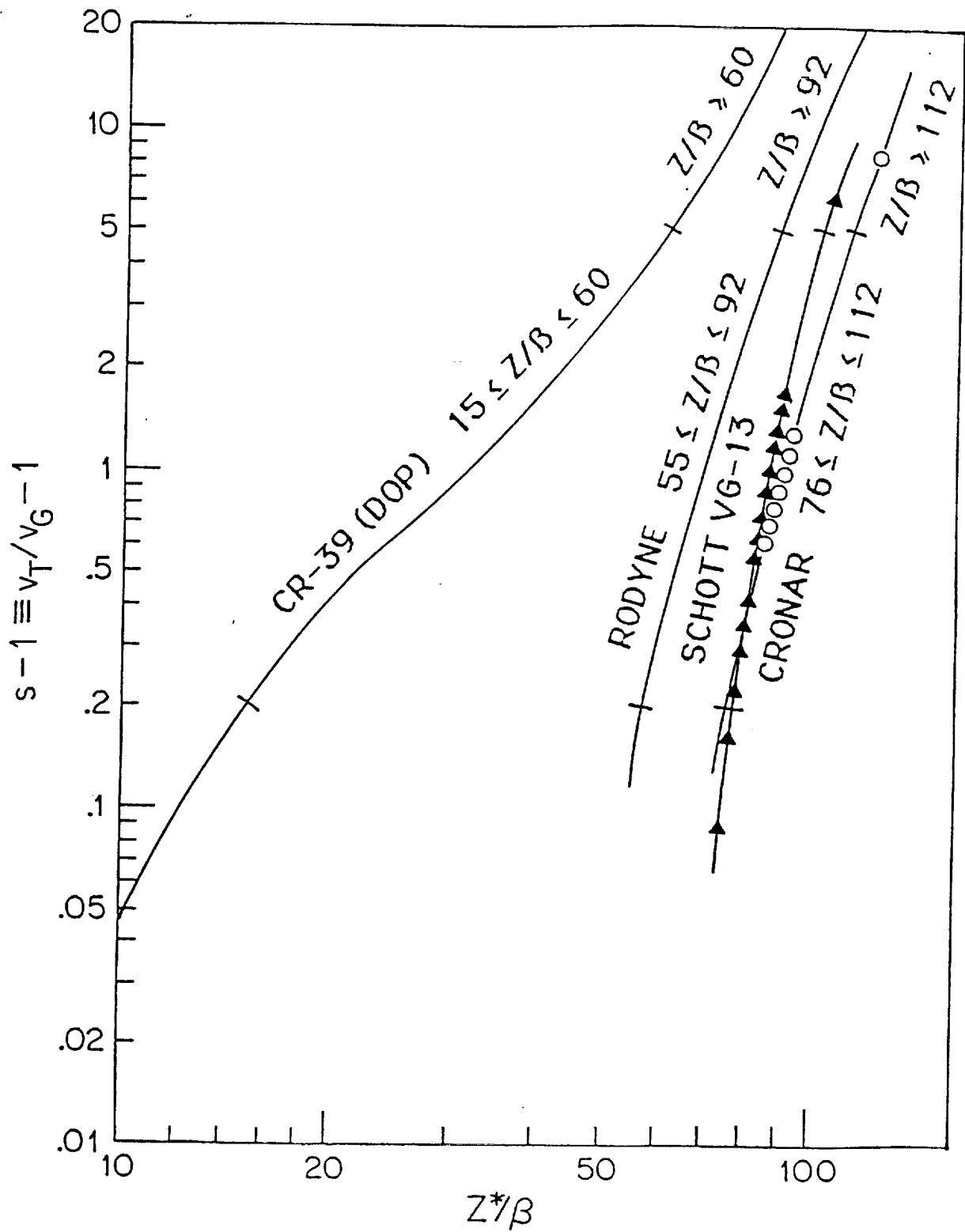


Fig. 1. Sensitivity of various types of track detectors as a function of Z/β . The tick marks indicate intervals where measurements of elliptical etch pit mouths provide the best measure of Z/β ($0.2 < s-1 < 5$) and where measurements of cone lengths give the best measure of Z/β ($s-1 > 5$).

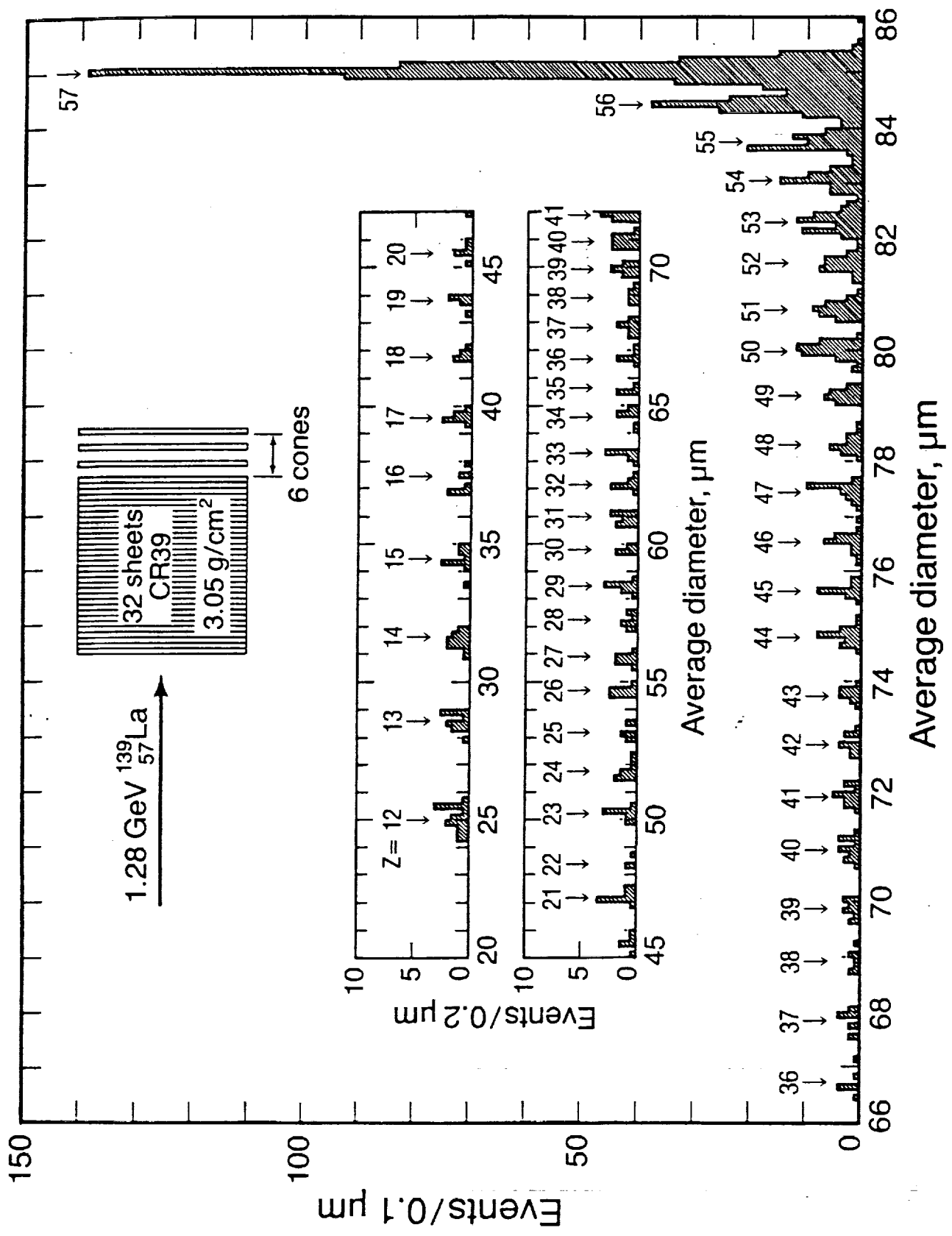


Fig. 2. Fragmentation of 1.28 GeV/N ^{139}La ($Z = 57$) in CR-39(DOP).

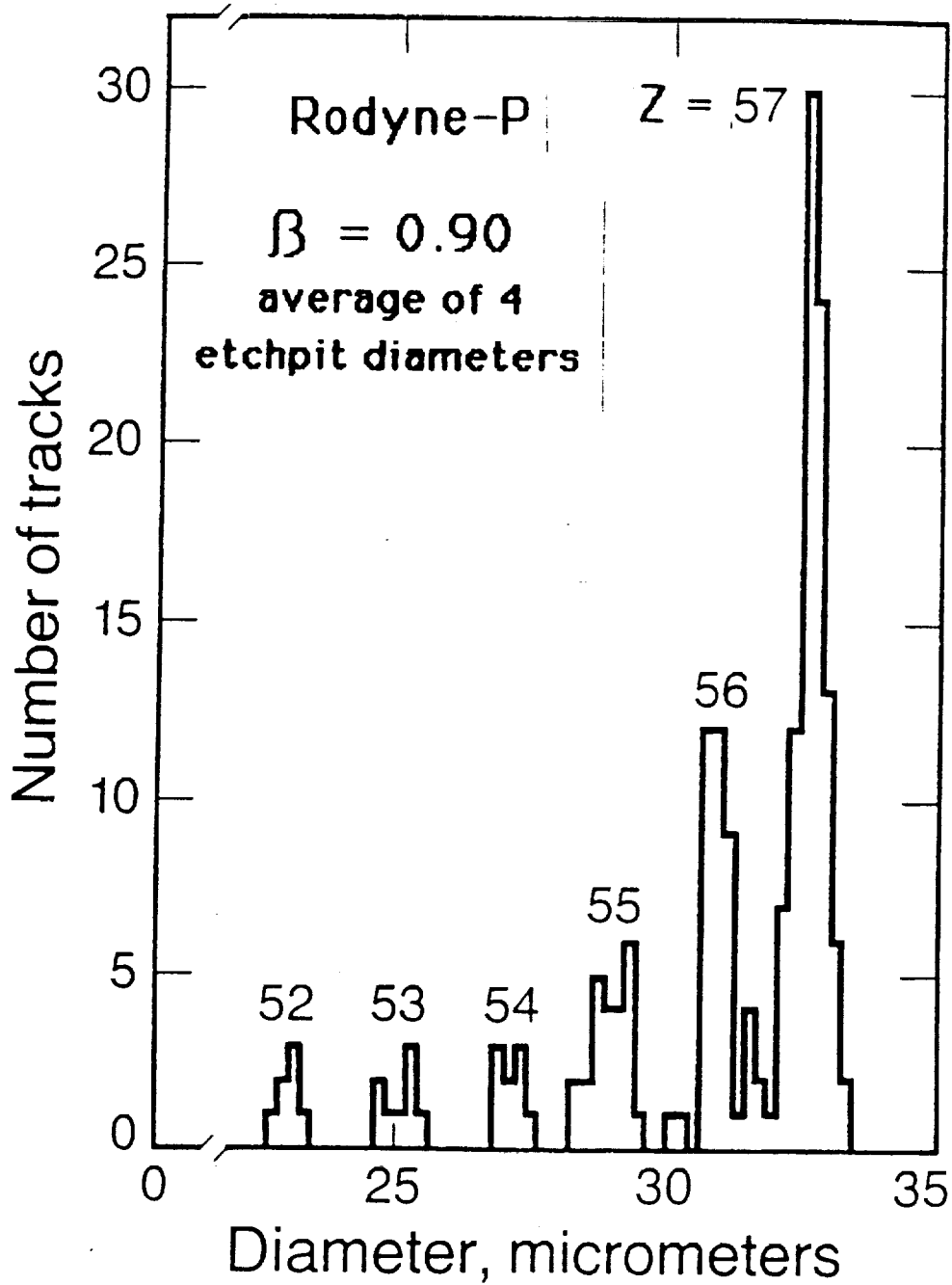


Fig. 3. Fragmentation of 1.28 GeV/N ^{139}La ($Z = 57$) in Rodyne.

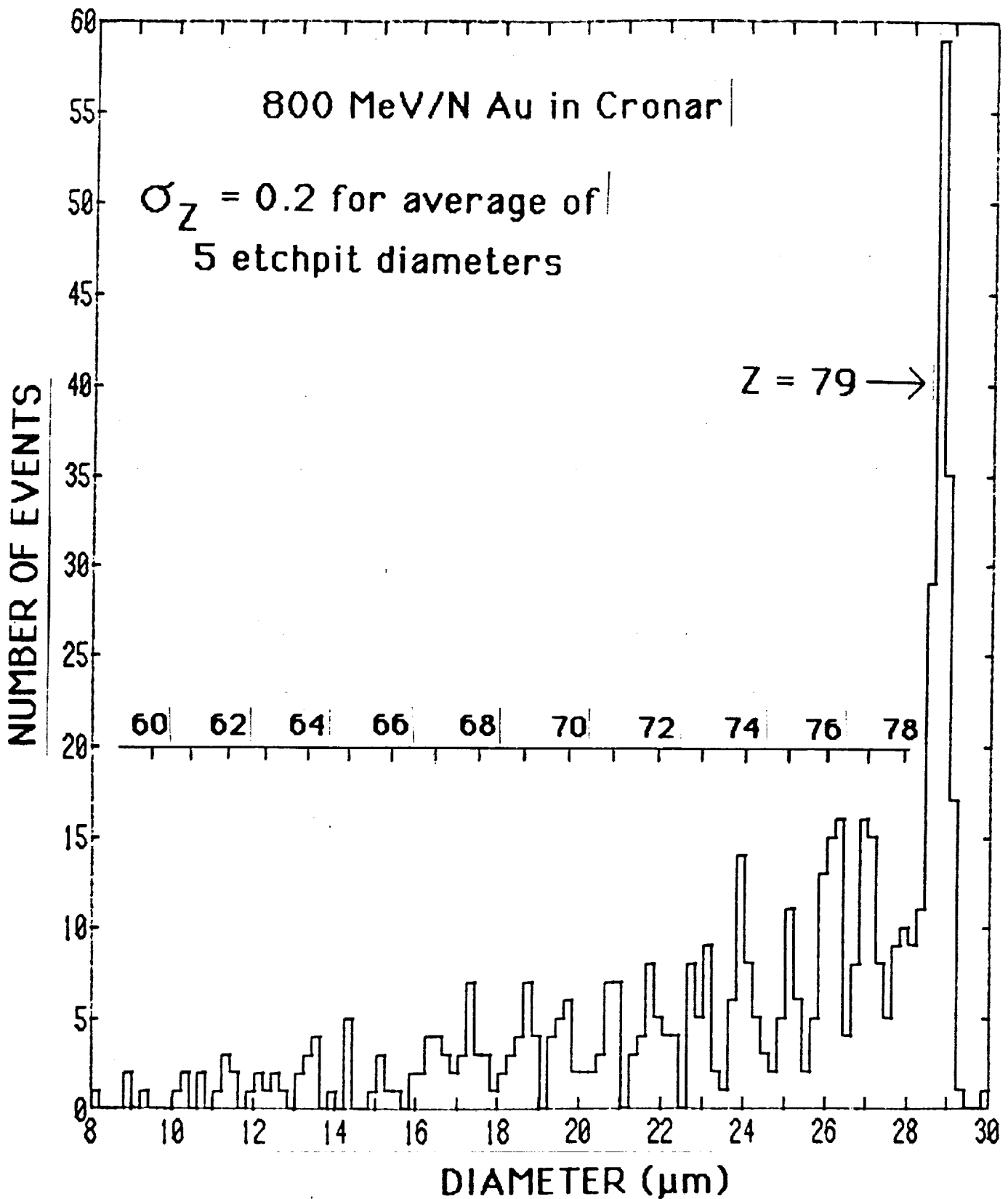


Fig. 4. Fragmentation of 1 GeV/N ^{197}Au ($Z = 97$) in a thick polyethylene target, followed by detection of projectile fragments with energy ~ 800 MeV/N in Cronar.

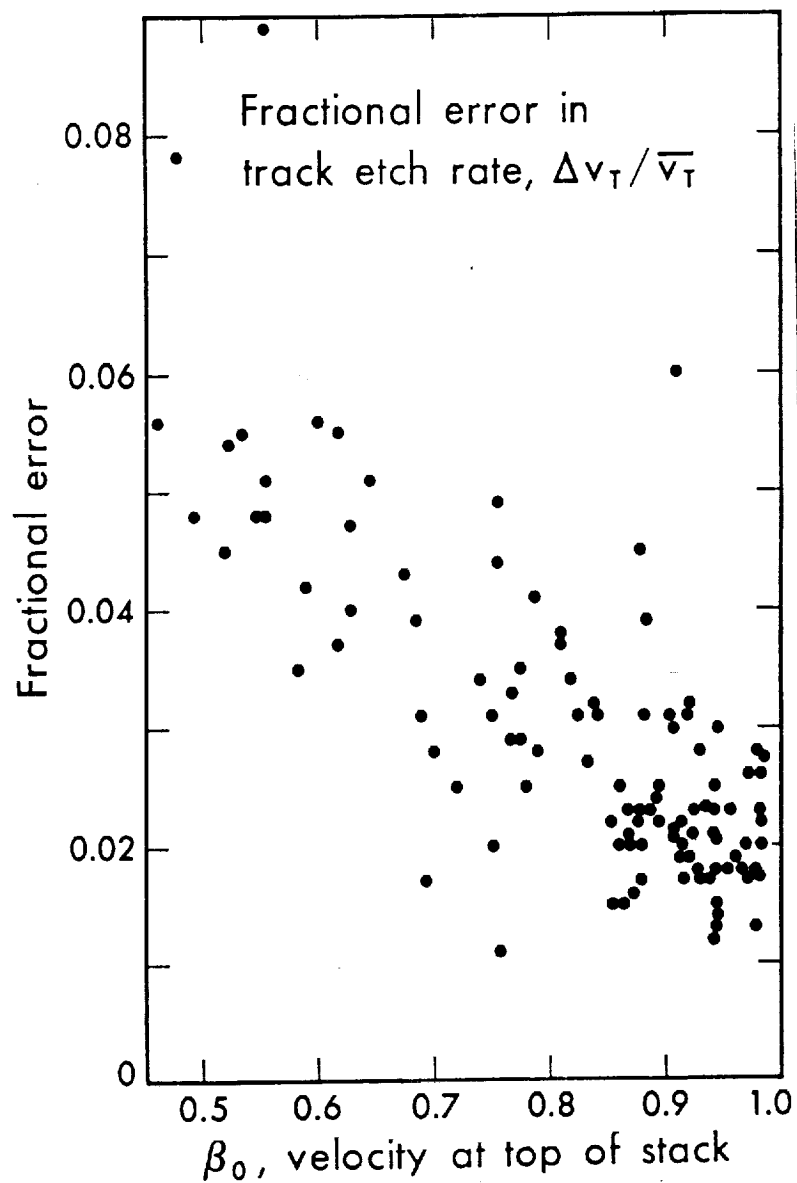


Fig. 5. Fractional standard deviation in track etch rate obtained for events with $Z > 65$ in Lexan stack on Skylab (Shirk and Price, *Ap. J.* **220**, 719 (1978)).

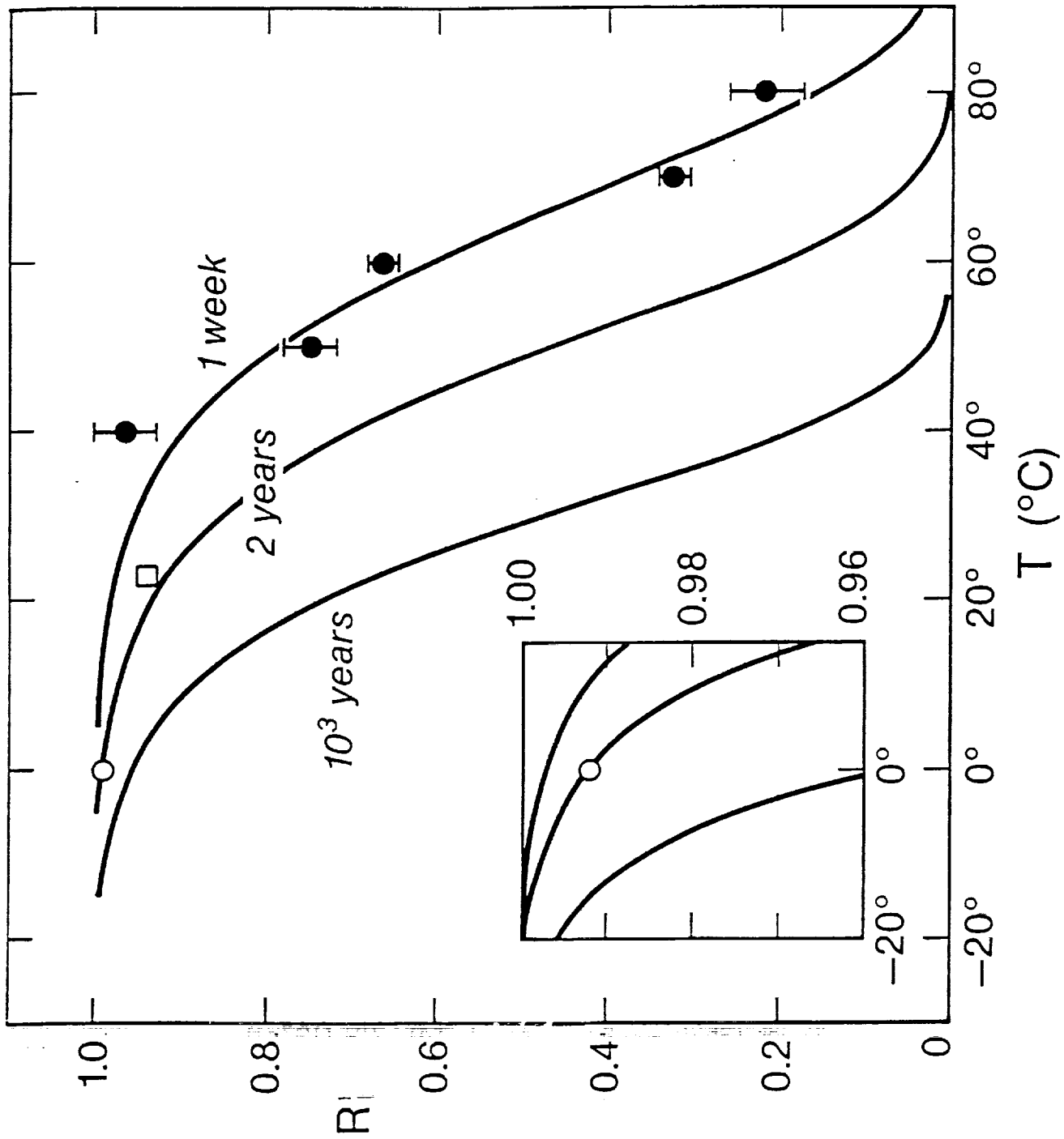


Fig. 6. Annealing of tracks with $Z/\beta \sim 120$ in Roddyne.

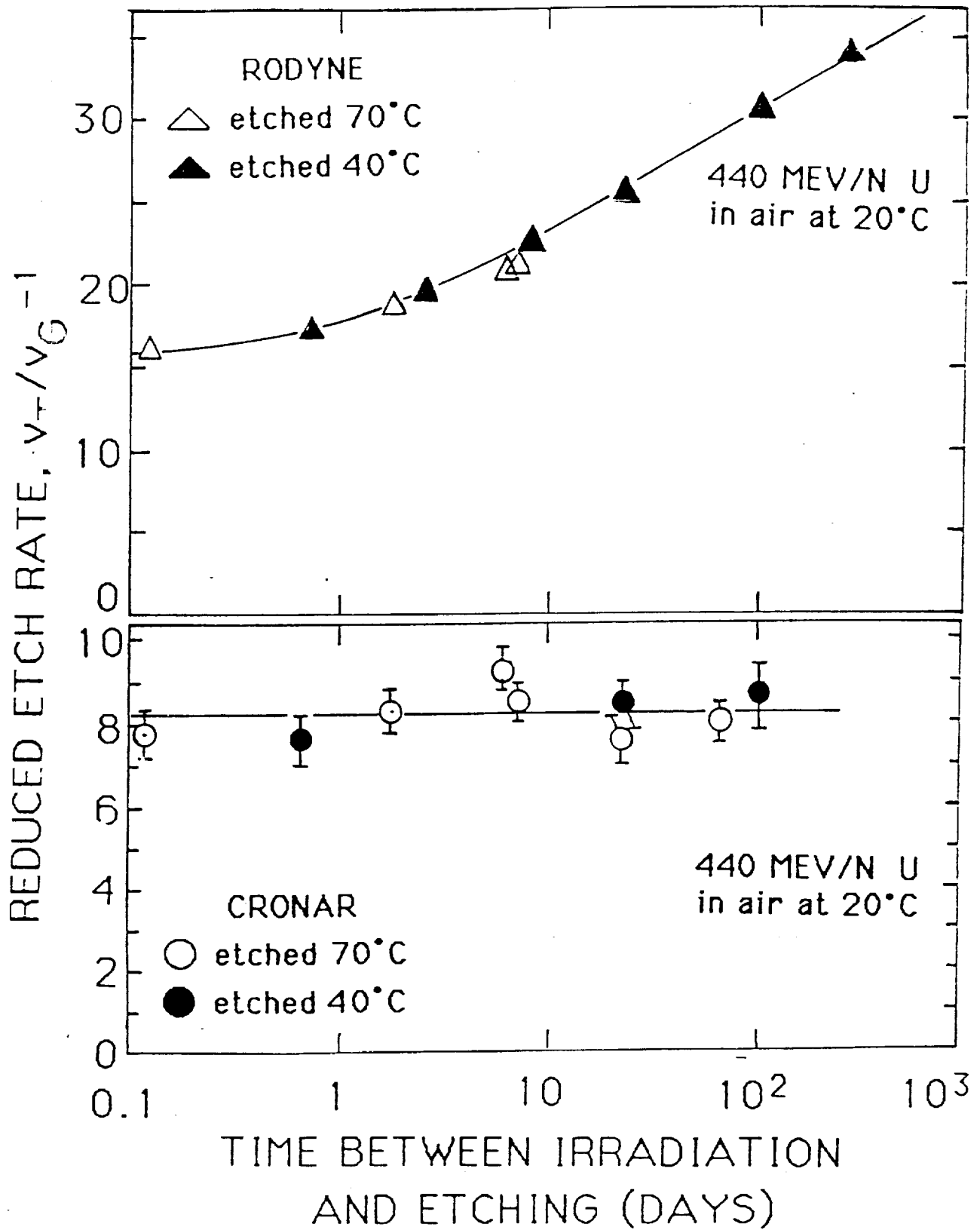
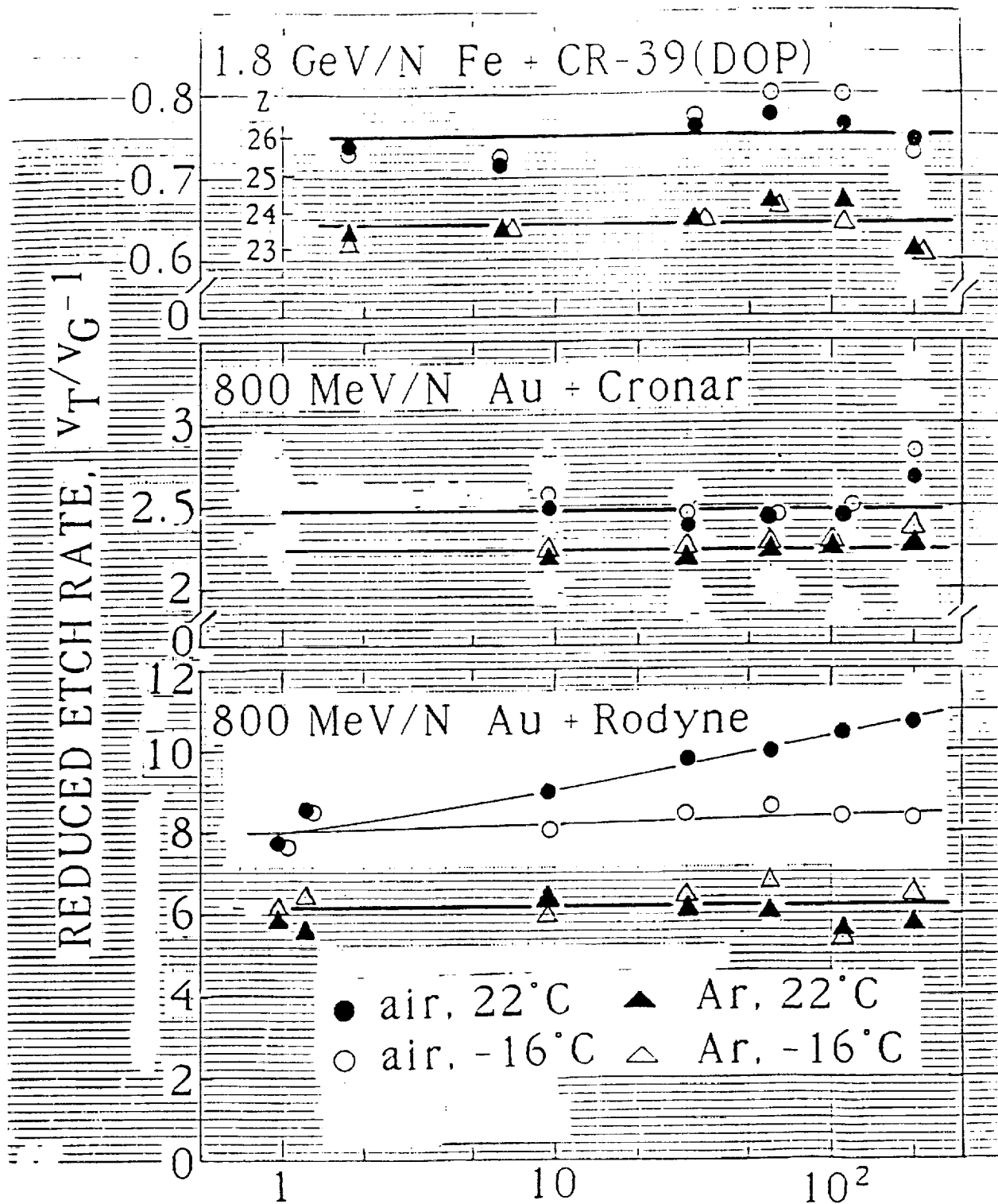


Fig. 7. Track-aging study for Rodyne and Cronar irradiated in air at 20°C with 440 MeV/N U ions.



TIME BETWEEN IRRADIATION AND ETCHING (DAYS)

Fig. 8. Track-aging results for detectors irradiated at 22°C in air or in argon, then aged at 22°C or -16°C in air or argon, and etched in 6.25N NaOH at 40°C.

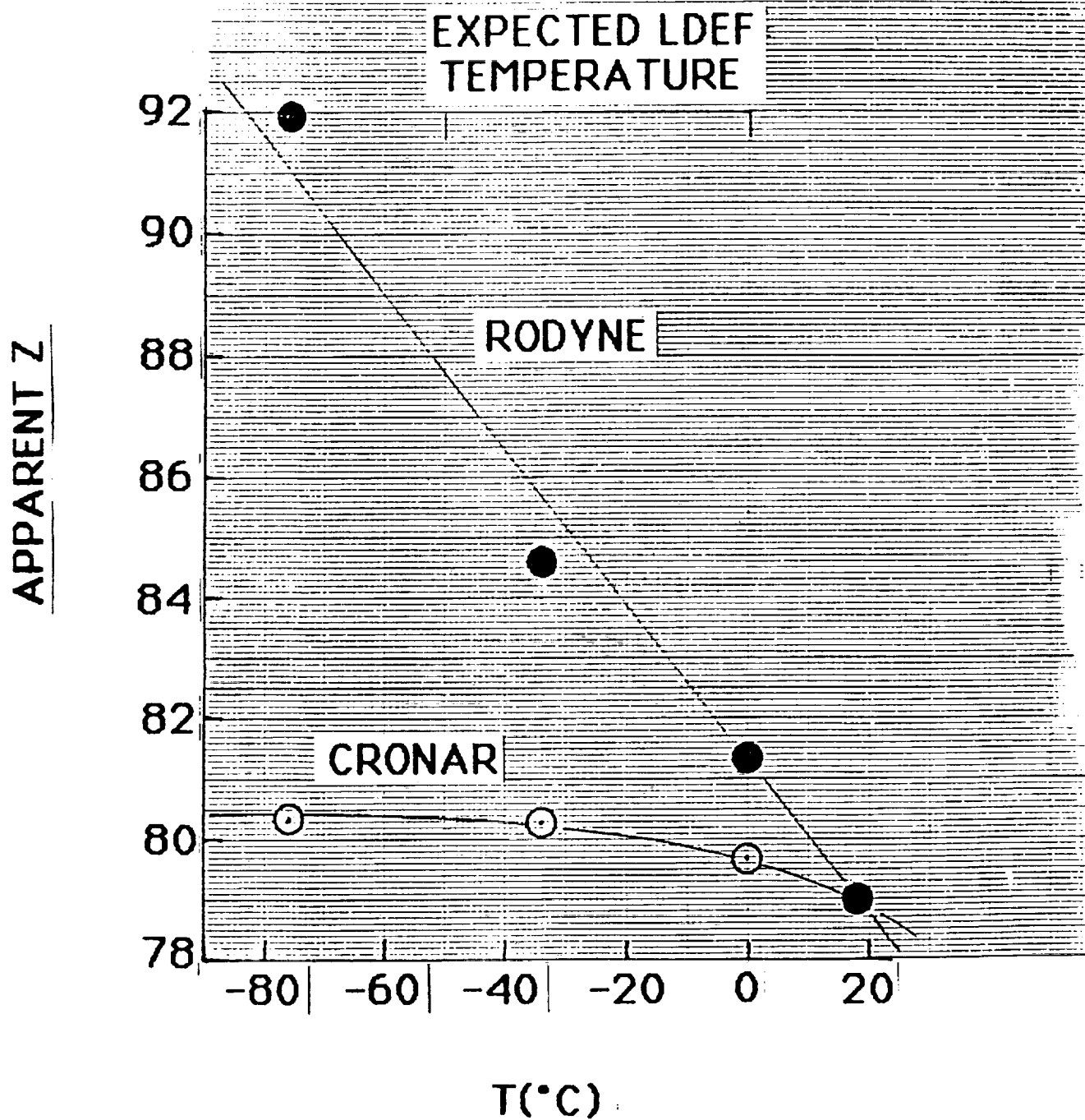


Fig. 9 Dependence of detector sensitivity on temperature at the time of track registration, expressed in terms of apparent charges of 800 MeV/N Au ($Z = 79$) ions.

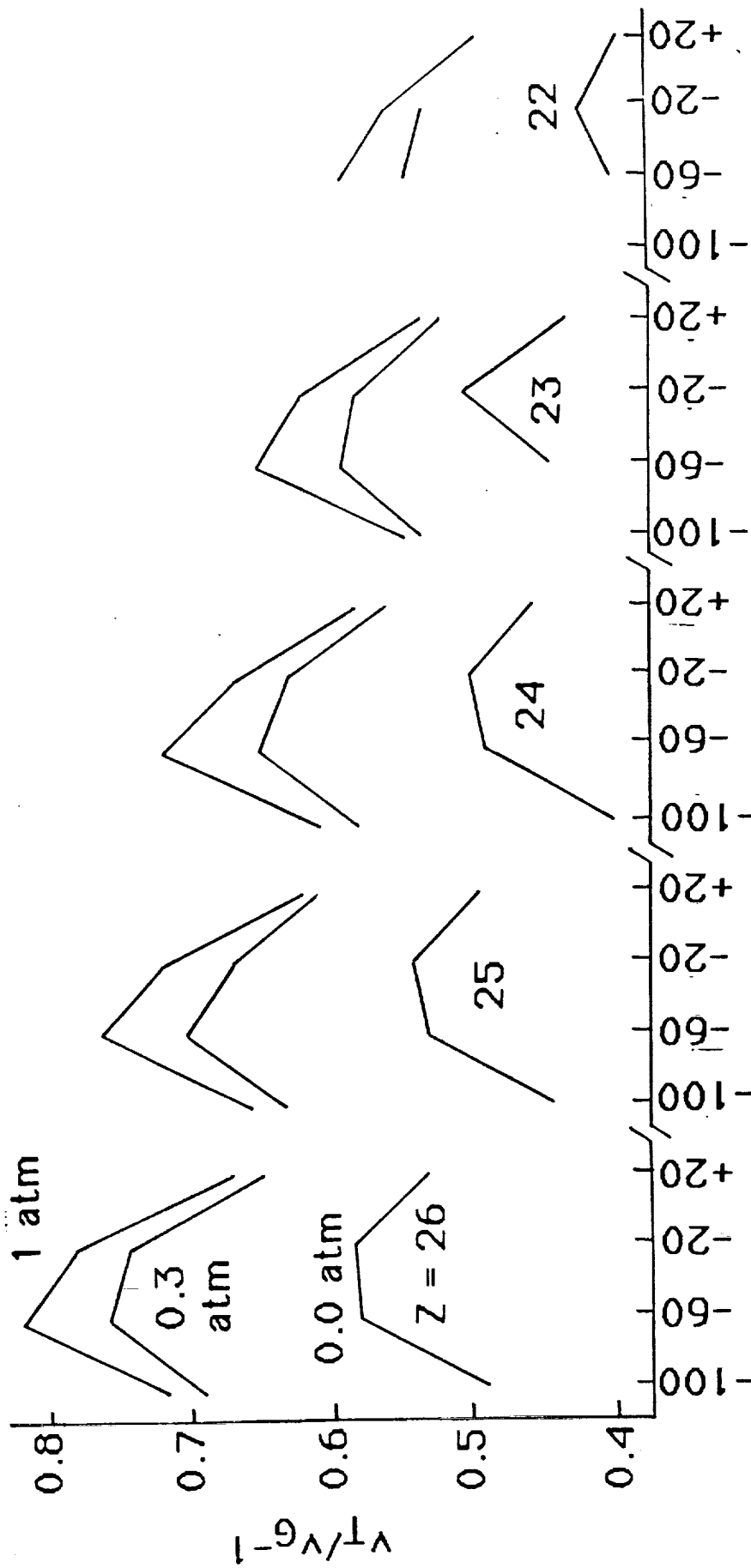
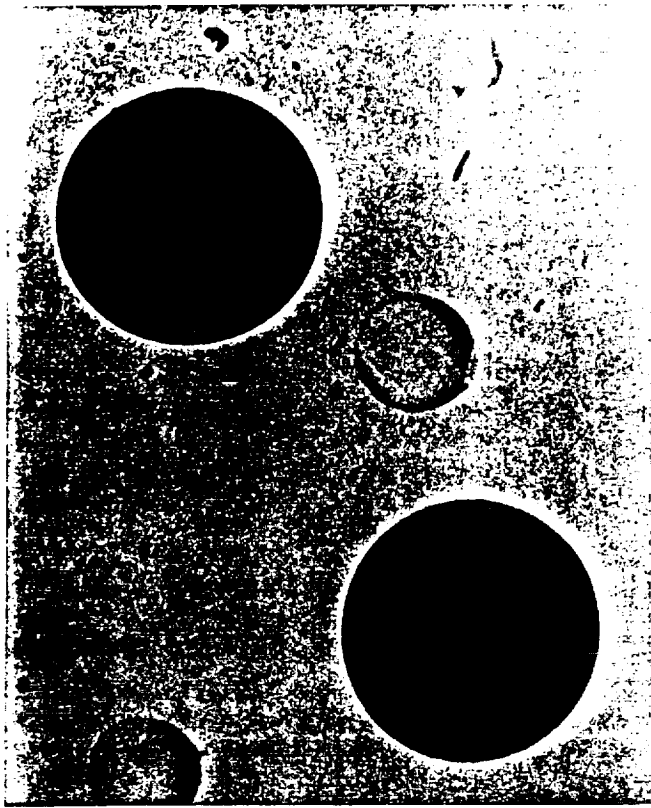
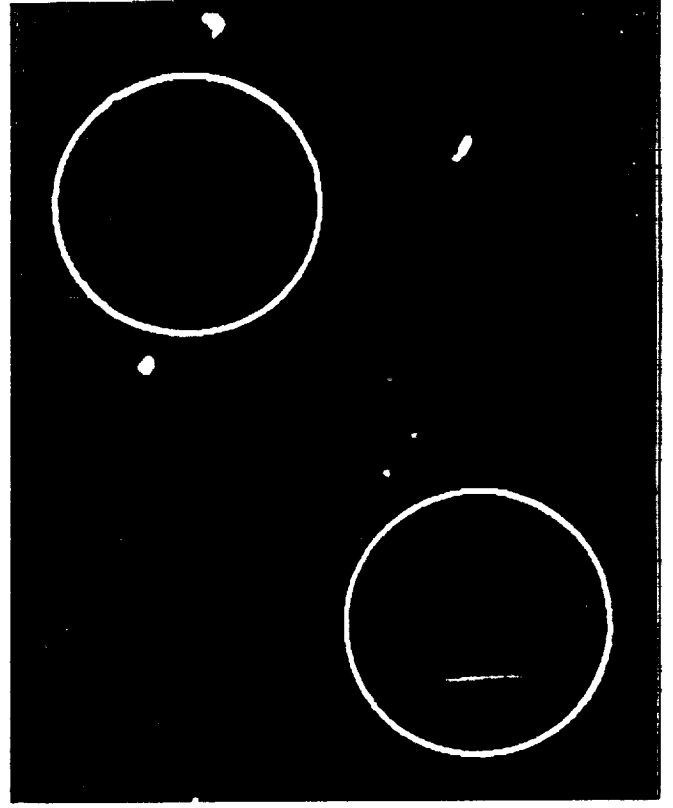


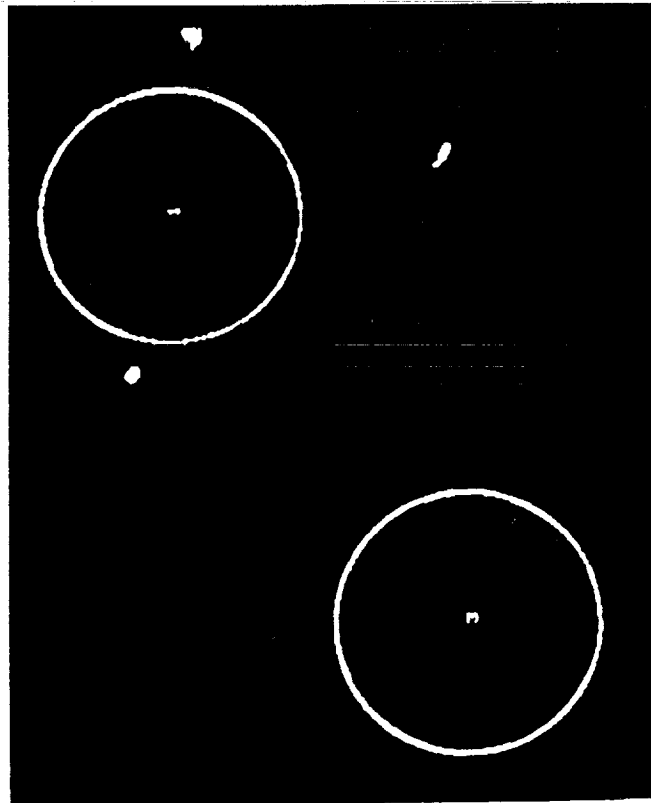
Fig. 10. Effects of air pressure and temperature on response of CR-39(DOP) to 1.8 GeV/N Fe nuclei and its projectile fragments.



(a)



(b)



(c)

Fig. 11. Steps in the analysis of circular etchpits: (a) digitized image; (b) thresholded binary image using an edge-detection algorithm; (c) superimposed best-fit circles.

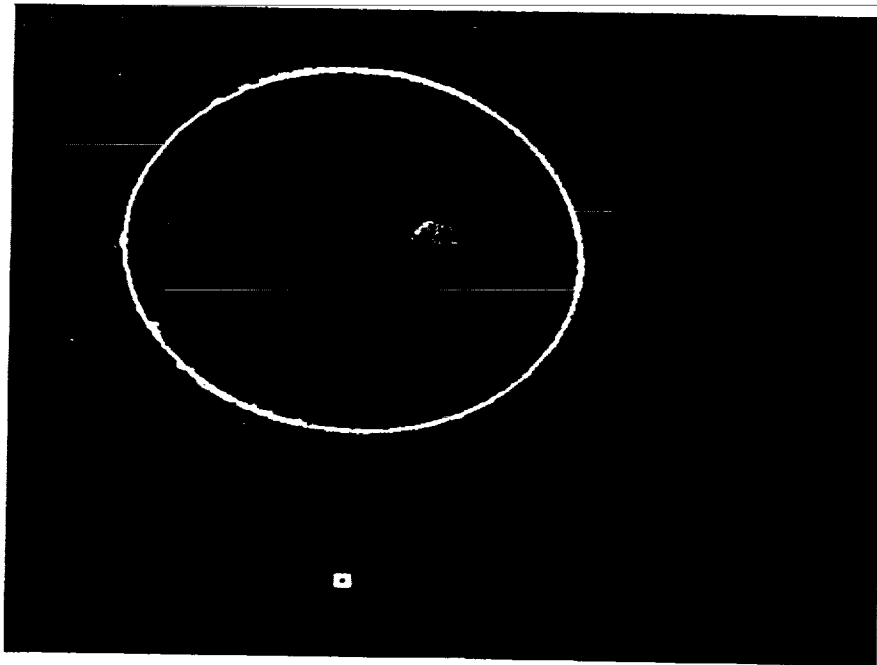


Fig. 12. Comparison of digitized binary image of edge of elliptical etchpit and superimposed best-fit ellipse.

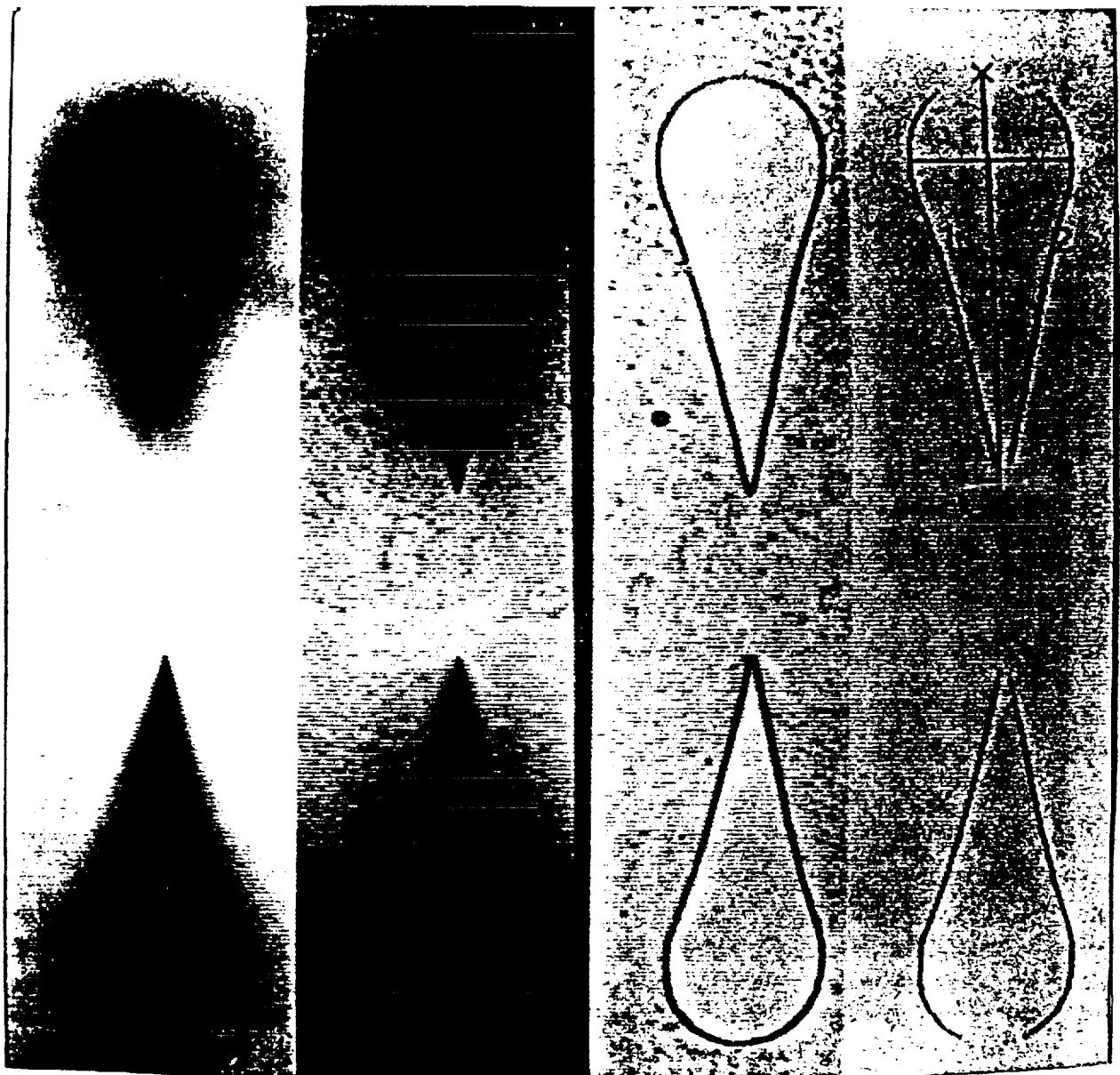


Fig. 13. Steps in the analysis of pair of conical etchpits using Krischer-Price minimization algorithm (ref. 16).

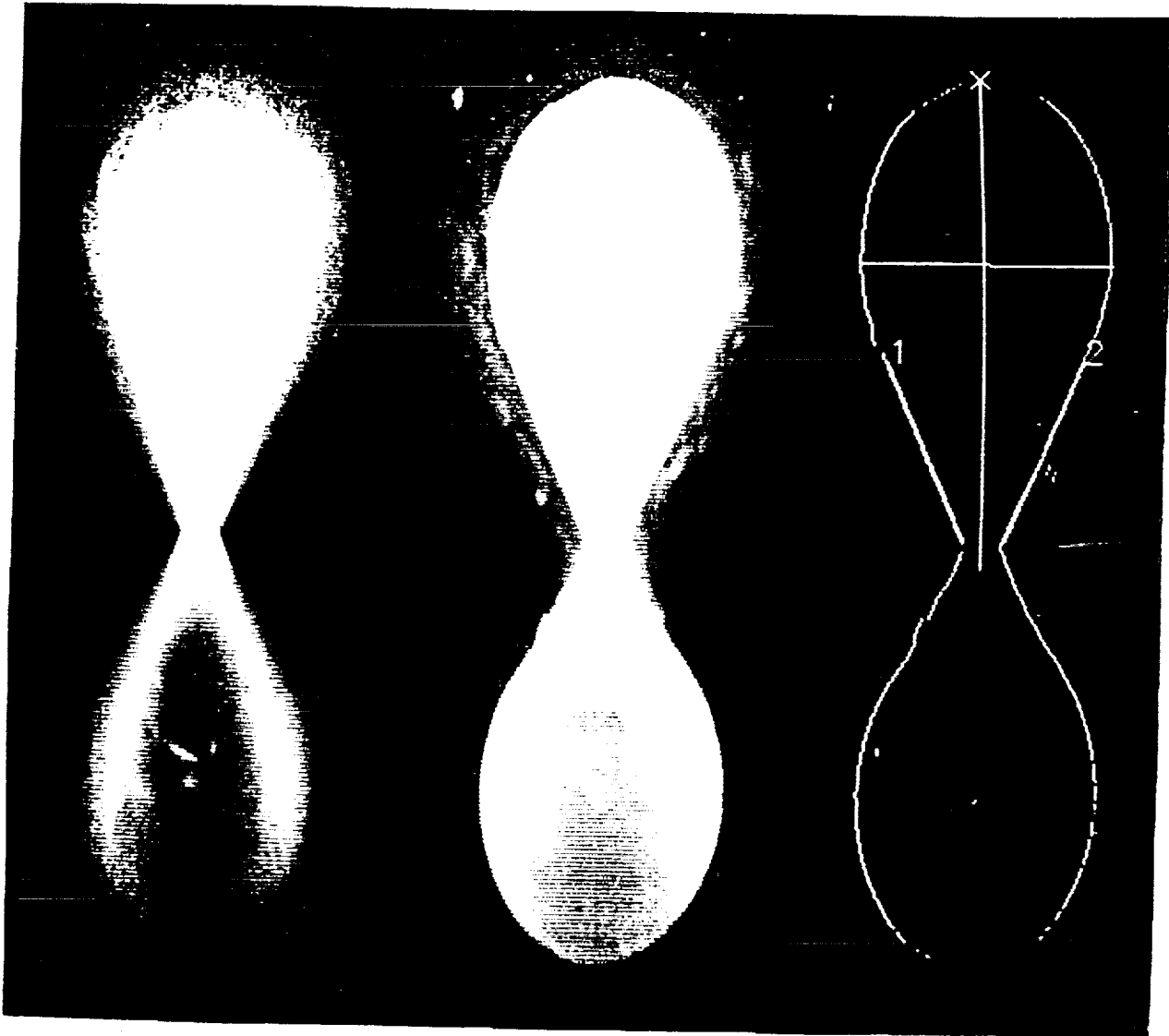


Fig. 14. Steps in the analysis of pair of connected etchpits using Krischer-Price algorithm (ref. 16).

Document 2:

Flowchart for HNC Postflight Processing and Data Analysis

P. B. Price

1. Introduction

In this document we amplify on the flowchart shown as Fig. 1. Since at least four years will elapse before the detectors are returned from orbit for processing and analysis, the final plan will involve more highly automated measuring techniques and more sophisticated computing techniques than are suggested below. The composition of the two types of stacks may undergo minor changes in the next few weeks, and the plan outlined below will certainly evolve in response to input from the steering committee and to our ongoing studies.

2. Protocol for detector storage and handling

As Table 1 shows, each of the 41 actinide trays consists of four modules containing 56 Cronar layers, 44 Rodyne layers, and 14 CR-39 layers -- a total of $456 \times 41 = 18696$ sheets. Polymers of like composition are grouped together to reduce transfer of additives that might alter the chemical response of another type of polymer. To exploit charge-stripping, Cronar and Rodyne are put immediately downstream from copper foils except near the beginning of each stack, where in order to identify very low-energy nuclei that do not penetrate far it would be desirable to have a number of consecutive plastic layers. The primary function of CR-39 in the actinide trays is to identify fission fragments and other fragmentation modes of actinide nuclei. A secondary function is to increase the statistics on rare mid-Z nuclei by an order of magnitude beyond that attainable with the mid-Z trays.

Each of the four mid-Z trays (Table 2) consists of four modules containing 27 Cronar layers, 28 Rodyne layers, and 47 CR-39 layers -- a total of $408 \times 4 = 1632$ sheets. In these trays the greater number of CR-39 sheets per module at the expense of Cronar and Rodyne should give high charge resolution of nuclei with $Z \leq 60$. There is sufficient Cronar and Rodyne to distinguish actinides from lighter nuclei. See the document on "Attainment of High Charge Resolution" for results of Monte Carlo simulations performed by J. Drach.

It is absolutely essential to drill accurate alignment holes through the four corners of each of the four stacks in each tray before disassembling them for storage and etching. Only if this is done will it be feasible to scan automatically for aligned etchpit pairs in "trigger layers" and thus locate high-Z events.

A major problem in HNC data analysis will be to keep track of the locations and treatments of all of the 20,328 plastic detector sheets as well as of the much greater number of small squares of plastic that might be cut out of the big sheets for individually tailored etch times. With an expected ~5000 events with $Z \geq 70$, which penetrate up to 114 plastic layers, we would in principle have to keep track of up to 5×10^5 squares of

plastic. (If mid-Z events are included, the number of squares would be well over a million.) The density of events with $Z \geq 70$ is expected to be about one per 60 cm². If each square has an area of 25 cm², then about 40% of the area of each sheet would be cut into small squares. Although this procedure was successfully used in the 1975 Skylab experiment, with a total detector area of 1.2 m², we regard it as impractical for the HNC experiment, and we favor a different procedure in the following document. Dealing with a mere 20,000 uncut sheets will still require that careful attention be paid to record-keeping. We propose to use a giant spreadsheet in a computer to record every operation performed on every sheet, as well as the location of every sheet at all times. Prior to etching, Cronar and CR-39 should be stored at -16 deg C and Rodyne should be stored at 0 to 10 deg C, as justified in a later section.

3. Skeleton etch of Rodyne for scanning and rough Z, β measurements

a) Etching facility

We propose to use four etch tanks, each of which will hold four stainless steel racks of 20 13" X 21" plastic sheets with 0.5" spacing for a total of 320 sheets per batch. All etching will be done in 6.25 N NaOH at 40 deg C. The etching room will be equipped with fume collectors to remove toxic vapors generated during etching of CR-39.

b) Test etch of one sheet of CR-39

Before beginning the Rodyne etch, we propose to etch one sheet of CR-39 to find out if the density of background etch pits from interactions of trapped protons in the plastic and from solar flare particles is low enough to make location and identification of mid-Z nuclei possible. If so, we will proceed with the plan discussed below. If the density of background etch pits is too high to use the CR-39, we will follow one of the alternative plans discussed in sections 8 a and b.

b) Skeleton etch of Rodyne

Nine layers of Rodyne will be taken from locations in the 41 trays marked in Table 1, and eight layers from locations in the 4 trays marked in Table 2, and etched in five batches each requiring 5 days of etching plus ~1 week of pre-etch and post-etch preparation. Total time = 60 days for these 1604 13" X 21" sheets.

c) Computer-controlled scan for sextets

The following discussion is based on the assumption that all 28 Cu sheets will be installed in the actinide stacks. If not, minor changes must be made in the location of the trigger sheets for locating high-Z events. We have investigated two approaches: In the first approach, the top three of the Rodyne skeleton etch layers, each originally separated by 1.42 mm or 0.6 g/cm² in the stack, would be carefully aligned, superimposed with glycerol coatings on all surfaces for optical coupling, scanned on a computer-controlled digitized stage, and viewed through a

3.2X objective with a CCD camera attached to an image processor that digitizes each field of view. The depth of field with a 3.2X objective is such that all six etch pits for a penetrating high-Z event would be approximately in focus. In collaboration with W. Krischer (CERN), we are investigating various fast algorithms for locating an approximately aligned array of three tracks forming a sextet of cones or a combination of cones and cylinders. We have considered an edge-detecting algorithm and various forms of skeletonization that convert a projected cone into a single line along the major axis. In this work we have been using Lexan sheets from the Skylab experiment. Of course, the density of tracks of slow iron-group nuclei that record only in one of the three layers will be much higher than in Skylab. Using the Monte Carlo calculation of Jim Adams for particles with $Z/\beta > 78$ and residual range $> 500 \mu\text{m}$, we expect $\sim 28/\text{cm}^2$ per layer, or ~ 56 per field of view. The size of a field of view in our 510×490 element CCD camera is $\sim 0.7 \text{ cm} \times 0.7 \text{ cm}$, and 1 pixel has an area of $13.7 \mu\text{m} \times 13.7 \mu\text{m}$, blurred by diffraction to $\sim 20 \mu\text{m} \times 20 \mu\text{m}$. For a five-day etch, cones will have a width of at least two pixels. The second approach, which we favor, is to use a low-power stereomicroscope to locate two penetrating events, one near each of opposite corners of a 13" by 21" sheet, and to use these two events as fiducials. We next would mount and scan one layer at a time, digitizing in turn each field of view and recording skeletonized binary images of all cones that exceed a threshold size. Only location, zenith and azimuth angles, and projected cone lengths would be stored. The two fiducial events would be used to determine the amount by which the layers should be rotated and translated in order to reconstruct the original alignment. Then all skeletonized images would be compared with neighbors within a distance corresponding to a zenith angle less than, say, 70 deg, and sextets and quartets found. After each set of trigger sheets is scanned, the penetrating events found by the computer are quickly inspected by a trained operator and fake events thrown out.

For vertical incidence on the actinide stacks and for a threshold $Z/\beta = 65$, nuclei with $Z \geq 28$ can produce a quartet in Rodyne and nuclei with $Z \geq 34$ can produce a sextet in Rodyne. For a threshold $Z/\beta = 78$, nuclei with $Z \geq 35$ can produce a quartet in Rodyne and nuclei with $Z \geq 44$ can produce a sextet. Because of the narrow range of velocities for which Z/β exceeds threshold, very few events with Z near the minimum allowable value will be detected. (For the mid-Z stacks the skeleton etch of Rodyne sheets might use a KOH - water - ethanol solution, called the FEW etch, in which case the minimum charges for quartets and sextets would be lower.)

With a 20% overlap, 2 sec per field of view, 3 min per change of sheet, a total area of $317,000 \text{ cm}^2$, and a 40 hr week, it would take about 50 weeks to locate all sextets using the second scheme in which sheets are not superimposed.

If, because of a giant solar flare, a longer space exposure than planned, or an unexpectedly rough surface of the Rodyne sheets, locating sextets in Rodyne turns out to be difficult or inefficient, we could scan for sextets in three Cronar layers, sacrificing some high-Z events at large zenith angles. (We have

investigated the FEW etch for Cronar and have found that it results in a decreased sensitivity, an effect opposite to that achieved by the FEW etch on Rodyne.

d) Estimates of Z , β for events with high Z/β

About 5000 events will be followed through the nine etched Rodyne layers and measured semi-automatically with a 20X, 32X, or 50X objective, using an improved version of the Krischer-Price three-dimensional minimization algorithm. Most of the time to measure $5000 \times 9 = 45,000$ etchpit pairs will be consumed in positioning and focussing the sheets on the stage.

Estimates of Z and β can be made by fitting curves through these data. The uncertainty in Z will increase with Z for several reasons: both the registration temperature effect and the aging effect increase with Z/β , and neither will be corrected for at this stage of the analysis; at high Z/β etchpit pairs will become tapered cylinders during a five-day etch, limiting the ability to determine track etch rate. Fragmentation of more than half of the nuclei with $Z > 70$ at some depth in the stack will also limit the resolution of Z and β . See "Attainment of High Charge Resolution for details.

4. Post-flight aging and processing of remaining Rodyne

a) What post-flight aging accomplishes

Our long-term aging studies (summarized in Figs. 2 and 3) show that chemical reactivity increases logarithmically with time in Rodyne at a rate that is an increasing function of Z/β . In Cronar and CR-39 the effect seems to be undetectably small. In Rodyne the rate of increase with $\log t$ appears to be smaller when the samples are kept in air at -16 deg C than at room temperature. When samples are irradiated and stored in argon, the effect seems to be absent, but the sensitivity is reduced by an undesirable amount. Because of this reduction in sensitivity, and because of our lack of knowledge of possible long-term effects of an argon atmosphere, we have decided not to switch from an air atmosphere to an argon atmosphere.

We have not yet characterized the aging effect well enough as a function of Z/β and of aging temperature to know the best way to correct for it. Events produced at different times during the mission will have a different thermal history in space. Probably the most pessimistic assumption is to assume that the temperature was always at its maximum permissible value, ~ 0 deg C. The rate of increase with $\log t$ would then be intermediate between the rate at 22 deg C and the rate at -16 deg C. Aging all detectors for a long time after flight should in principle reduce the fractional difference in reduced etch rate between old and young events, but what should be the storage temperature? Storage at -16 deg C would reduce the rate of aging but would probably also decrease the rate of reduction of fractional difference in reduced etch rate for events of different ages. Storage at 20 deg C for times of one or more years might permit some track-fading to occur in Rodyne. The best strategy would seem to be to age all Rodyne detectors except those used in the

skeleton etch and in the event thermometer at an intermediate temperature of 0 to 10 deg C for 22 years or more during which time the Cronar and CR-37 detectors are being etched and analyzed.

Figure 4 illustrates how post-flight aging for times of two and three years at 22 deg C could decrease the spread in apparent values of Z/β , assuming a 2.5-year LDEF mission at 22 deg C. In this calculation thermal fading is assumed not to occur. A population of events with $Z/\beta = 93$ uniformly distributed in time would, according to this calculation, have a very asymmetric distribution of apparent charges and a total spread of 0.75 in apparent Z for $\beta = 1$. About 75% of the events would have an apparent Z within 0.38 charge unit of $Z = 93$. For three years of aging, the total spread in apparent Z would be reduced to 0.59 charge unit, and 75% of the events would have an apparent Z within 0.28 charge unit of $Z = 93$. Presumably, with mission temperatures always lower than 0 deg C instead of the 22 deg C assumed in the above model, the spread of apparent Z values at the end of the mission would be less than in the model, and less still after two or three years of post-flight aging. For events with larger Z/β as in Fig. 2, the aging effect is greater and the spread in apparent Z after several years of aging would also be greater.

b) Etching of aged Rodyne layers for times that depend on depth

To avoid handling over a million squares of plastic, we propose to cut out squares only along the trajectories of actinide events, of which we expect ~30 to 100. These events would be identified in the analysis of the sheets from the skeleton etch. The etch times for these 1300 to 4400 squares of Rodyne would be quantized in multiples of 3, in order to optimize cone lengths and avoid producing cylinders. Special stainless steel frames will be designed for rapid mounting and demounting.

Following the skeleton etch and analysis, we propose to etch 20 complete layers of Rodyne in the actinide stacks and 13 in the mid- Z stacks for times that vary periodically with depth in a pattern such as the following -- 120 hours, 40 hours, and 12 hours -- based on a Monte Carlo calculation of the frequency of occurrence of various values of Z/β for a standard model of cosmic ray charge abundances and energies along a 57 deg orbit. Although some portions of trajectories will be overetched and others will be underetched, there is sufficient redundancy in the number of layers to permit us to use this strategy and avoid the labor of dealing with $\sim 10^6$ squares. To etch these layers will require 11 changes of each of the four etch tanks and will take approximately 100 days.

A computer program can select only those portions of trajectories for which a useful measurement can be made, taking into account the necessity to sample often for interactions.

5. Analysis of the event thermometer

As shown in Fig. 5, we have recently found that the track

registration temperature effect in Cronar is at least an order of magnitude smaller than in Rodyne for particles at the same Z/β and smaller still than in CR-39. Specifically, for $Z/\beta = 93.9$, in the temperature interval -50 deg to 0 deg C relevant to the HNC mission, the change in apparent charge at $Z = 79$ is only 0.012 per degree for Cronar, compared with 0.13 per degree for Rodyne and 0.4 per degree for CR-39. The effect for Cronar is so small that a reasonably good charge spectrum could be obtained without making any correction. Thus, even if the event thermometer were to fail completely, the Cronar could be used to fulfill many of the goals of the HNC mission.

To etch the two $508 \mu\text{m}$ layers of Rodyne constituting the event thermometer will require about one filling of each of the four etch tanks. We propose first to etch small test areas in the standard 6.25 N NaOH solution and in the PEW solution, and to irradiate a test area with UV and etch it. We would select the method that would give the largest number of usable events without substantial interference from background tracks.

One research group, not necessarily the one at UCB, could take on the task of locating in the event thermometer the events with coordinates and azimuth and zenith angles determined from analyses of Rodyne etched in the skeleton etch of the actinide stacks and of CR-39 etched in the skeleton etch of the mid-Z stacks. Based on current studies of the track registration temperature effect in Rodyne by the Dublin group, by other groups, and by ourselves, they could determine the displacements of the two members of the event thermometer and thus the temperature for each of the events. They could also participate in the task of correcting the signals in CR-39, Rodyne, and Cronar.

6. Use of CR-39 to study fragmentation of actinide nuclei

The fission channel comprises a fraction of the total cross section that increases rapidly with Z^2/A for nuclei with $Z \geq 80$, as shown in Fig. 6. For actinide nuclei the partial cross section for fission exceeds 50% of the total cross section. Detection of fission fragments in a large fraction of interactions of events thought to be actinides would thus provide confirmation of their correct identification, at least on a statistical basis. Rodyne and Cronar are not sensitive enough to detect fission fragments, which typically have $Z < 50$ (but see section 8, in which we discuss the possibility of using a UV irradiation to sensitize Rodyne enough to detect fission fragments). We propose to cut out and etch small squares of CR-39 at points along trajectories of putative actinide nuclei below interaction points. The etch times would be chosen to produce long but not touching cones if the interactions were indeed fissions. Because of the high density of background etch pits of short length at the surfaces of CR-39, due mainly to spallation of trapped protons, it will probably be necessary to focus below the surface and measure cone lengths, so it is important to choose etch times so that etch cones do not touch.

7. Use of Cronar to study nuclei with $Z/\beta \geq 78$

a) General remarks

Although less sensitive than Rodyne, Cronar has a number of advantages that should simplify data acquisition and analysis. It seems to show no track-fading with time at room temperature and no change of response with aging time after irradiation, and its response is about a factor ten less sensitive to detector temperature than is the response of Rodyne. Its surface is far smoother than that of Rodyne after etching. Because of its lower sensitivity, the density of background etch pits will be much smaller than in Rodyne, and reduced track etch rates can be determined simply by measuring the dimensions of elliptical etch pit mouths, at least for values of Z/β up to about 115 or 120. Being only $\sim 100 \mu\text{m}$ thick, Cronar sheets are easily damaged or lost during etching, and great care must be taken in mounting and demounting them.

b) Skeleton etch of Cronar and ellipse measurements

We propose that, independently of the rough Z, β data from the skeleton etch of Rodyne, five layers of Cronar be etched for a time corresponding to a reduction of sheet thickness from 100 to about $50 \mu\text{m}$. Between a quarter and a half of the ~ 5000 events we expect in the Rodyne should be detectable in the Cronar. Analysis of ellipse mouths can be done more rapidly in Cronar than can three-dimensional cone measurements be made in Rodyne.

c) Further etching and measurements in Cronar

We propose to etch and measure events in another 23 layers of Cronar in the actinide stacks and 15 layers in the mid-Z stacks for a time such as to reduce the thickness from 100 to $50 \mu\text{m}$, reserving the remaining layers for future use or for unraveling puzzling cases of several closely spaced fragmentations that cannot easily be deciphered. This might well be necessary for some of the actinides. Future use of some of the Cronar might be a new method of post-flight treatment or a new chemical etchant capable of higher sensitivity than NaOH. To etch these layers will require 13 changes of each of the four etch tanks.

d) Final charge and energy assignments

We expect to use data from Cronar, Rodyne, CR-39 and the event thermometer to make the final, accurate charge and energy assignments for the actinides and for those platinum-peak and lead-peak nuclei at zenith angles small enough to be recordable in Cronar.

8. Study of mid-Z nuclei ($40 \leq Z \leq 60$)

a) Analysis of tracks in CR-39

After cutting out squares of CR-39 for the study of actinide interactions, we propose that one research group, not necessarily UCB, etch the remaining portions in the actinide stacks for times that vary cyclically with depth in a fashion similar to that proposed earlier in this document for the Rodyne. In the mid-Z stacks there is enough CR-39 that that group could first do a skeleton etch of the 7 layers labeled with daggers in Table 2,

make preliminary charge assignments including corrections from the event thermometer data, and cut out squares of certain events deemed to be particularly important to study with the utmost accuracy. Since this activity would require transporting large volumes of plastic to a laser-cutting firm to have the squares cut out, and is thus extremely laborious, the number of events treated in this way would of necessity be limited. The group would then etch additional layers of CR-39 in the mid-Z stacks.

b) Analysis of tracks in Rodyne using the PEW etch

In the event of an excessive background of tracks in CR-39 due either to solar flares or to the trapped radiation, Rodyne, which is much less sensitive than CR-39 even when etched in the PEW etch, might replace CR-39 as the primary detector. Many years ago we found that Lexan etched in a solution of NaOH and ethanol showed a response that varied strongly with zenith angle, a phenomenon that we attributed to a competition between diffusion of reagent through the volume of the polymer and normal etching along the track. We plan to study the charge resolution and the angular dependence of response of Rodyne for the PEW etch using Bevalac beams of nuclei with $40 < Z < 60$. (Preliminary results show that the PEW etch leaves a very rough surface and irregular elliptical cone mouths, which suggests that the charge resolution may be inadequate.) We estimate that minimum-ionizing nuclei with Z as low as 55 could be detected in the trigger sheets with an acceptance that increases rapidly with Z . It is thus worth exploring some minor variants of the PEW composition that would preserve this high sensitivity. By including the actinide stacks, etching trigger sheets for these stacks in an acceptable variant of the PEW etch instead of the normal NaOH etch, and accepting sub-relativistic nuclei, one might, without too great a compromise of the major objective of the HNC mission, collect good statistics on mid-Z nuclei down to Z as low as 40.

c) Sensitization of Rodyne by UV irradiation

If the background track density in CR-39 during the 2.5 year spcae exposure were to be too high for useful measurements, an alternative to the PEW etch suggested in 8 (b) would be to irradiate some of the Rodyne with UV, which could easily increase its sensitivity enough to enable minimum-ionizing nuclei with $Z > 40$ to be studied, but not so much as to produce a high background track density. Calibrations with Bevalac beams at various zenith angles would be necessary to establish whether charge resolution would be adequate. Such a procedure would be extremely laborious but might be necessary if an acceptable variant of the PEW etch cannot be found.

9. Events with $Z/\beta \geq 120$

Judging from our experience with Skylab, whose orbit of 53 deg was rather similar to that for HNC, about 20% of the nuclei with $Z \geq 70$ would have $Z/\beta \geq 120$ at all points along their trajectories. The measurement of elliptical etchpit mouth dimensions in Cronar becomes inadequate for $Z/\beta \geq 120$, and the measurement of cone lengths in Cronar is infeasible both because of the birefringence of the plastic and because it is so thin

(100 μm) that cone lengths could not, in general, be allowed to exceed $\sim 50 \mu\text{m}$ without forming cylinders. Despite the large aging effect for large Z/β , Rodyne may provide adequate information about events with $Z/\beta \geq 120$.

In recent work with a 1 GeV/nucleon gold beam, we have found a superb new detector that is somewhat more sensitive than Cronar, has a very steep response, $v_{T/G} \approx 1 + a(Z/\beta)^{9.8}$, has a charge standard deviation $\sigma_Z = 0.2e$ (!) for a single etchpit at gold, has enough barium and zinc in it that we could omit the copper stripping sheets on HNC, and has superb optical properties. This detector is a phosphate glass made by Schott. Figure 7 shows a set of measurements of gold ions and projectile fragments using a single etch pit diameter. Although it is probably too late now to incorporate phosphate glass into HNC, we are continuing to study it for possible future applications.

10. Summary of etch tank requirements

To etch all of the plastic layers in 45 trays and in the event thermometer would require 259 tankfuls or 65 refillings of each of the four tanks. We have suggested procedures that would require processing about 60% of the layers plus the event thermometer sheets. With this plan we would need 40 refillings of each of the four tanks. The alternative of cutting out and working with over a million squares would insure optimum etch times for each portion of the trajectory of each event and would reduce the total area to be etched by about a factor two but would very greatly increase the labor. We favor the former approach.

Table 1. Actinide Stack Configuration

1.	RR†(Cu)	C†CCC	(Cu)	RR†R	CR
2.	Cu	CCCC	Cu	RR†R	CR
3.	Cu	CCCC	Cu	RRR	CR
4.	Cu	C†CCC	Cu	R†RR	CR
5.	Cu	CCCC	Cu	RRR	CR
6.	Cu	CCCC	Cu	R†RR	CR
7.	Cu	C†CCC	Cu	RRR	CR
8.	Cu	CC*CC	Cu	R†R*R	CR*
9.	Cu	CCCC	Cu	RRR	CR
10.	Cu	C†CCC	Cu	R†RR	CR
11.	Cu	CCCC	Cu	RRR	CR
12.	Cu	CCCC	Cu	R†RR	CR
13.	Cu	C†CCC	Cu	RRR	CR
14.	Cu	CCCC	Cu	R†RR	CR

$$28 \text{ Cu} = 28 \times 0.2266 = 6.3448$$

$$56 \text{ C} = 56 \times 0.014 = 0.7840$$

$$44 \text{ R} = 44 \times 0.0306 = 1.3464$$

$$14 \text{ CR} = 14 \times 0.0335 = 0.4690$$

$$\text{TOTAL} \qquad \qquad \qquad 8.944 \text{ g/cm}^2$$

- Cu/Plastic = 2.441
- Cu = 250 μm Cu
- R = 250 μm Rodyne
- CR = 250 μm CR-39
- C = 100 μm Cronar

*Calibration sheets

†Skeleton etch

() can we omit these Cu sheets? If so, choice of top 3 skeleton etch sheets will change.

Table 2. Mid-Z Stack Configuration

1.	(Cu)	R†RR		CR† CR
2.	(Cu)	C†CC		CR CR CR
3.	Cu	R†RR	Cu	CR CR
4.	Cu	R†C†CC	Cu	CR† CR CR
5.	Cu	RR		CR CR
6.	Cu	CC		CR CR
7.	Cu	R†RR		CR† CR
8.	Cu	C†CC		CR CR CR
9.	Cu	R†R*R	Cu	CR CR
10.	Cu	CC*C	Cu	CR† CR* CR
11.	Cu	RR		CR CR
12.	Cu	CC		CR CR
13.	Cu	R†RR		CR† CR
14.	Cu	C†CC		CR CR CR
15.	Cu	R†RR	Cu	CR CR
16.	Cu	CCC	Cu	CR† CR CR
17.	Cu	RR		CR CR
18.	Cu	CC		CR CR
19.	Cu	R†RR	Cu	CR CR
20.	Cu	C†CC	Cu	CR† CR CR

28 Cu = 28 x 0.2266 = 6.3448
 27 C = 27 x 0.014 = 0.3780
 28 R = 28 x 0.0153 = 0.4284
 47 CR = 47 x 0.0335 = 1.5745

TOTAL 8.7257 g/cm²

Cu/Plastic = 2.665

Cu = 250 μm Cu

R = 125 μm Rodyne (half as thick as in actinide stacks)

CR = 250 μm CR-39

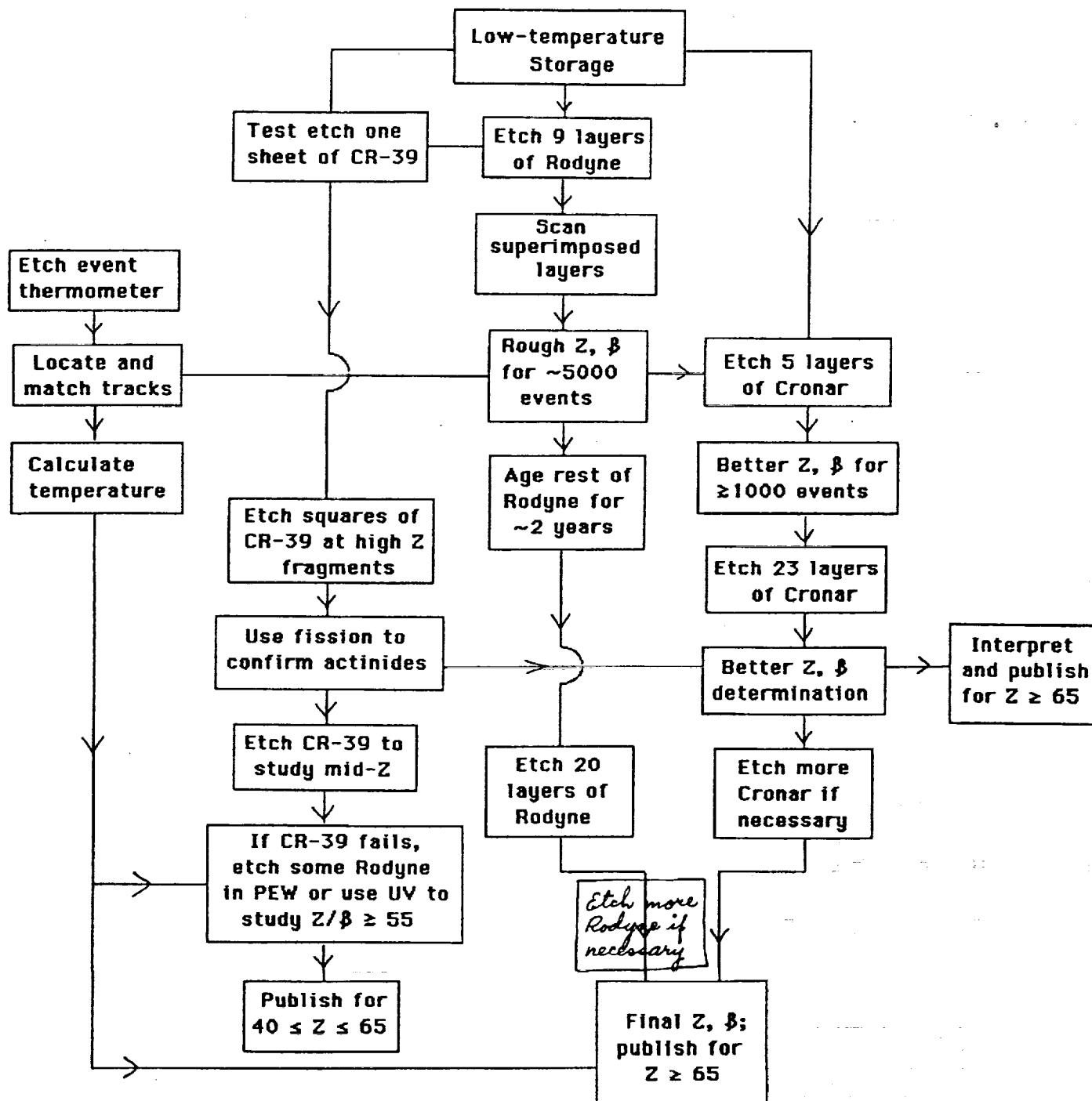
C = 100 μm Cronar

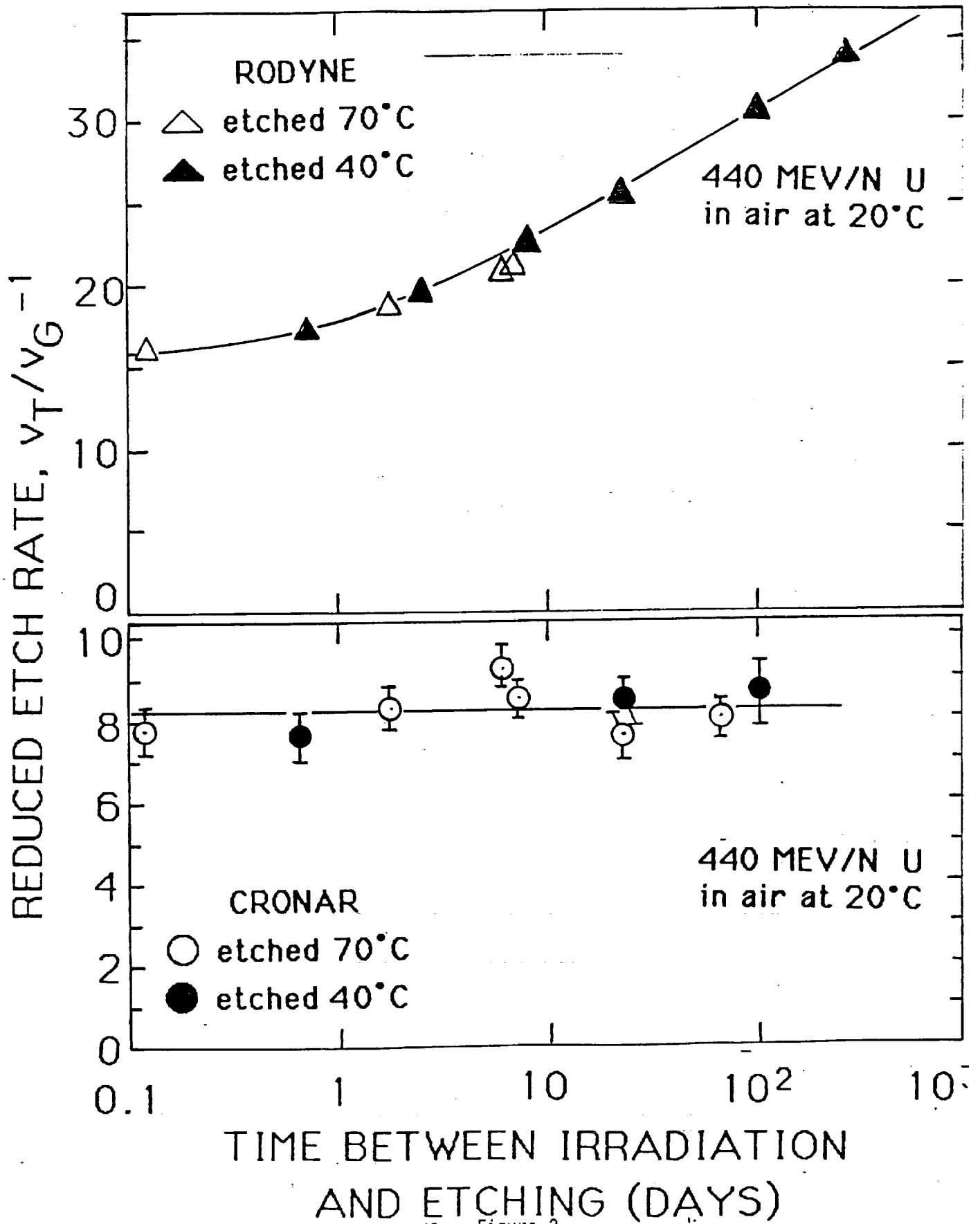
*Calibration sheets

†Skeleton etch

() can we omit these Cu sheets? If so, choice of top 3 skeleton etch sheets will change.

FIG. 1. PROCESSING AND DATA ANALYSIS





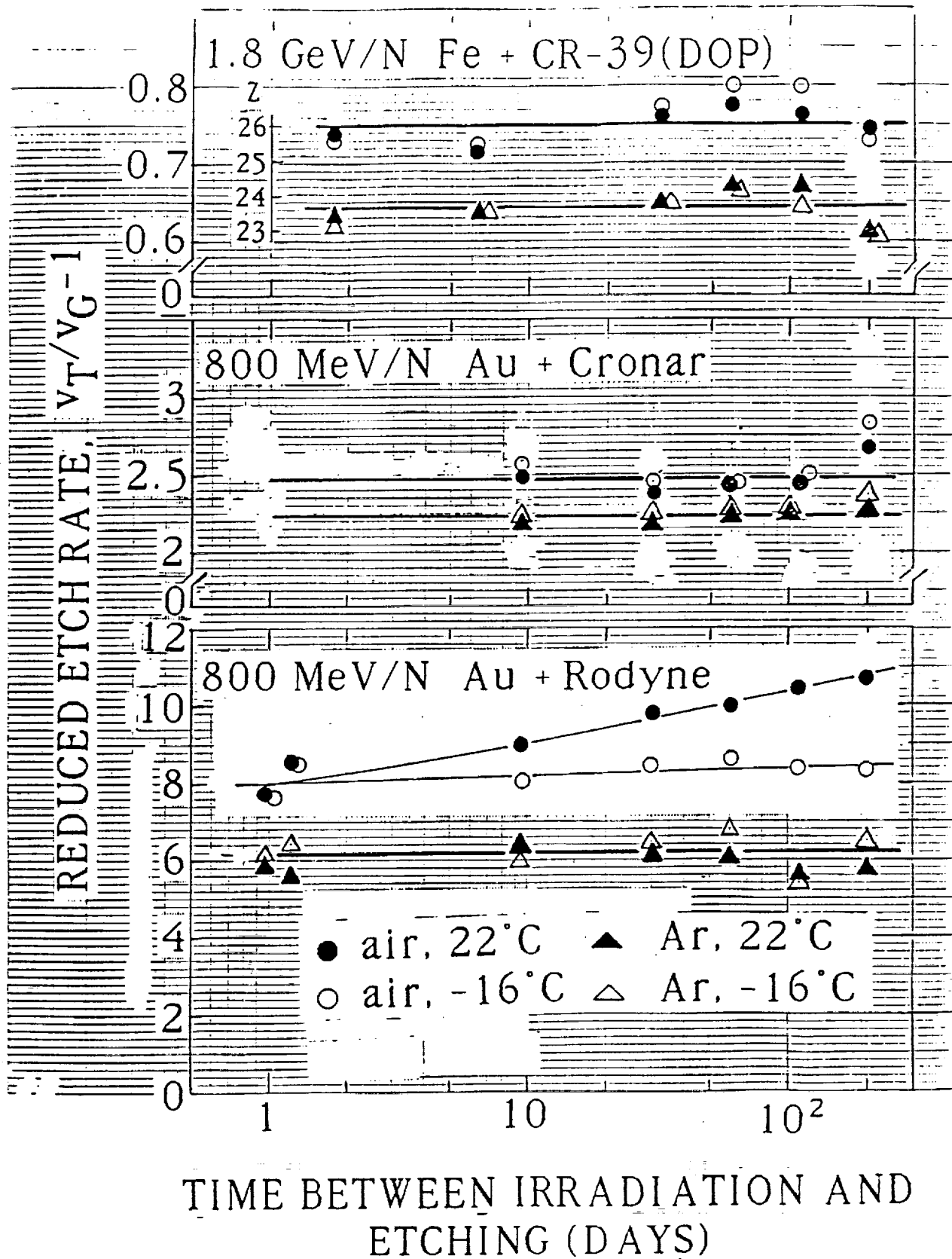


Fig. 3. Track-aging results for detectors irradiated at 22°C in air or in argon, then aged at 22°C or -16°C in air or argon, and etched in 6.25N NaOH at 40°C.

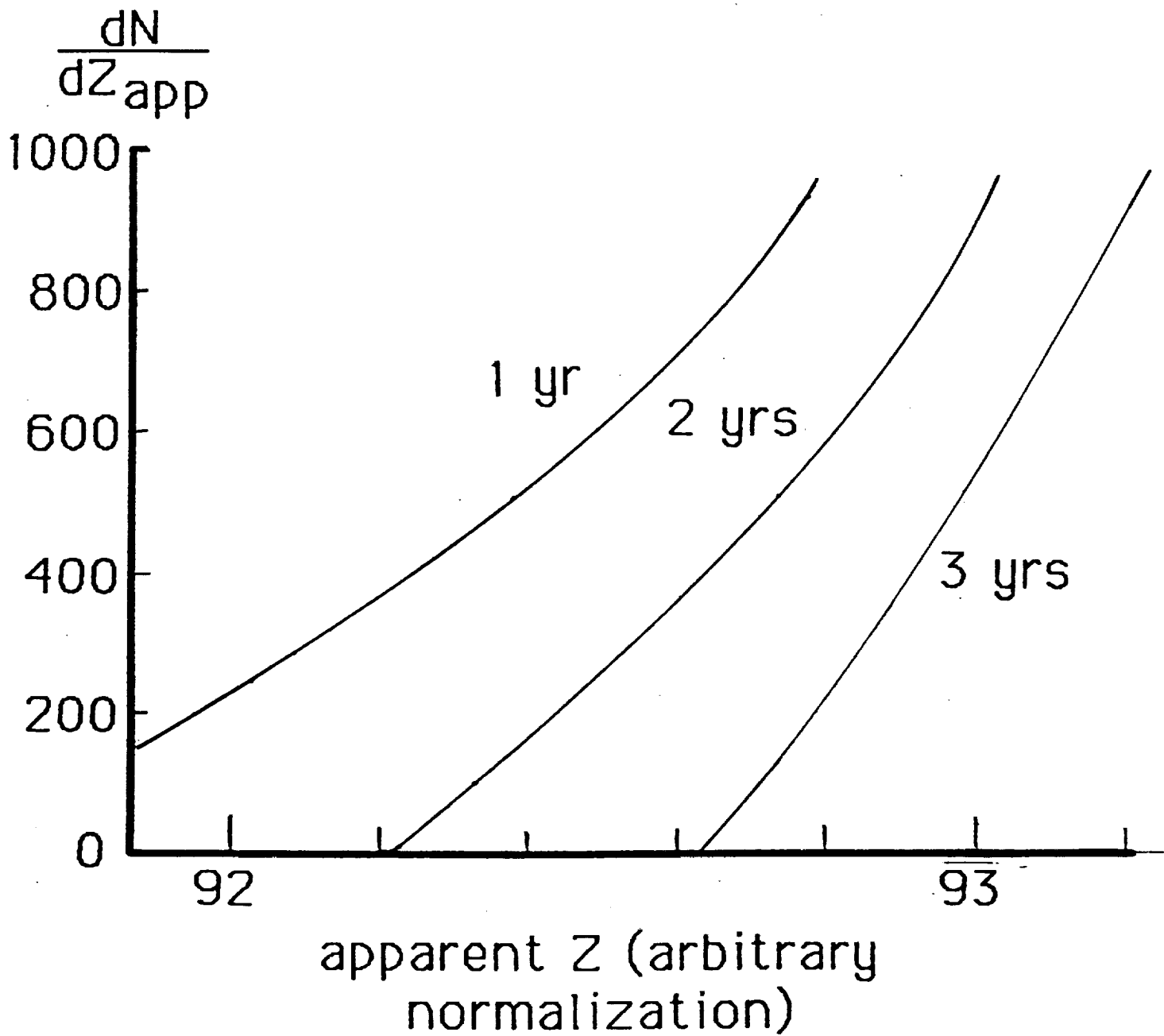


Fig. 4. Distribution of apparent charges for events with $Z/\beta = 93$, uniformly distributed in arrival times and ages for an additional 1, 2 and 2 years after the mission.

APPARENT Z

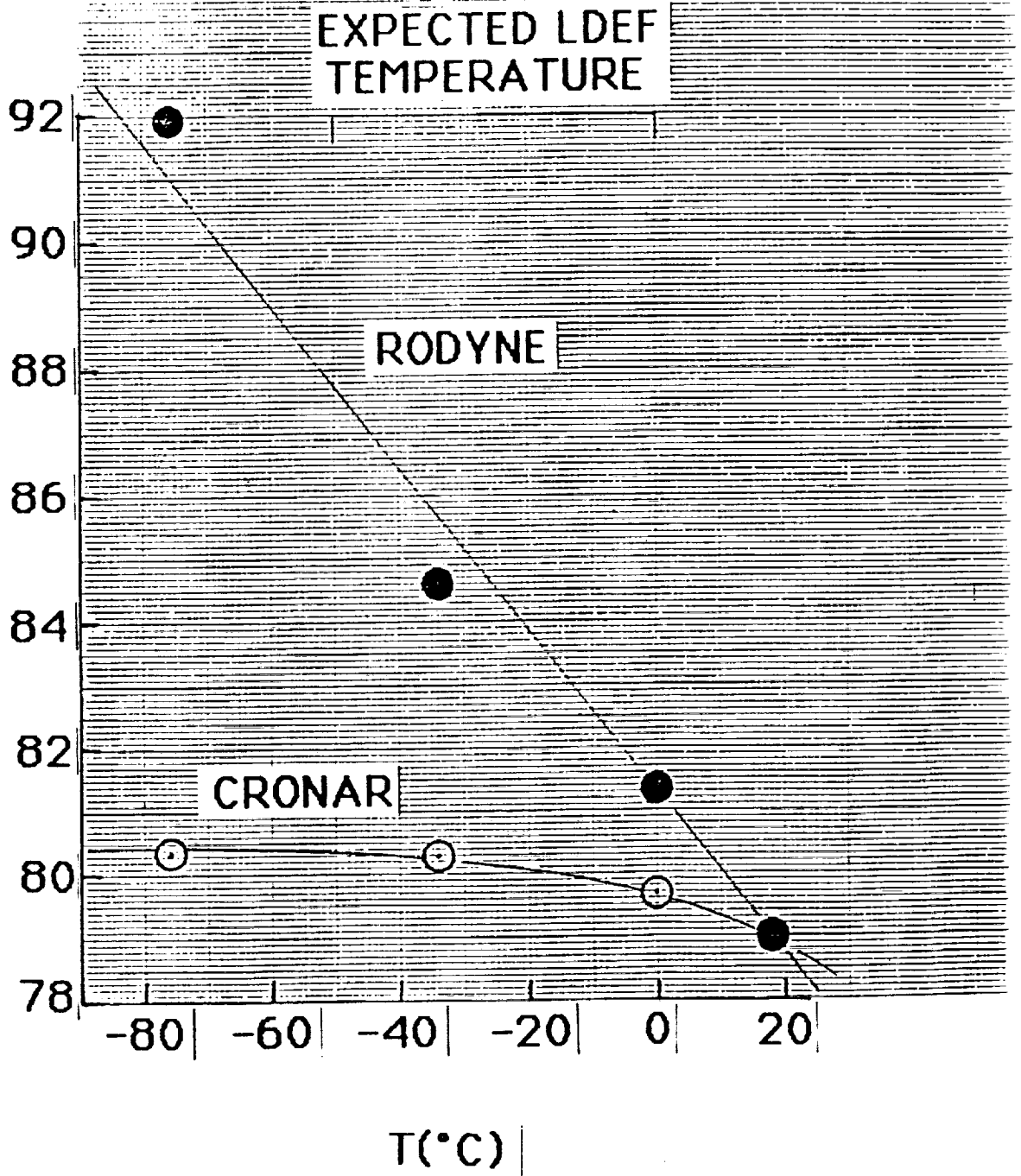
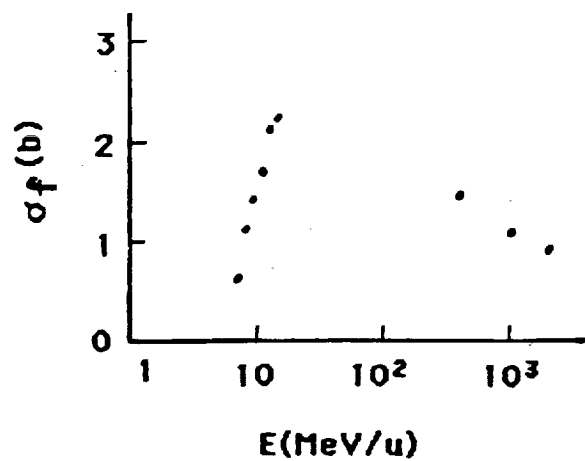
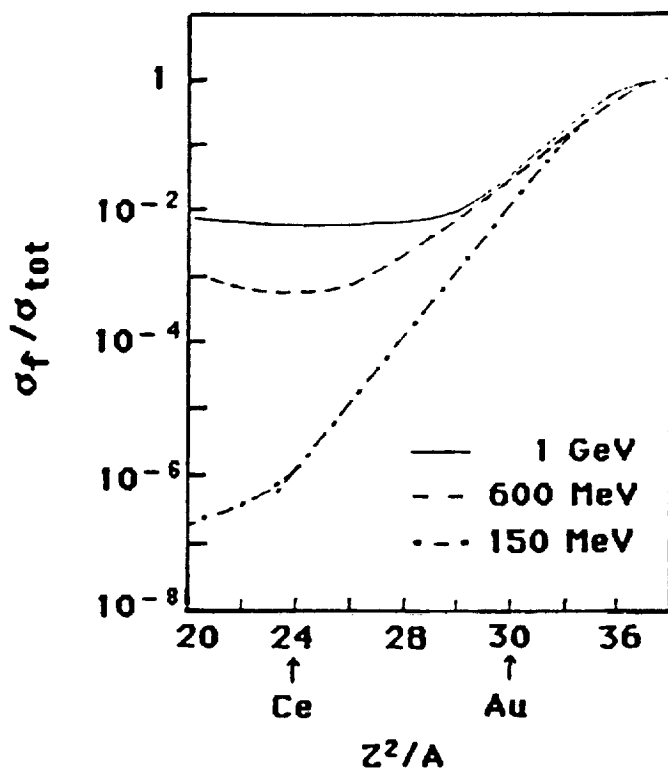
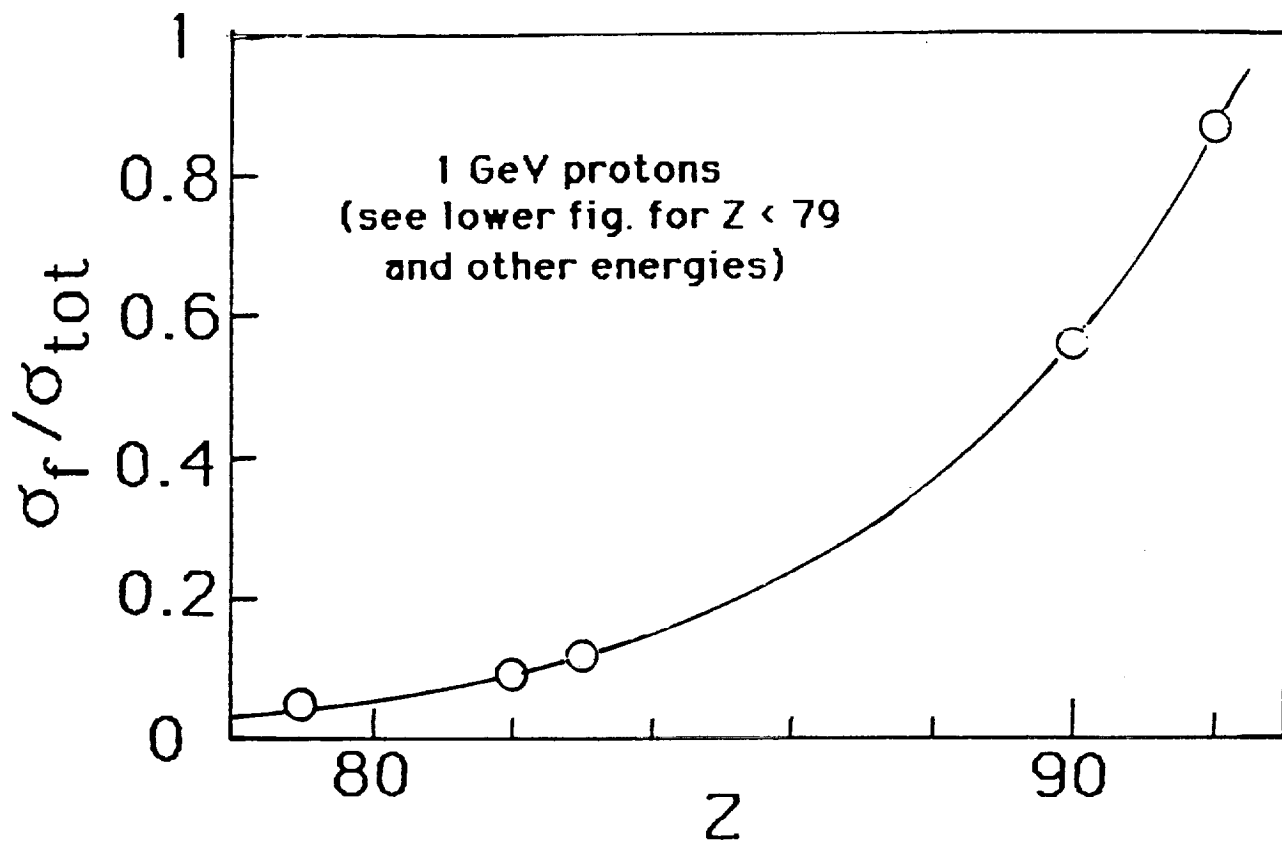


Figure 5



Fission cross section as a function of energy for ^4He ions on U (Meyer et al., Phys. Rev. C 22, 179 (1980)).

Dependence of fission probability on Z^2/A and on proton bombarding energy (Becchetti et al., Phys. Rev. C 28, 276 (1983)).

Figure 6

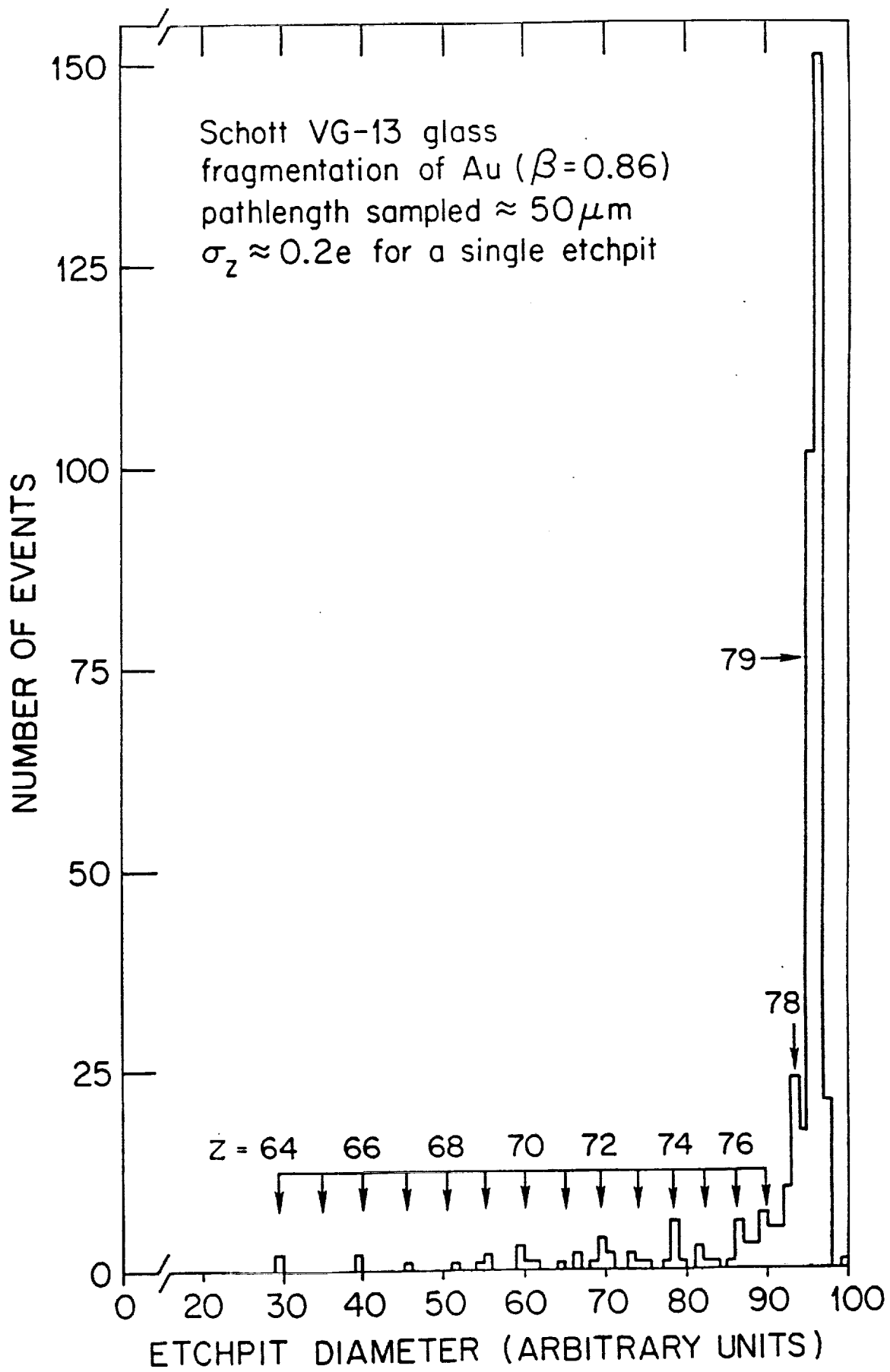


Figure 7

Document 3

Research Proposal to the
National Aeronautics and Space Administration

submitted by

The Regents of the University of California
Space Sciences Laboratory
c/o Sponsored Projects Office
Attn: P. A. Gates or M. A. Barnato
University of California
2111 Bancroft Way, 5th Floor
Berkeley, California 94720
(415) 642-8109

UCBSSL 1457/88

Flight Proposal In Response to A.O. No. OSSA 3-88:

**HEAVY NUCLEUS COLLECTOR (HNC):
A SPACE STATION ATTACHED PAYLOAD**

Volume 1: Investigation and Technical Plan

Principal Investigator

Prof. P. Buford Price
Space Sciences Laboratory
University of California
Berkeley, California 94720
(415) 642-4982

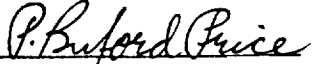
Co-Investigators at Other Institutions

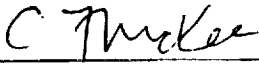
Prof. Gregory Tarlé
University of Michigan
Prof. Michael H. Salamon
University of Utah
Dr. William H. Kinard
NASA Langley Research Center

Period of Performance

October 1, 1989 - September 30, 2003

November 11, 1988


P. Buford Price
Principal Investigator


Christopher F. McKee
Director
Space Sciences Laboratory

David F. Mears
University Contracts and
Grants Coordinator

Table of Contents

Investigative and Technical Plan	2
Summary	2
Background	2
Science Objectives	4
Identification of Ultraheavy Cosmic Rays with BP-1 Glass Detectors	8
Instrumentation	12
Overview	12
Detector Concept	13
Tray Mounting Frames	13
Pallet	14
LDEF Concept	14
Thermal Control Concept	15
Ground Operations	15
Flight Operations	15
Data Reduction and Analysis	15
Orbiter Crew of Payload Specialist Training Requirements	16
Summary	16
References	17
Figures	19
Appendices	24
Curricula Vitae and Recent Publications of P. B. Price and G. Tarlé	24
Technical Data Sheets (Fact Sheets)	30

Section I

1. Investigative and Technical Plan

Summary

The HNC is a passive array of stacks of a special glass, 14 sheets thick, that record tracks of ultraheavy cosmic rays for later readout by automated systems on earth. The primary goal is to determine the relative abundances of both the odd- and even-Z cosmic rays with $Z \geq 50$ with statistics a factor at least 60 greater than obtained in HEAO-3 and to obtain charge resolution at least as good as 0.25 charge unit. The secondary goal is to search for hypothetical particles such as superheavy elements. The HNC detector array will have a cumulative collection power equivalent to flying 32 m² of detectors in space for 4 years. The array will be flown as a free-flight spacecraft and/or attached to Space Station Freedom.

Background

Details of the origin and history of the cosmic radiation have remained a mystery despite over seven decades of research. A measurement with high statistics and high resolution of the composition of the heaviest elements in the cosmic rays could do more to advance our understanding of the sources and time-history of cosmic rays than any experiment yet done. The extremely low abundances of ultraheavy cosmic rays and the extremely high precision needed to resolve individual elements at high atomic charge have stood in the way of progress in this area.

In the early 1970's balloons were used to carry passive nuclear track detectors measuring tens of square meters in size to the top of the atmosphere where they would float for one or two days collecting tracks of ultraheavy nuclei. These experiments reported apparently high fluxes of actinide and transuranic elements which, if correct, indicated a recent origin in an explosive environment for the heavy cosmic rays. In 1973 Shirk and Price¹ exposed a 1 m² array of Lexan polycarbonate sheets on the Skylab. This experiment also reported a high flux of actinide elements, but because of weight limitations only a thin stack could be flown, and it was not possible to resolve individual elements. The need for better resolution and collecting power provided much of the impetus for the HEAO-3 Heavy Nuclei Experiment² and the ARIEL-6 experiment³ which utilized Cerenkov and ionization detectors. Although neither HEAO-3 nor ARIEL-6 achieved individual element separation, they did provide measurements of the even-Z nuclei up to $Z=60$ and showed that the actinide flux was not as large as had been indicated by Skylab and the balloon-borne visual detectors.

It became clear that a decisive ultraheavy experiment would require a high resolution instrument having an exposure factor ≥ 100 m² years. For a number of years NASA funded feasibility studies at Berkeley of a large-area passive free-flyer. In 1978, in response to a Spacelab AO, Price, Shirk and Tarle' proposed a large deployable array of plastic detectors. Although it was not accepted, we were encouraged to redesign it for possible inclusion on an LDEF reflight. Then, in the late 1970's, beams of relativistic heavy ions up to U became available at the Lawrence Berkeley Laboratory Bevalac. These beams not only permitted a dramatic

improvement in the quality and resolution of track detectors but led to an explanation for the poor resolution achieved in balloon experiments. Thompson and co-workers⁴ discovered that the response of plastic detectors depended on the temperature at which they were exposed, an effect which undoubtedly caused problems with charge identification in the balloon experiments, due to large day-night temperature excursions. From laboratory annealing experiments⁵ we now believe that partial fading of tracks at room temperature during the 250 day mission may have degraded the resolution of the Skylab experiment. Then, in 1978, a discovery was made that greatly increased the attractiveness of visual detectors. A new plastic track detector, CR-39, with unprecedented resolution and sensitivity was discovered by Cartwright et al.⁶ and improved by Tarle et al.⁷, who demonstrated that both in principle and by examination of the charges of projectile fragmentation at the Bevalac, certain nuclear track detectors have superior charge resolution to that of any other detector that responds to deposited energy. It is now clear that environmental conditions and lack of uniformity had previously resulted in the degradation of the high intrinsic charge resolution of plastic track detectors.

In 1984 a European group built a large array of pressurized plastic stacks that has been collecting tracks of cosmic ray nuclei with $Z > 65$ on the LDEF-I passive free flyer for several years⁸. Plans are now underway to recover LDEF. Unfortunately, the understanding of the role of environmental factors such as the time-dependence of reactivity of latent tracks⁹ and the dependence of response on detector temperature⁴ came too late to affect the design of the LDEF-I cosmic ray experiment. However, we showed that by using thermal isolation and by employing an "event thermometer" (a track recording sheet that moved relative to a fixed sheet in response to temperature changes), the original LDEF could be transformed into a suitable carrier for a high-resolution ultraheavy experiment and reflown. Improvements in the resolution of passive detectors and understanding of the many environmental factors, coupled with the ability to carry out an experiment on an existing low-cost platform, convinced NASA's Cosmic Ray Program Planning Working Group to endorse a reflight of the LDEF as a dedicated ultraheavy experiment. The Associate Administrator of the Office of Space Science and Applications concurred with the Cosmic Ray Working Group and approved the Heavy Nucleus Experiment (HNC)¹⁰ as a Shuttle-launched free-flyer within the Explorer program. Contracts were awarded to the University of California at Berkeley and to the University of Michigan to develop the HNC instrument. The HNC experiment was manifested on the Challenger as mission 71-K to be launched in May, 1987. In the aftermath of the Challenger disaster, the HNC science steering committee was asked to consider ways to redesign the HNC carrier so that it could fit into a smaller volume of the shuttle. Several simple and inexpensive platforms that could occupy as little as 1/8 of the volume required for LDEF were conceived. Within a year many approved experiments, including HNC, were cancelled.

With the resumption of flight opportunities, it continues to be of great scientific importance to carry out the HNC experiment. In the last two years, as the product of an extensive and ongoing program of research on new detectors, the Berkeley group has developed a new class of nuclear track detectors, made of phosphate glass, with spectacular properties.¹¹ These glasses can cleanly resolve individual minimum-ionizing nuclei in the charge region extending from $Z = 50$ (Sn) all the way to the end

of the Periodic Table; they can be used to resolve low-energy isotopes of nuclei heavier than iron; and they are nearly immune to environmental effects, as we will explain later. A far simpler instrument design is now possible, reducing the requirements on the carrier and greatly simplifying post-flight analysis. A mini-LDEF pallet, designed at Langley, fits into a small volume of the shuttle. Such pallets can be joined together and mounted on the Space Station or flown as a free-flyer. The pallets can be integrated into the Shuttle cargo bay as a Payload of Opportunity only months before a flight. The unique capability of a permanent Space Station allows a continuing and flexible HNC program to be carried out: pallets can be exposed on the Space Station very soon after it has been constructed, since they require no electronic connections. After a year or so they can be replaced by other pallets and returned to Earth for analysis so that a new exposure can begin while data analysis is carried out concurrently. An attractive feature of this program is that new detectors can be installed on future pallets if scientific returns from the first pallets justify continuation. The LDEF retrieval is now manifested for late 1989. Thus, a reflight of this facility may again be considered for the HNC.

Science Objectives

Accurate measurements of the elemental composition of the ultraheavy cosmic rays (defined here as those with $Z \geq 50$) should greatly increase our understanding of their nucleosynthetic origin and their subsequent acceleration and propagation through our Galaxy. The relative abundances of certain elements, among them Os, Ir, Pt, and the long-lived actinides ($Z > 89$), probe the extent to which cosmic rays are enriched in products of explosive nucleosynthesis. The abundances of elements of varying volatility and ionization potential, such as Pb, Sn, and Ge, may enable us to distinguish among models of their acceleration. Relative abundances of the long-lived radioactive species -- the actinides, and in particular the transuranic actinides -- will enable us to determine their age. The abundances of the largely secondary elements, such as the odd-Z elements and the rare-earths, together with existing knowledge of the abundances of the lighter secondary elements such as Li, Be, and B, can complete the picture of propagation of the cosmic rays, both light and heavy.

The distribution of abundances of the heavy and ultraheavy elements found in solar system material -- the sun and the meteorites -- is shown in Fig. 1. Detailed analyses of the data¹² have shown that the great majority of these elements were synthesized in stars by two dominant processes involving neutron capture and subsequent beta decay. In the s-process (synthesis by slow neutron capture), seed nuclei in the iron peak ($Z \sim 26$) are transformed into nuclei that lie along the nuclear stability line by capturing neutrons over time scales that are long compared to their beta decay lifetimes. The s-process synthesizes new nuclei from the iron peak further and further up the stability line by a succession of neutron captures and beta decays until they encounter bottlenecks at nuclides with closed shells, which have high cross sections for neutron capture. These bottlenecks build up abundance peaks at ^{50}Sn , ^{56}Ba and ^{82}Pb , as can be seen in Fig. 1. The s-process is believed to take place over thousands of years during the late stages of stellar evolution. The contribution of the s-process to the solar abundances is shown as circles in Fig. 1.

In order to reproduce the entire abundance pattern an additional process is required. In the r-process (synthesis by rapid neutron capture) an intense flux of neutrons drives nuclei in the iron peak far to the right of the beta stability line on a timescale shorter than beta decay can bring them back. Synthesis follows a line approximately parallel to and 10 to 15 neutrons to the neutron-rich side of the stability line. Bottlenecks for this process also occur at closed nuclear shells but on nuclides very far to the neutron-rich side of stability. When the neutron flux terminates, these nuclei undergo beta decay, producing characteristic abundance peaks at elements of somewhat lower charge. The abundance peaks at ^{52}Te and ^{54}Xe and at ^{76}Os , ^{77}Ir , and ^{78}Pt , labeled in Fig. 1 as triangles, are due mainly to the r-process.

Because of the short lifetimes (<1600 years) of all the nuclides with $83 < Z < 90$, only the r-process is capable of bridging this gap and synthesizing still heavier elements, the so-called long-lived actinides. In this class, only ^{90}Th and ^{92}U have isotopes with half-lives long enough to have survived in present-day solar system material. All of the other elements have isotopes with half lives much shorter than the age of the solar system (about 4.5×10^9 years). Although the r-process produces more ^{92}U than ^{90}Th , more ^{90}Th is found today in solar material because one of its isotopes, ^{232}Th , has a longer lifetime than that of any of the isotopes of U. The r-process is believed to take place over a time scale of only a few seconds during supernovae explosions that both synthesize and eject the products of stellar synthesis into the interstellar medium.

Just as the abundance distribution of solar system material has led to an understanding of its origin, the abundances of the elements in the cosmic radiation should hold the key to their origin. Because the cosmic rays come to us from outside the solar system, they are likely to consist of a different mix of r- and s-process elements from solar-system material. If a substantial fraction of the ultraheavy cosmic rays are synthesized by supernovae explosions, then they may be enriched in elements such as ^{52}Te , ^{54}Xe , ^{76}Os , ^{77}Ir , ^{78}Pt and the actinide elements ^{90}Th and ^{92}U which are synthesized in the r-process. If the cosmic rays are synthesized and promptly accelerated by supernovae then their nucleosynthetic age, meaning the time since they were synthesized, would be comparable to the cosmic ray age of about 10^7 years inferred from abundance measurements of "secondary" nuclides such as ^{10}Be , which are created in collisions with interstellar gas. In this case, the transuranic elements ^{93}Np , ^{94}Pu and ^{96}Cm , which have lifetimes ranging from a few 10^6 to about 10^8 years, may be present in the cosmic rays, and ^{92}U will be more abundant than ^{90}Th , as it was when the solar system material was synthesized between 4.6 and 10×10^9 years ago. If, however, the cosmic rays are just a sample of the local interstellar medium that has been swept up and accelerated by supernovae shock waves, then no transuranic elements should be seen and ^{90}Th will be more abundant than ^{92}U as is the case in the solar system material today. Table 1 gives examples of possible numbers of actinide cosmic ray nuclei that might be collected by a detector with an acceptance of $100 \text{ m}^2\text{sr}$ in a four-year exposure in a 28.5 degree orbit (relevant to the Space Station) at solar minimum. Detection of even a fairly small number of actinide nuclei, if achieved with a charge resolution capable of separating elements differing by even as much as two units of charge, would be sufficient to determine the nucleosynthetic age of the cosmic rays and decide between competing theories of their origin.

Table 1. Examples of Possible Numbers of Actinide Events for LDEF-2 HNC

	Th	U	Np	Pu	Cm	TOTAL
Solar System abundances at birth	30	10	0	0	0	40
Solar System abundances now (SS)	21	5	0	0	0	26
80% SS + 20% 10^6 y-old r-process material	19	18	6	4	5	52
80% SS + 20% 10^7 y-old r-process material	20	21	0.4	4.6	3.4	49
80% SS + 20% 10^8 y-old r-process material	24	20	0	2.2	0.1	46
50% SS + 50% 10^6 y-old r-process material	16	39	16	10	13	84
50% SS + 50% 10^7 y-old r-process material	18	44	1.1	12	9	84
50% SS + 50% 10^8 y-old r-process material	30	42	0	5	0.2	77

The composition of the cosmic rays is altered by their nuclear interactions with the gas of the interstellar medium. Fortunately, in the case of the even-Z elements it is possible to correct for this distortion of the composition rather accurately. The reasons are as follows. Nuclear interactions produce lighter nuclei. Because the abundances generally decrease with Z from the iron peak to the region of the actinides, the products of interactions of nuclei of an ultraheavy element have lighter charge and contaminate the more abundant nuclei very little. What contamination is produced can be estimated fairly reliably because of the regular systematics of total interaction cross sections among the ultraheavy nuclei. Furthermore, actinide nuclei tend to fission when they interact, and their fission products do not contaminate the sample of nuclei with $Z > 50$ at all. These features make the even-Z nuclei in the ultraheavy region some of the most accurate indicators of cosmic ray source composition available. In contrast, the odd-Z nuclei are much less abundant than their even-Z neighbors, and the nuclei which have charges just below the abundance peaks are much less abundant than their heavier neighbors, and these less abundant elements tend to get built up by spallation. These predominantly secondary nuclei can be used in the same way that Li, Be, and B and the secondary elements below the iron peak are used, to determine the conditions under which their progenitors have propagated in the Galaxy. The ability to resolve individual adjacent even- and odd-Z elements is mandatory if one is to separate secondary from primary nuclei without the uncertainties of model-dependent background subtraction.

Within the limitations of statistics and charge resolution to date, the elemental composition of the cosmic radiation throughout the Periodic Table roughly tracks the solar system abundances up to $Z \approx 60$ when proper account of selective injection and secondary production during propagation is taken. For the latter, accurate partial and total nuclear interaction cross sections are being measured¹³ through the use of beams of relativistic ultraheavy nuclei at the Lawrence Berkeley Laboratory's Bevalac facility. For the former, elemental abundance ratios, corrected back to the cosmic ray source and compared to solar system abundances, seem to depend on their first ionization potential (FIP).¹⁴ The interpretation is obvious -- elements with lower FIP are preferentially injected into the cosmic ray acceleration process. An alternative explanation is that the selection of cosmic ray nuclei favors elements with high

volatility, as would be expected if they originated in interstellar grains. In the ultraheavy region the refractory (low volatility) elements are also those with high FIP except in the case of Ge and Pb which have low FIPs but are highly refractory. An underabundance of these elements would favor the grain hypothesis.¹⁵ Implicit in this determination is that accurate solar system abundances are available for comparison. In this regard, solar photospheric abundance measurements may be more appropriate than meteoritic measurements.

Figure 2a shows the abundance distribution of nuclei with $Z > 50$ observed with HEAO-3 (ref. 2) and Fig. 2b shows data from the same charge region obtained with ARIEL-6 (ref. 3). As the inset in Fig. 2a shows, the HEAO-3 investigators have succeeded in finding a portion of their data for which the even-Z elements up to $Z = 60$ are resolved. Beyond $Z = 60$ there is inadequate statistics and resolution to determine even the abundances of even-Z elements, but the HEAO-3 investigators believe they can measure the ratio of abundances of elements in the Pt peak, the Pb peak, and the actinides. Figure 3 compares the observed abundances of elements with Z from 36 up to the Pb peak, relative to those predicted for source material that is like the composition of the solar system, like a pure s-process, and like a pure r-process. The interpretation of this graph by the authors of ref. 16 is that the elements with $60 < Z < 80$ are enriched relative to solar system composition and that the Pb-peak elements are depleted. The HEAO-3 group has reported one possible actinide, and ARIEL-6, with less good charge resolution, may have seen two or three. Neither has sufficient charge resolution to determine whether these events are Th, U, or possibly transuranic, nor to separate the Pt-Pb peak elements into anything other than charge groups. Still, the results are intriguing. The large actinide abundances seen earlier in balloon flights and Skylab are absent. The ARIEL-6 actinide abundance, if all three events are correctly identified, suggests an enrichment in pure r-process elements, but the issue is open. The Pb/Pt ratio is significantly lower than the solar system value. This might indicate an enhancement in the r-process contribution in this region or simply a depletion of Pb due to its low volatility.¹⁵ Another possibility is that the solar system abundance of Pb (determined from meteorites) may be in error. Photospheric determinations seem to give lower Pb abundance.

An examination of Fig 2 shows clearly that the next step in the study of ultraheavy nuclei requires an increase in the number of events by a factor of at least 10, and a charge resolution about an order of magnitude better than that attained on HEAO-3 or ARIEL-6. Figure 2c, based on Monte Carlo calculations by Drach¹⁷, shows what might be obtained with an instrument with 100 times the collecting power of HEAO-3 and a charge resolution of 0.25 charge unit. The actinide elements are clearly resolved (see inset), and there is a sufficiently large number of events to determine the cosmic ray age. The elements in the Pt-Pb region are also clearly resolved, allowing both a determination of the dominant source of primary elements and a measurement of the abundance of the odd-Z secondary elements. The LDEF-I cosmic ray instrument was designed before all of the environmental effects on plastic track detectors were understood, and consequently it will almost certainly not be able to match the resolution of HEAO-3. If the Challenger disaster had not occurred, the LDEF-II HNC experiment would have been launched in 1987 and would have already completed 1/5 of such an exposure. An electronic instrument one to two orders of magnitude larger than HEAO-3 would be prohibitively costly and would not achieve

the needed charge resolution. Fortunately, advances in passive detectors have now made it possible to greatly simplify the design and data analysis requirements of a completely passive instrument with the collecting power and resolution necessary to obtain data of the quantity and quality indicated in Fig. 2c.

The primary goal of HNC is to measure the relative abundances of both the odd- and even-Z cosmic rays with $Z \geq 50$ with statistics a factor at least 60 greater than obtained in HEAO-3 and to obtain a charge resolution better than 0.25 charge unit over most of the accessible energy region. In addition, the large collecting power makes HNC an attractive instrument with which to search for hypothetical particles that have been discussed by physicists and chemists but that have not yet been discovered. A secondary goal is to search for hypothetical particles such as the following:

- **superheavy elements**, defined as elements heavier than the transuranic elements that have been produced at accelerators. To date, the heaviest element for which some isotope has been produced at a heavy ion accelerator is $Z = 109$. Shell effects are expected to increase the stability of certain isotopes of elements with $Z \sim 110$ to 114, but current models of the r-process and of the fission barriers of superheavy elements do not hold out great hope that they can be made in r-process synthesis. Still, nature may have found a way to do it.

- **magnetic monopoles**. Many experimenters are now searching for supermassive magnetic monopoles that are predicted to exist in grand unified theories, and this class of monopoles would easily penetrate the earth because of their enormous mass and inertia. For such monopoles there would be no need to have a detector above the earth's atmosphere. The HNC would have a unique advantage over sea-level detectors in a search for monopoles that would thermalize before penetrating the earth's atmosphere.

- **quark nuggets**. Witten¹⁸ has calculated that particles with large mass and roughly equal numbers of up-, down-, and strange-quarks will be stable and may have survived the phase change from a quark-gluon plasma to hadrons that is believed to have taken place in the early universe. DeRujula and Glashow¹⁹ have argued that "nuggets" of the quark phase may account for much of the dark matter in our Galaxy. A striking attribute of quark nuggets is their very large mass to charge ratio, as well as their very large mass, in an object of nuclear density. Such particles might produce anomalously large ionization rates in the HNC detectors.

Identification of Ultraheavy Cosmic Rays with BP-1 Glass Detectors

The original concept of HNC was to achieve high charge resolution by tracking particles through 120 layers of plastic, which would have required measuring 240 etchpits (at top and bottom of each sheet) per event. Procedures were developed to deal with the problems associated with temperature-dependent response,⁴ growth of track reactivity with time,⁹ necessity for an oxygen atmosphere,²⁰ degradation by ultraviolet radiation, and so forth. The discovery in 1987 of the remarkable performance of certain phosphate glasses¹¹ as track detectors has made possible a great reduction in the complexity of the HNC mission. With only 14 layers of glass, the labor involved in data analysis is reduced enormously. Furthermore, the superb

properties of the glass eliminate the necessity to take the precautions that had been developed for the plastics, as well as the necessity for elaborate Bevalac calibrations. (Because of significant variations in response from sheet to sheet, each stack of plastics would have had to be separately calibrated. With the glass this is not necessary.) The experiment is now much simpler to construct and analyze. Furthermore, techniques developed for the production of huge laser rods made of very high-purity, homogeneous glass enable Schott (and other companies) to produce precision glass plates with uniform response to charged particles in any quantity that we need. The extremely precisely specified refractive index listed in the next paragraph is an indication of the uniformity of composition attained in Schott's glass products.

BP-1 glass²¹ has the composition (wt%): 65.6 P₂O₅; 25.8 BaO; 4.05 Na₂O; 4.55 SiO₂. It has a density 3.00 g/cm², a refractive index $n_D = 1.54435$; a coefficient of expansion $\alpha = 1.25 \times 10^{-5}$; an annealing temperature 352⁰C; and a softening temperature 467⁰C. It is transparent and colorless. Its properties and behavior as a particle track detector are similar to VG-13, which we discovered in 1987 and have used in several experiments²², but it has several advantages over VG-13: it is more sensitive, that is, it can detect nuclei down to lower atomic numbers; it contains no uranium, and can thus be manufactured in the U.S. and can be used in a radiation environment without accumulating a fission background; it is more resistant to track-fading; and its rate of corrosion in moist air is far lower. Schott Glass Laboratories has demonstrated that it can make plates to our specifications.

An extensive set of measurements²³ on samples that we irradiated with relativistic heavy nuclei at the LBL Bevalac has shown that BP-1 is sensitive to all relativistic nuclei with $Z \geq 48$, that it has almost unbelievably good charge resolution, and that it can survive the adverse environmental conditions in space for many years without significant degradation of stored tracks or of its ability to record new tracks. Figure 4 compares the response of BP-1 with that of the plastic track detectors that we had originally planned to use on the HNC mission.¹⁰ It is more sensitive than Rodyne polycarbonate, and its response as a function of Z/β is far steeper than that of both Rodyne and CR-39, which implies that it should be better able to discriminate between neighboring charges.

Figures 5 and 6 demonstrate its fantastic charge resolution. The peaks in Fig. 5, obtained in fragmentation of 900 MeV/N gold ($Z = 79$), where the velocity is known, have a width $\sigma_z \sim 0.06$ charge unit. Figure 6 gives examples of a string of charge measurements on the tops and bottoms of five sheets of glass. These data demonstrate that the single-etchpit charge resolution is so good that the occasional pickup and subsequent stripping of an orbital electron (Fig. 6a) is easily detected and is readily distinguished from a fragmentation with loss of one proton (Fig. 6b). The distinction is, of course, that in electron pickup the instantaneous charge fluctuates up and down, between that of the fully stripped nucleus and that of the nucleus with one attached electron, whereas in fragmentation the nuclear charge permanently decreases. The ability of BP-1 (and VG-13) to record instantaneous charge changes of one unit at very high Z in a pathlength as short as $\sim 30 \mu\text{m}$ is unique.

The great majority of the ultraheavy nuclei that penetrate the geomagnetic field at a 28.5° orbit have energies greater than 1 GeV/N, which simplifies the charge identification, since there are no particles with rapidly changing ionization rate. One simply measures the sizes of the etched cones at the top and bottom surfaces of all 14 sheets of glass and fits a straight line to the track etch rate (inferred from the etchpit size)²⁴ as a function of distance in the stack. This gives the charge and velocity. Bevalac calibrations²³ show that for $\beta > 0.8$, the track etch rate is a simple function of Z/β , approximately a power law, $\sim(Z/\beta)^{8.5}$.

Figure 7 shows the results of Monte Carlo calculations¹⁷ in which the charge standard deviation was evaluated for lanthanum ($Z = 57$), gold ($Z = 79$) and uranium ($Z = 92$) nuclei impinging isotropically on a stack of fourteen 2-mm-thick sheets. The calculations took into account detector resolution and response as a function of Z/β ; slowing, electron attachment and stripping, and nuclear interactions of fast nuclei in the stack, at zenith angles from 0° out to 60° . Only in the energy interval from about 3 to 6 GeV/N does the net charge resolution become worse than one-third of a charge unit, and only for $Z \Delta 90$ between 3 and 6 GeV/N does it extend up to one-half a charge unit. Fortunately, in the region $Z \Delta 90$ the even- Z nuclei 90, 92, 94, 96 have much longer half-lives and would be expected to be much more abundant than their odd- Z neighbors, so we can tolerate a charge resolution as poor as 0.5 charge unit in a restricted energy interval for the actinides. In the case of the nuclei with $Z \leq 83$ we can eliminate events with charge resolution worse than ~ 0.3 charge unit by cutting out those within a particular band of etch rate gradients (see Fig. 7).

Calibrations of a large batch of glass made for us by Schott showed that it is extraordinarily uniform in properties: its thickness is 2.0 ± 0.01 mm over an entire 10 cm x 10 cm sheet; its response is independent of zenith angle of entry of relativistic nuclei (as shown in Fig. 8) and is the same from sheet to sheet; the bulk etching rate is also the same from sheet to sheet.

We have found²³ that latent tracks in BP-1 are unaffected during a five-month interval at a temperature as high as 60°C . The response to monoenergetic 1060 MeV/N gold nuclei is only weakly dependent on the temperature of the glass at the time of irradiation, over a wide range of temperatures,²³ as shown in Fig. 9. This insensitivity to temperature saves us from having to construct an elaborate "event thermometer", which would have been required if we had used plastic detectors.²³ The dependence of response on detector temperature is weakest at the lowest temperatures. In order to achieve the best possible resolution it is desirable to maintain the detectors at the lowest temperature attainable with passive coatings -- below -20°C or even below -50°C if convenient.

In contrast to plastic track detectors, whose response is very sensitive to the partial pressure of oxygen, we found, using beams of gold and uranium nuclei, that the response of the glass is exactly the same when it is irradiated in vacuum as in air⁹, and that it does not depend on the delay time between irradiation and etching.⁹ In order to maintain an oxygen atmosphere, the plastic detectors would have had to be sealed in a pressure vessel. The 0.5 g/cm^2 thick cover, together with the event

thermometer, would have fragmented ~10% of heavy nuclei before they could reach the plastic stack. In our new design (see Fig. 10) there is no need for a cover. The glass stacks are mounted only at the sides, in a window frame arrangement, so that they are exposed directly to space from both faces of each stack.

The glass is superior to plastic detectors in several other respects not explicitly stated above:

1. Its σ_z is only about one-fifth that of plastic; a stack of 14 sheets gives a charge resolution better than 120 sheets of plastic would have given.

2. Not having any hydrogen in its structure, it is much more effective at slowing nuclei without fragmenting them than are plastic detectors; about 70% of Pb ($Z = 82$) nuclei would pass through the glass stack without interacting, compared with less than 30% for a plastic stack interleaved with copper sheets.

3. There is no swelling or shape change of glass during etching (except for the uniform decrease in thickness due to bulk etching), and it lies flat on a microscope stage.

Table 2 gives an estimate of the numbers of events for various known elements that we expect to collect, assuming a one-year exposure of 16 trays followed by a four-year exposure of another 16 trays, taking into account the area, solid angle, and expected energy spectrum along a 28.5⁰ orbit. The expected number is based on the data from the HEAO-3 and ARIEL-6 experiments.^{2,3} As Fig. 11 shows, the solid angle of acceptance is a function of charge. Nuclei with $Z \hat{O} 70$ are accepted out to the maximum zenith angle of 70⁰; nuclei with smaller Z are accepted out to a smaller maximum zenith angle. The lightest nuclei to be studied, those with $Z = 50$, have an acceptance ~20% that of the heaviest nuclei, but because of their greater abundance, the number of events to be collected will still be very large. Because the acceptance depends differently on charge for HNC, HEAO-3 and ARIEL-6, the numbers of events in Table 1 do not scale exactly with flux.

Table 2. Number of events expected on two HNC missions
(taking into account charge-dependent acceptance)

Z	seen on HEAO-3	seen on ARIEL-6	1-yr HNC mission	4-yr HNC mission
49-50	50	52	126	504
51-52	50	68	140	560
53-54	34	39	147	588
55-56	54	69	319	1276
57-58	34	17	142	568
59-60	14	22	113	452
61-70	46	76	515	2060
$\Delta 71$	58	75	840	3360
$\Delta 90^*$	1?	3	5 to 50*	20 to 200*
Total no.	340	420	2350**	9400**

* Estimate is ~5/yr for 4.6 billion year old solar system composition, propagated through exponential pathlength distribution, corrected for first ionization potential; estimate is ~10/yr based on one possible actinide seen by HEAO-3 experiment²; estimate is ~50/yr based on three possible actinides reported by Ariel experiment³.
** Event density is expected to be ~1.5 per 10 cm x 10 cm glass plate per year.

Two points about the table should be noted:

1. Because of our relatively small acceptance for nuclei with $Z < 70$, the total number of events expected for a four-year HNC experiment is only a factor 27 greater than seen by HEAO-3. However, for the most interesting nuclei -- those with $Z > 70$ -- we expect to detect ~60 times more events.

2. The charge resolution reported for the HEAO-3 experiment was $\sigma_Z = 0.016Z - 0.1$ for $Z \Delta 50$,² and was less good for ARIEL-6.³ The abundances found in these two experiments were reported for pairs of elements rather than for individual elements. Because of our far superior charge resolution, it will be possible for us to separately identify odd-Z as well as even-Z nuclei, and to resolve individual elements in the platinum and lead peaks as well as in the actinide peak. We request the reader to note that grouping the events by twos in Table 1 obscures this very important advantage of HNC, which cannot be overemphasized.

2. Instrumentation

Overview

The elemental distribution of the ultraheavy cosmic ray nuclei will be measured using an array of passive, track-recording detectors which will be exposed in space for the equivalent of 130 m² years as an attached payload on Space Station Freedom and, if an earlier opportunity can be developed, as a free-flying payload. After the exposure in space, the array will be returned to earth for etching of the detectors and automated analysis of the tracks that will result from penetration by the ultraheavy nuclei. The Space Shuttle will be used for the transportation of the detector array to and from space.

Individual HNC phosphate glass detectors will be grouped and mounted in LDEF-type trays which will in turn be mounted on pallets or on the existing LDEF to form the array. The pallets will be designed to interface with the Orbiter for transportation, with the Orbiter and the Freedom Remote Manipulator Systems (RMS) for handling in space, and with the Freedom Payload Interface Adaptor (PIA) for mounting on the Station Interface Adaptor (SIA).

Since the HNC detector array will require only structural support from the Freedom, it can easily be accommodated during the early man-tended phase of the Freedom assembly. It can be mounted at any location which can provide the required structural support (an SIA) and which will allow the array to view space with minimal obstructions. Although a Freedom "utility port" can be used, none of the utilities provided there other than the SIA are needed. The array is truly passive: it requires

no power, no command or data interface, no active thermal control, no pointing other than a general orientation to view space, and no crew servicing. The Freedom crew will need only to attach the detector array to the Freedom truss at the start of the space exposure and to detach the array after the end of the exposure. The HNC detector array will not be sensitive to contamination (line of sight or deposition) or to electromagnetic interference, and it will not generate any contamination or electromagnetic interference.

It would be very desirable to have an opportunity for a mission before the Freedom is available. To this end, the HNC pallets will be designed such that they can be coupled and deployed by the Orbiter as a free-flying spacecraft. The trays will be designed so that they can be mounted either on the existing LDEF or on the pallets. A reflight mission with the LDEF may also provide an opportunity to carry out part of the HNC mission before the Freedom is available. The passive thermal design of the detectors, trays, and pallets will be compatible with a mission involving either attachment to the Freedom, free-flight of two or more pallets, or attachment of the trays to the LDEF.

The HNC detector, mounting tray, and pallet concepts will employ proven technology. Much of this technology has already been demonstrated on the first LDEF mission. All of the hardware required for HNC can be designed, manufactured, flown in the Orbiter, mounted on the Freedom, flown as a free-flying spacecraft, or carried on a reflight of the LDEF with minimal risk as to performance, schedule, or cost.

The detailed design, manufacture, and qualification testing of the HNC hardware will be performed by qualified aerospace contractors under the direction of the NASA Langley Research Center (LaRC). The hardware will meet all of the HNC experiment requirements established by the Principal Investigators at the University of California at Berkeley and at the University of Michigan and all of the requirements for hardware to fly on the Shuttle and Freedom. Much of the engineering required for the HNC hardware has already been done by personnel at Langley, U. C. Berkeley, and U. of Michigan during previous HNC-related studies.

Detector Concept

The HNC will employ track-recording detectors of a proven design. The detector material will be a phosphate glass, type BP-1, with the following composition by weight: 65.5% P₂O₅; 25.8% BaO; 4.05% Na₂O; and 4.55% SiO₂. The BP-1 glass will be transparent and colorless with a density of 3.00 g/cm³, a refractive index (n_D) of 1.54435, a coefficient of expansion of 1.25 X 10⁻⁵, an annealing temperature of 352° C, and a softening temperature of 467° C. Three firms have the capability to manufacture the glass plates to meet specifications. They are Schott Glass Laboratories, Corning Glass, and Hoya Glass. All three have submitted bids, and a decision will be made after comparing their plant facilities and manufacturing techniques as well as the costs.

Tray Mounting Frames

The concept for the trays for mounting the HNC detectors was developed and qualified at the LaRC for an HNC experiment anticipated on the first reflight of the LDEF. The 6061-T6 aluminum tray is shown in Fig. 10. The glass stack of each detector will be placed in a premolded silicone rubber gasket and secured to the tray structure with a mounting frame as illustrated. The silicone rubber to be used for the gaskets, which will remain elastic at the low temperatures to be encountered during the mission, will accommodate the differential thermal expansion between the glass stacks and the aluminum structure and will provide vibration damping during the launch and retrieval environments. This technique has been used successfully to secure glass test specimens in aluminum trays on the first LDEF mission. This mounting technique allows the undisturbed detection of ultraheavy nuclei entering the detector from either side and allows the detectors to be easily disassembled after recovery for etching and track analysis. Each glass plate in the detectors will be coded to document its location in the stack and in the array. An HNC tray, fully loaded with detectors, will measure ~1m x 1.3m x 0.3m and will weigh ~100 kg.

Pallet

Figure 12 illustrates the concept of the HNC pallet, which will have the same tray/structure mechanical interface as the LDEF. This pallet will be fabricated from standard aluminum structural elements bolted together and will accommodate 8 trays of detectors. It will be designed with two main trunnions and a keel trunnion for attachment in the Orbiter cargo bay during transportation to and from space. The pallet will also be designed with fittings to accommodate the Orbiter and Freedom RMS end effectors for handling in space. When the HNC pallets are to be attached to Freedom, a PIA will be mounted on them to interface with an SIA on Freedom's truss as illustrated. One option for mounting pallets on the Freedom is illustrated in Fig. 13.

If the pallets are to be used as a free-flying HNC spacecraft, two will be attached together as shown in Fig. 14. The latching mechanism to be used in this attachment will be activated by the Orbiter RMS End Effector. The deployment sequence for two free-flying HNC pallets will be as follows: After achieving orbit, the Orbiter RMS attaches to an active grapple fixture on one pallet, unlocking the latching mechanism when it is rigidized. The main trunnion latches in the Orbiter for that pallet are then released and the RMS moves that pallet into position on top of the second pallet which is still retained in the Orbiter. The RMS end effector then derigidizes, allowing the latching mechanism to lock the two pallets in position together. The RMS then attaches to a fixed grapple fixture on the second pallet; the main trunnion latches in the Orbiter for that pallet are released; the RMS removes the joined pallets from the payload bay, places them in the required attitude for gravity gradient stabilization, and then releases them for free flight.

A pallet fully loaded with detector trays will be ~5 m in diameter and 0.3m in length. It will weigh ~1700 kg. The size and weight of these pallets should permit them to be easily manifested with other payloads on Shuttle missions.

LDEF Concept

The existing LDEF is manifested for retrieval from space in the latter part of 1989. If a reflight of this facility is approved, HNC detector trays may be included on the reflight mission. The HNC detector tray concept will be fully compatible with this mission possibility. The LDEF, shown in Fig. 15, is ~5 m in diameter and 10 m long. It can accommodate up to ~6800 kg of experiment hardware. Thirty of the HNC detector trays could be accommodated on an LDEF reflight.

Thermal Control Concept

To ensure optimum performance, the HNC detector stacks will be maintained at temperatures below ~20° F while in space. This will be done passively by blocking the conduction and radiation of thermal energy to the detectors. The thermal isolators, shown in Fig. 10, will block the conduction of heat to the trays. Superinsulation blankets and coatings will be employed to block radiant heat. This concept was analyzed in detail during previous studies for an HNC mission on an LDEF reflight.

Ground Operations

The ground operations at Kennedy Space Center (KSC) for the launch of the HNC experiment will be limited to those necessary to assemble the detector trays on the pallets, or the LDEF as the case may be, and to integrate the pallets or LDEF in the Orbiter. After retrieval, the hardware will be deintegrated at KSC and the detector trays will then be shipped back to the Principal Investigators for etching and data analysis. There are no unique ground support requirements. Only a mechanical fit check will be required at KSC. As the experiment is passive, no electrical or electronic checks are required.

Flight Operations

The HNC experiment flight operations will be limited to those necessary to transport the experiment to the Station, attach it to the Station, and return the experiment after the required space exposure or, if the experiment is to be performed as a free-flying spacecraft, simply to transport the experiment to and from the orbit. There are no constraints on launch window or orbit, and there is no need for communication while on orbit. If it is a free-flying spacecraft, ground tracking will be required in order to plan the retrieval mission.

3. Data Reduction and Analysis

After the first pair of pallets is returned to earth, half of the glass will be processed and analyzed at Berkeley and half at Michigan. Each institution will have 11200 plates to analyze. Before being etched, the plates can be stored and handled at room temperature in ordinary air and illumination. We will etch the plates in 49% fluoboric acid for four weeks at 50°C. Each institution will have an etch tank with a capacity of 600 liters of fluoboric acid and will etch 2800 plates in four batches, replacing the acid for each new batch of plates. The total time for etching, including intervals for mounting and demounting, will be about 18 weeks. Scanning and analysis can begin on the first batch of plates as soon as they are etched.

To scan one 10 cm x 10 cm plate with a 5X microscope objective and locate all tracks, using one of the automated systems now working at each institution, will take one hour, with present technology. The additional time to go back at high magnification and measure all tracks located in the initial scan will take 30 seconds per event. We expect about 1.5 events per plate per year in space. Thus, measurement time is negligible compared with scanning time. We will employ a cassette system for the automated loading and unloading of plates onto the microscope stage. We routinely run an automated scanning and measuring system continuously around the clock. To measure all of the 1600 plates in one of the 14 layers will take 800 hours at each institution. Since all of the particles will have energies high enough to penetrate all of the layers with little change in ionization rate, it is not necessary to scan independently each of the 14 layers. A reasonable strategy is to do a redundant scan of four of the 14 layers, and in the intervening layers to look only at the locations of the small number of events per plate. Thus, the scanning at each institution can be done in about 3200 hours, and the approximately 2400 events expected per year (see Table 2 above) can be quickly found in the intervening layers and measured in less than about four minutes per plate. Most of this time will be spent taking plates in and out of inventory and loading them and unloading them from the cassettes. The total time for measurement of tracks in the intervening layers will be less than 1000 hours. With one system per institution it would take about six months to do the analysis for the first mission. The rates quoted above are realistic, based on our current technology. The time required to analyze the roughly 9400 events for a four-year mission, at ~6 events per plate, is still only ~3200 hours per institution for the complete scans and ~1000 hours per institution for measurement of the events in the intervening layers.

At a 28.5° inclination there will be essentially no background due to slow particles (these will be excluded by the geomagnetic field) or solar flares, and the density of low-energy recoil nuclei due to spallation by trapped protons will not be high enough to cause any problem.

4. Orbiter Crew or Payload Specialist Training Requirements

The HNC experiment has no crew training requirements other than the standard training necessary to transfer the hardware on orbit to the Space Station and later to retrieve it, or, if it is to be a free-flying spacecraft, to deploy the spacecraft in orbit and subsequently retrieve it from orbit after the required exposure. These tasks will be standard RMS operations.

5. Summary

It is worth emphasizing that the HNC mission as envisaged here is much superior to what had been planned, approved, and scheduled for launch in a 57° orbit in May, 1987:

- the glass detectors have much better charge resolution than plastic detectors, are simpler to work with, and are immune to adverse environmental conditions;
- at 28.5° there is virtually no background, and all particles are at approximately the ionization minimum;

- no power is required in space, and there are no moving parts;
- automated scanning and measuring systems quite adequate for the HNC mission are being used routinely in our laboratories in a variety of applications that demonstrate their capabilities;
 - with only 14 layers of glass, as contrasted to 120 layers of plastic, the mission can be carried out easily with only two institutions doing the etching, scanning, and measuring, and with one other institution participating in the interpretation;
 - four pallets can be manufactured and filled with a total of 32 trays of detectors within one to two years after the HNC mission is approved, and they can be kept available as a target of opportunity.

The primary science goals are as follows:

- determine the relative abundances of each of the elements, both odd and even, in the ultraheavy cosmic rays ($Z \geq 50$);
- determine the age of the ultraheavy cosmic rays since their nucleosynthesis;
- determine the major sources of the ultraheavy cosmic rays;
- determine details of nucleosynthesis and propagation of ultraheavy cosmic rays, and also the composition of the interstellar medium, if it turns out that the ISM is the dominant source;
 - search, with a sensitivity a factor $\sim 10^2$ greater than previously, for transuranic elements and for hypothetical superheavy elements ($Z > 100$), magnetic monopoles, and quark nuggets.

6. References

1. E. K. Shirk and P. B. Price, *Ap. J.*, **220**, 719 (1978).
2. For a summary of the current status of HEAO-3 data analysis, see W. Robert Binns, in *Genesis and Propagation of Cosmic Rays*, ed. M. M. Shapiro and J. P. Wefel (D. Reidel, New York, 1988), p. 71.
3. P. H. Fowler et al., *Ap. J.* **314**, 739 (1987).
4. A. Thompson et al., *Proc. 11th Inter. Conf. on Solid State Nuclear Track Detectors*, Bristol, England, 1981.
5. M. H. Salamon, P. B. Price and J. Drach, *Nucl. Instr. Meth.* **B17**, 173 (1986).
6. B. G. Cartwright, E. K. Shirk and P. B. Price, *Nucl. Instr. Meth.* **153**, 457 (1978).
7. G. Tarle', S. P. Ahlen and P. B. Price, *Nature* **293**, 556 (1981).
8. A. Thompson et al., *Proc. 16th Inter. Cosmic Ray Conf.*, Kyoto, **11**, 103 (1979).
9. P. B. Price and J. Drach, *Nucl. Instr. Meth.* **B28**, 275 (1987).
10. J. Drach et al., *Proc. 19th Inter. Cosmic Ray Conf.*, La Jolla, CA **2**, 131 (1985).
11. P. B. Price et al., *Nucl. Instr. Meth.* **B21**, 60 (1987).
12. A. G. W. Cameron, in *Essays in Nuclear Astrophysics*, ed. C. A. Barnes, D. D. Clayton and D. N. Schramm (Cambridge University Press, 1982), p. 23.
13. W. R. Binns et al., *Phys. Rev. C* **36**, 1870 (1987).
14. J.-P. Meyer, *Ap. J. Suppl.* **57**, 173 (1985).
15. M. H. Israel et al., *Proc. 18th Inter. Cosmic Ray Conf.*, Bangalore, **9**, 305 (1983).
16. E. C. Stone et al., *Proc. 20th Inter. Cosmic Ray Conf.*, Moscow, **1**, 366 (1987).
17. J. Drach, "HNC: a Detector to Study Ultraheavy Cosmic Rays," Ph.D. thesis, University of California, Berkeley, 1987.
18. E. Witten, *Phys. Rev.* **D30**, 272 (1984).

19. A. deRujula and S. L. Glashow, *Nature* 312, 734 (1984).
20. J. Drach, M. Solarz, Ren Guoxiao, and P. B. Price, *Nucl. Instr. Meth.* B28, 364 (1987).
21. Shicheng Wang, S. W. Barwick, D. Ifft, P. B. Price, and A. J. Westphal, "Phosphate Glass Detectors with High Sensitivity to Nuclear Particles," *Nucl. Instr. Meth.* (in press).
22. G. Gerbier, Ren Guoxiao, and P. B. Price, *Phys. Rev. Lett.* 60, 2258 (1988).
23. A. J. Westphal, S. W. Barwick, D. Ifft, and P. B. Price, to be published.
24. R. L. Fleischer, P. B. Price and R. M. Walker, *Nuclear Tracks in Solids* (California Press, Berkeley, 1975).

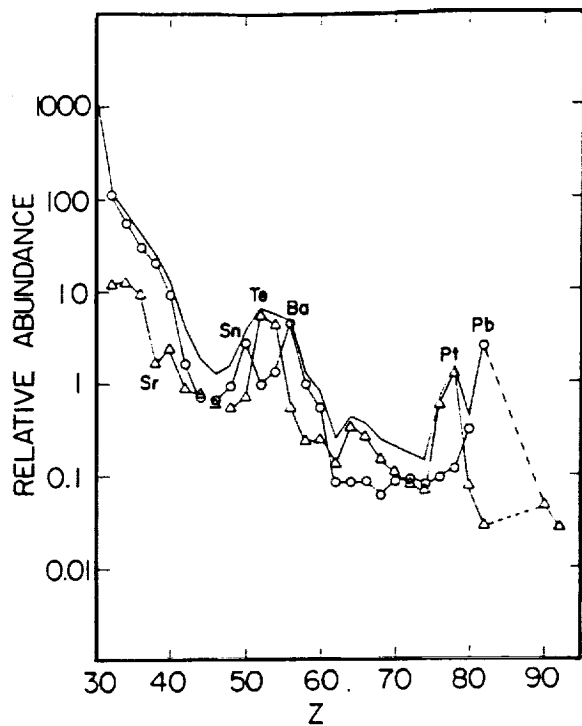


Fig. 1 Contribution of the r-process (triangles) and the s-process (circles) to the total solar system abundance of each even-Z element (upper line).

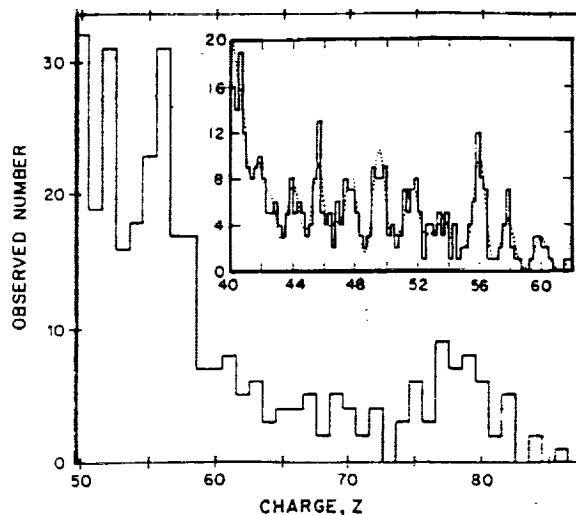


Fig. 2 (a)

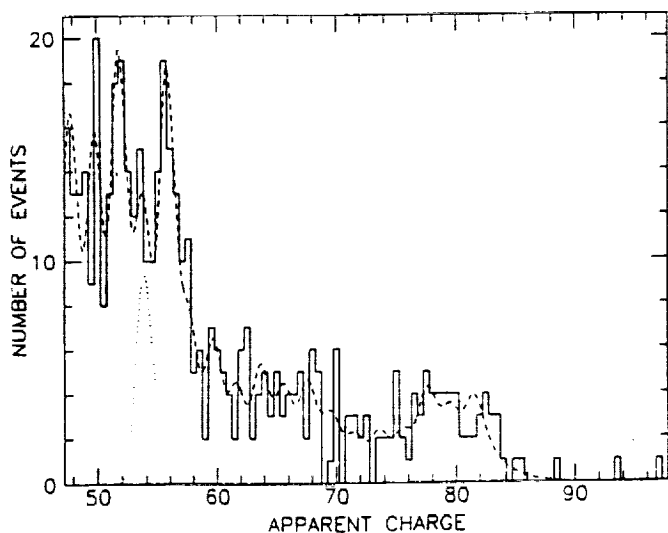


Fig. 2 (b)

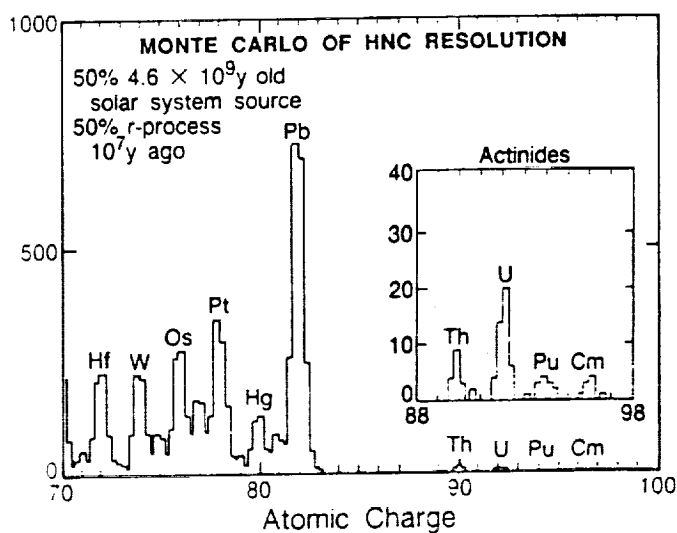


Fig. 2 (c)

Fig. 2 Relative abundances of ultraheavy cosmic rays. (a) HEAO-3 experiment; (b) Ariel-6 experiment; (c) expected resolution and number of events for HNC experiment.

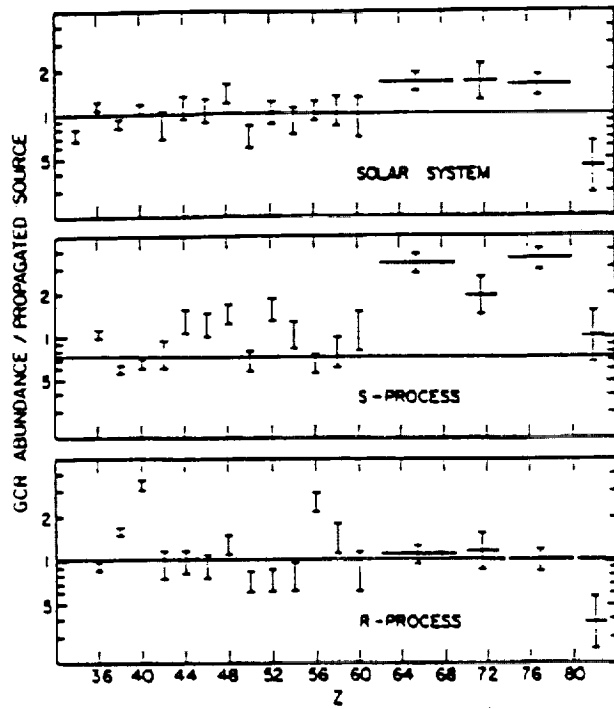


Fig. 3 Ratio of galactic cosmic ray abundances to calculated abundances near earth, for three hypotheses regarding source composition: FIP - fractionated solar-mix materials; pure s-process; and pure r-process (from ref. 16).

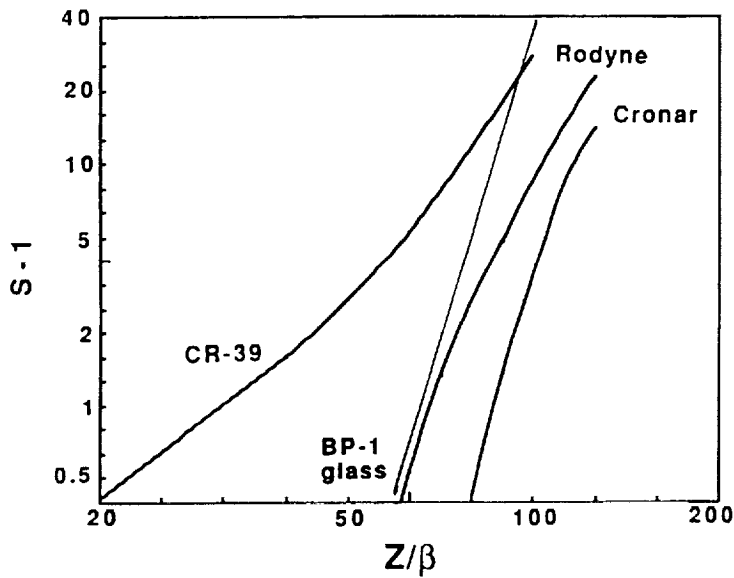


Fig. 4 Response of BP-1 glass, proposed for HNC, as compared with plastic track detectors.

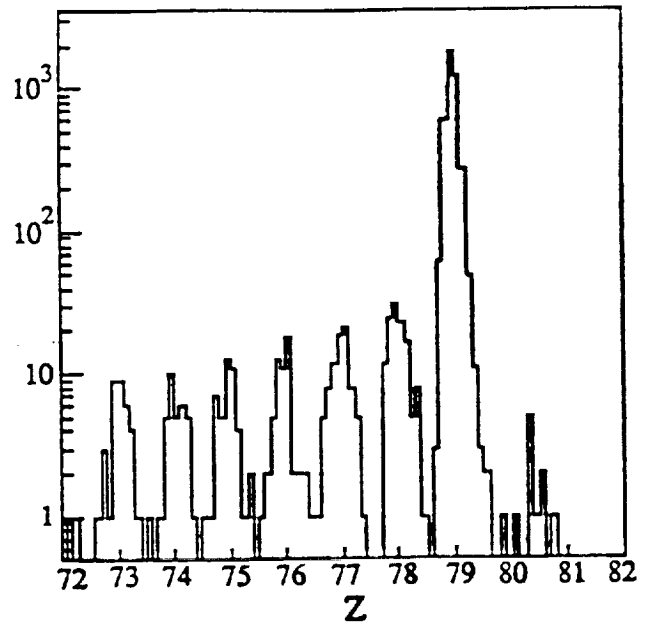


Fig. 5 Data on fragmentation of 200 GeV gold ($Z=79$), showing the excellent charge resolution of BP-1 glass detectors.

Fig. 7 Examples of charge resolution expected for the HNC mission.

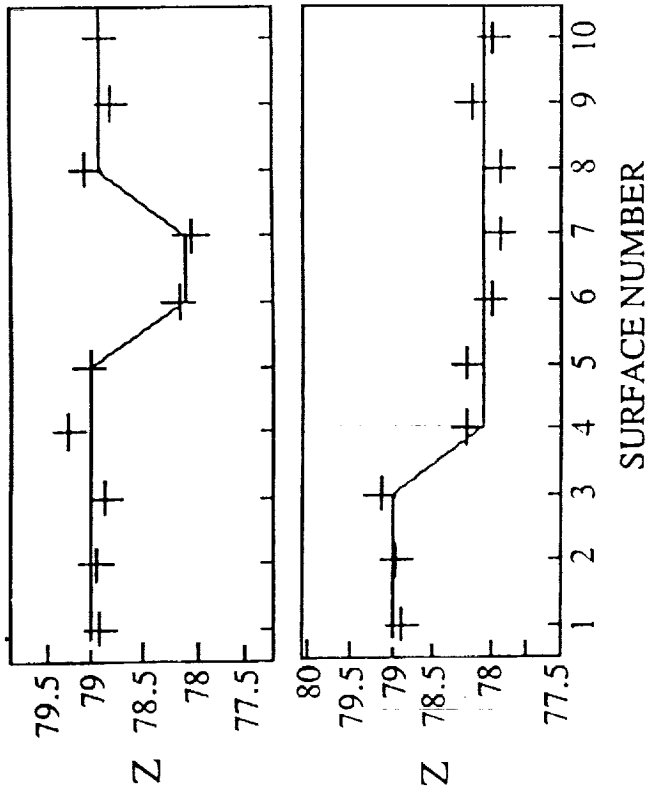
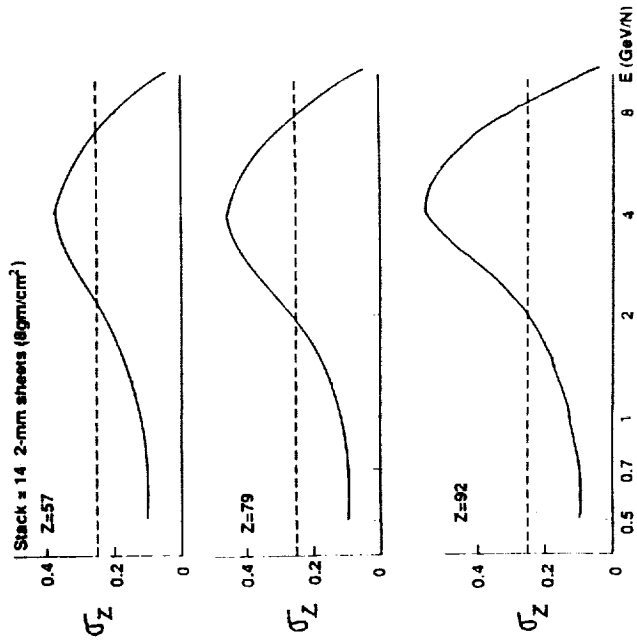


Fig. 6 Measurements of charge state at top and bottom surfaces of a stack of five glass plates.

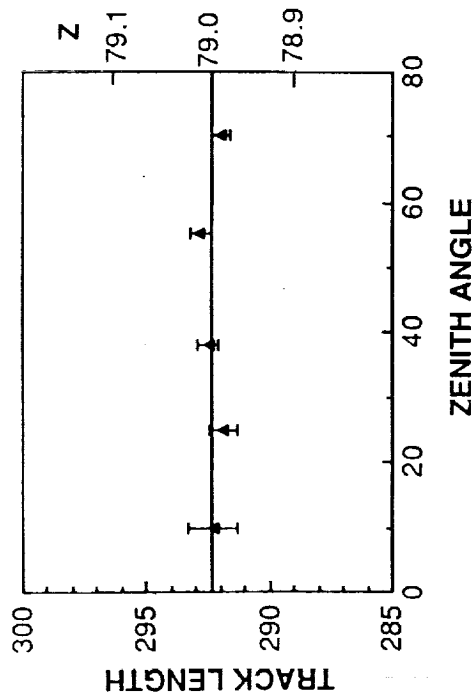
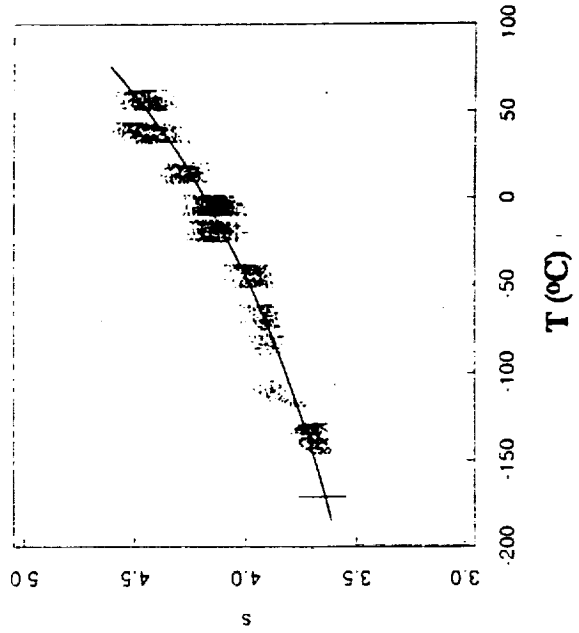


Fig. 8 Independence of response of BP-1 glass detector on zenith angle of a particle's trajectory.

Fig. 9 Dependence of response on detector temperature.



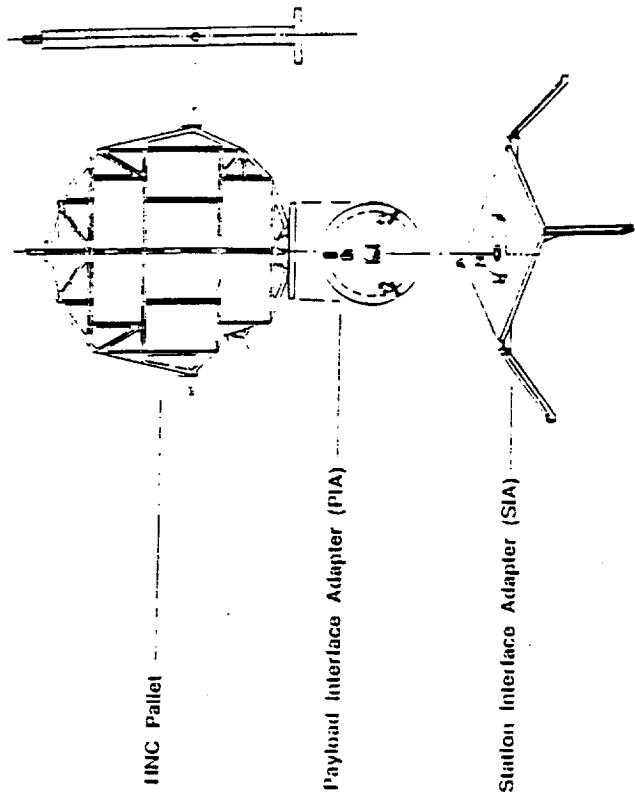


Figure 12 - IINC Pallet Concept

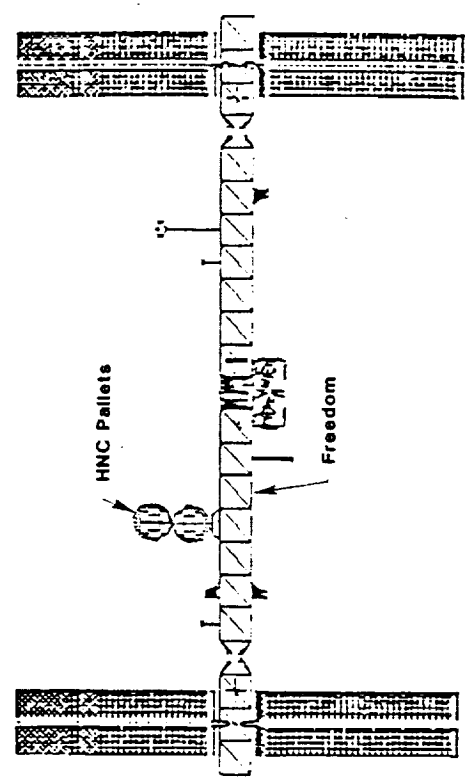


Figure 13 - Two IINC Pallets on Freedom

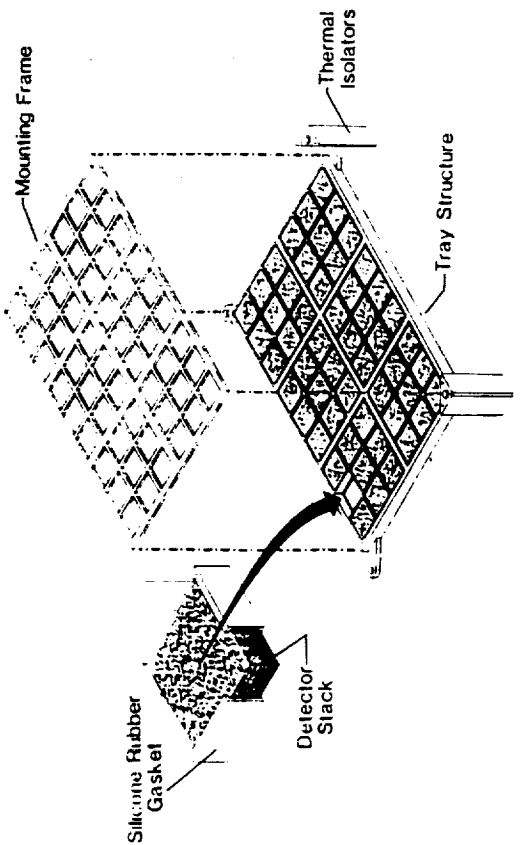


Figure 10 - IINC Detector and Tray Assembly Concept

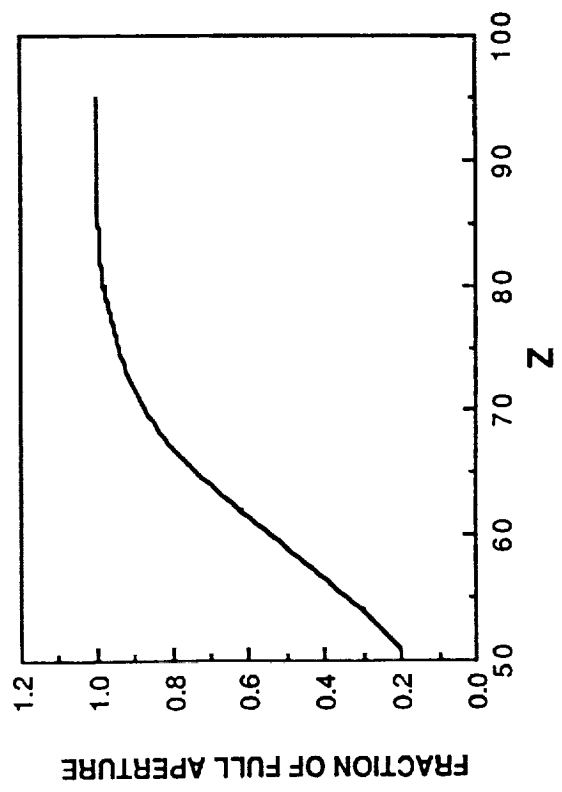


Fig. 11 Fraction of full collecting power as a function of Z for BP-1 glass detectors.

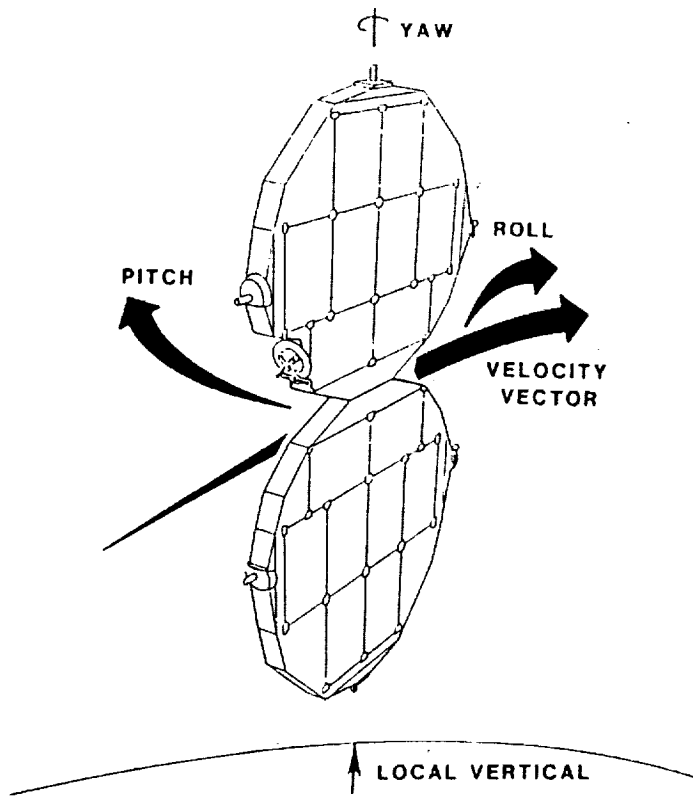


FIGURE 14 - FREE-FLYING HNC CONCEPT

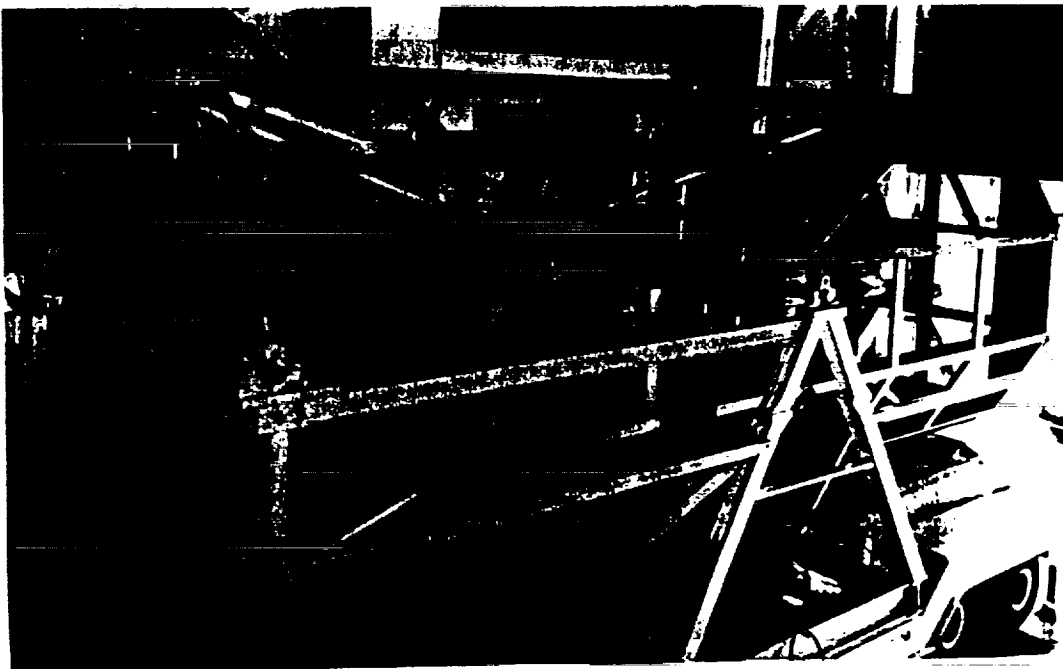


FIGURE 15 - LONG DURATION EXPOSURE FACILITY

ORIGINAL PAGE IS
OF POOR QUALITY

HEAVY NUCLEUS COLLECTOR FOR SPACE STATION

P. B. Price

Physics Department, University of California, Berkeley, CA 94720

ABSTRACT

Two opportunities exist in the next decade for measuring the charge distribution of ultraheavy cosmic rays with unprecedented statistics and elemental resolution. Groups at Berkeley, University of Michigan, and University of Utah will expose an array of track-recording phosphate glass plates $\sim 16 \text{ m}^2$ in area for five years at an orbital inclination of 28.5° on Space Station Freedom. In addition, negotiations are underway between Berkeley and Soviet colleagues to expose 1 to 3 m^2 of glass for 2 years at an inclination of 51.6° on Space Station Mir. The elemental resolution for the two sets of experiments is expected to be ~ 0.25 charge unit. If negotiations are successful, the Mir experiment will be launched in 1991 and will collect about six times as many events with $Z > 50$ as were studied on HEAO-3 and about one-fifth as many events as will be collected on Freedom.

INTRODUCTION

HEAO-3¹ and Ariel-6² experiments have provided interesting data on the abundances of ultraheavy cosmic rays with $Z > 30$. Each instrument collected between 300 and 400 events with $Z > 50$. On HEAO-3 the charge resolution was adequate to detect even-Z peaks up to $Z = 60$. One possible actinide event was detected on HEAO-3 and perhaps two or three on Ariel-6. The next study of ultraheavy cosmic rays must obtain much higher statistics and must attain charge resolution sufficient to resolve both odd-Z and even-Z nuclei. In its original conception, the Heavy Nucleus Collector (HNC) would have used large arrays of track-recording plastic films on a reflight of the Long-Duration Exposure Facility (LDEF), with an event thermometer by means of which the temperature-dependence of the response of the plastic films could be corrected. The Challenger accident dashed hopes for this version of HNC. Since the accident, we have developed a new class of detectors made of phosphate glass, which have several advantages over the plastic films.³ The version of HNC that will fly as an attached payload on Freedom will not require an event thermometer and will require the analysis of only 16 layers of glass, in contrast to the ~ 120 layers of plastic for the old HNC. The reduction in the number of dE/dx detectors is a consequence of the much higher charge resolution of glass than of plastic.

ASTROPHYSICAL GOALS AND EXPECTED NUMBER OF EVENTS

With the ability to measure both odd-Z and even-Z elements with good statistics, a number of astrophysical goals can be achieved. First and foremost is the goal of determining the source of the ultraheavy cosmic rays. Neutron capture is the dominant process of nucleosynthesis for the elements beyond the iron peak. The analyses of HEAO-3 and Ariel-6 data showed that the abundances of the even-Z elements 32 to 60 are consistent with a cosmic ray source having a composition similar to that of the solar system, but subject to source fractionation correlated with the first ionization potential of each element. For $Z > 60$ statistics and resolution were limited, such that elements had to be analyzed by groups. The conclusion was that the

abundances of both the platinum group, $74 \leq Z \leq 80$, and of the largely secondary elements $62 \leq Z \leq 73$, are enhanced relative to those in a propagated solar system source. These results suggest that there is an enhancement of the r-process contribution to the source nuclei in the charge region $Z > 60$. Over the entire region of charge with $Z > 32$, standard leaky box models of propagation account satisfactorily for secondary production. Statistics and resolution were inadequate to draw conclusions about the actinide elements, $Z \geq 90$. Thus, although much has been learned from the HEAO-3 and Ariel-6 experiments, details of the nature of the source of ultraheavy cosmic rays are still obscure.

If the goal of collection of at least 40 actinide events can be achieved, it should be possible to estimate the age of the ultraheavy cosmic rays since they were synthesized. This is done by comparing the relative numbers of Th, U, and transuranic nuclides, which span halflives from $\sim 10^6$ to $\sim 10^{10}$ years. For example, if the cosmic rays were simply swept-up interstellar matter uncontaminated by supernova debris since early in the history of the Galaxy, the Th/U ratio would be ~ 4 , as is the case for the solar system material today. If the cosmic rays were made up of equal parts of old material and supernova debris added within the last $\sim 10^7$ years, the Th/U ratio would be < 0.4 , and a number of transuranic cosmic ray nuclei would be detected.

In addition to the astrophysical goals, one can use HNC to search for admittedly improbable particles such as long-lived superheavy elements ($Z \sim 110$), magnetic monopoles, and quark nuggets.

The table below compares the number of nuclei in various charge intervals seen in the HEAO-3 experiment with the number expected for a one-year Freedom exposure and a two-year Mir exposure. If the decision is made to leave the HNC detectors on the

Table 1. Expected Number of Ultraheavy Cosmic Rays

Z	seen on HEAO-3	estimated, 28.5° 16 m^2 for 1 yr (NASA Freedom)	est., 51.6° 3.2 m^2 , 2 yr (Soviet Mir)
49-50	50	126	95
51-52	50	140	119
53-54	34	147	78
55-56	54	319	171
57-58	34	142	62
59-60	14	113	56
62-69	48	450	414
70-73	15	180	259
74-80	36	570	734
81-83	8	160	218
>88	1?	15	18
Total no.	340	2362	2224

[HEAO-3 + Ariel-6 data, and dependence of aperture on ionization rate, were used to predict fluxes at solar min.; at solar max., fluxes will be lower.]

Freedom for a full five years, the numbers in column 3 can be multiplied by five. Thus, in round numbers, a Mir experiment with $6 \text{ m}^2 \text{ yr}$ would improve the statistics by a factor ~ 6 over the HEAO-3 data, and a Freedom experiment with $80 \text{ m}^2 \text{ yr}$ would lead

to a factor ~ 35 improvement. Either of these possibilities would lead to good statistics in the collection of odd-Z and actinide elements, with resolution sufficient to provide firm charge identification.

PHOSPHATE GLASS DETECTION SYSTEM

Figure 1, from ref. 4, shows the unprecedented charge resolution exhibited by phosphate glass. The main peak is that of a beam of gold ($Z = 79$) nuclei of energy 800 MeV/N produced at the LBL Bevalac. The other peaks are due to projectile fragmentation of gold. The charge standard deviation is $\sim 0.06 e$. An extraordinary feature of these detectors is that instantaneous charge states are recorded at each surface of a stack, and pickup and stripping of single electrons are unambiguously seen.

Ref. 4 gives the composition and properties of BP-1, the phosphate glass that we developed and that will be used on the HNC. Aside from its remarkable charge resolution, two noteworthy features are that its response is independent of the ambient atmosphere and far less sensitive to ambient temperature than is the response of the plastic detectors originally planned for HNC.

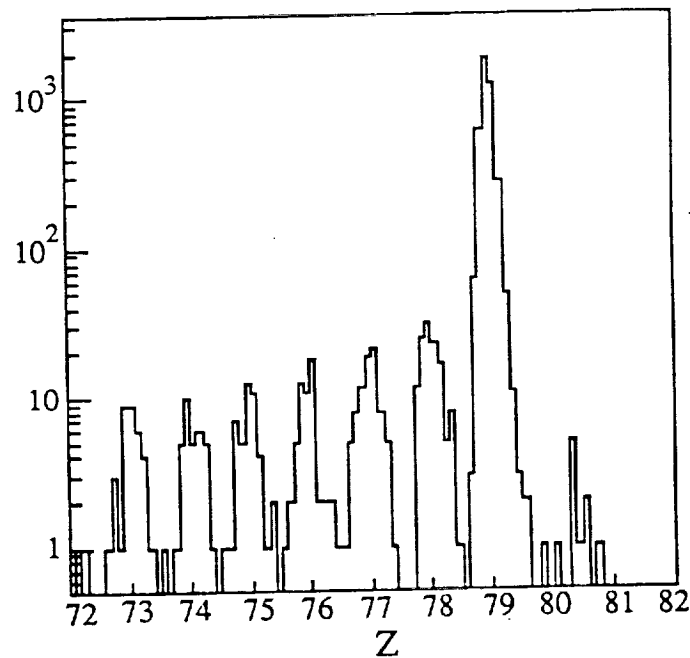


Figure 1. Charge distribution of fragments produced in fragmentation of 800 MeV/N Au projectiles at LBL Bevalac. Standard deviation is 0.06 e.

TWO POSSIBLE SPACE STATION EXPERIMENTS

At this writing, NASA has given its provisional approval of HNC for early deployment as an attached payload on Freedom. The glass plates will be processed and analyzed with automated scanning and measuring systems at the Universities of California (Berkeley) and Michigan. Charge, Z , and velocity, βc , are determined from the value of the ratio Z/β inferred from the ratio of the track etch rate to the general etch rate, v_T/v_G , at the point of entrance of the particle into the stack, and from the rate of change of Z/β as the particle slows. G. Tarle' will be in charge of the Michigan effort, and M. H. Salamon (University of Utah) will participate in data analysis. The requirement of a space exposure of several years will put the beginning of data analysis several years into the next millenium.

Soviet physicists at the Soviet Space Research Institute and at Moscow State University are interested in collaborating with the Berkeley group (together with D. O'Sullivan of the Dublin Institute of Advanced Studies) in a scaled-down version of HNC that could be deployed by Cosmonauts on the outside wall of the Mir, which will remain in space until toward the end of 1993. Details and a definite commitment have yet to be worked out, but the prospect of having the first really high-resolution data on ultraheavy cosmic rays a decade before the Freedom experiment is complete is very attractive.

REFERENCES

1. For a summary of the current status of HEAO-3 data, see W. Robert Binns, in Genesis and Propagation of Cosmic Rays, ed. M.M. Shapiro and J. P. Wefel (D. Reidel, New York, 1988), p. 71.
2. P. H. Fowler et al., Ap. J. **314**, 739 (1987).
3. Shicheng Wang et al., Nucl. Instr. Meth. **B35** 43 (1988).
4. G. Gerbier, Ren Guoxiao, and P. B. Price, Phys. Rev. Lett. **60**, 2258 (1988).



Report Documentation Page

1. Report No. NASA CR-187527		2. Government Accession No.		3. Recipient's Catalog No.	
4. Title and Subtitle Science Requirements for Heavy Nuclei Collection (HNC) Experiment on NASA Long Duration Exposure Facility (LDEF) Mission II			5. Report Date June 1991		
			6. Performing Organization Code		
7. Author(s) P. Buford Price			8. Performing Organization Report No.		
			10. Work Unit No. 871-00-00-04		
9. Performing Organization Name and Address University of California Berkeley, CA 94720			11. Contract or Grant No. NAS1-17806		
			13. Type of Report and Period Covered Contractor Report		
12. Sponsoring Agency Name and Address National Aeronautics and Space Administration Langley Research Center Hampton, VA 23665-5225			14. Sponsoring Agency Code		
			15. Supplementary Notes Langley Technical Monitor: William H. Kinard Final Report		
16. Abstract The HNC is a passive array of stacks of a special glass, 14 sheets thick, that record tracks of ultraheavy cosmic rays for later readout by automated systems on Earth. The primary goal is to determine the relative abundances of both the odd- and even-Z cosmic rays with $Z > 50$ with statistics a factor at least 60 greater than obtained in HEAO-3 and to obtain charge resolution at least as good as 0.25 charge unit. The secondary goal is to search for hypothetical particles such as superheavy elements. The HNC detector array will have a cumulative collection power equivalent to flying 32 M ² of detectors in space for 4 years. The array will be flown as a free-flight spacecraft and/or attached to Space Station Freedom. Upon return to Earth, detectors would be removed for analysis. Ultraheavy nuclei would have left tracks through the detector sheets that would be made visible after etching in a hot sodium hydroxide solution.					
17. Key Words (Suggested by Author(s)) cosmic ray, heavy nuclei, space, LDEF			18. Distribution Statement Unclassified - Unlimited Subject Category 73		
19. Security Classif. (of this report) Unclassified		20. Security Classif. (of this page) Unclassified		21. No. of pages 77	22. Price A05

